博 士 学 位 論 文

論文題目　Research on Decommissioning Simulation Based on Plant Lifecycle Information Management for Nuclear Power Plants

提　出　者　　東北大学大学院情報科学研究科

応用情報科学　　　　　　専　攻

氏　名　　関　　洋

TOHOKU UNIVERSITY
Graduate School of Information Sciences

Research on Decommissioning Simulation Based on Plant Lifecycle Information Management for Nuclear Power Plants

（原子力プラントのライフサイクル情報管理に基づく

廃炉シミュレーションに関する研究）

A dissertation submitted for the degree of Doctor of Philosophy (Information Sciences)

Department of Applied Information Sciences

by

Hiroshi SEKI

July 7，2022

Research on Decommissioning Simulation Based on Plant Lifecycle Information Management for Nuclear Power Plants

Hiroshi Seki

Abstract

Many sections in an engineering company are conducting partial engineering work concurrently in the engineering activities during the lifecycle, which consists of design, construction, operation&maintenance, and decommissioning for nuclear power plants (NPPs).

At first, an engineering data warehouse was developed to integrate and exchange data through the lifecycle of NPPs. Based on a standard information model, CAD data translators from 2D drawings and 3D models were built, and their browsers were also made in this research. To adopt every task in the plant-related work with its design data, such as process and instrumentation 2D drawings, a continuous refining system for drawing data has been built. The developed system is applied to maintain consistency between actual project and design data.

Secondly, there are many cases in which it is reasonable to decommission NPPs in Japan and overseas concerning balances between investment costs of heavy safety measures and speculated profits by operating plants for generating electricity. Based on the standard information model, a decommissioning engineering support system was developed using three-dimensional models for NPPs. As for the calculation of the duration related to dismantling work and costs, based on the spatial distribution of the dose rate around equipment and piping components, it is essential to evaluate difficulty levels of dismantling work and waste quantities consisting of contaminated equipment and piping components with radioactive materials in the decommissioning project. Furthermore, it is necessary to assess person-hours for large equipment and waste containers being carried out from the installed or packed places to designated temporary areas or outside areas of the plant building. In this system, radioactive inventory data is mapped to 3D objects of equipment and piping components for a decommissioning NPP. Based on the mapped radioactive inventory data to 3D objects, the spatial dose rate distribution is automatically calculated, and waste container models are automatically generated. Using generated data, carrying out paths for large equipment and waste containers are automatically calculated. Results of an evaluation showed that the developed system could support decommissioning engineering tasks systematically and effectively.

Thirdly, equipment and piping components contaminated by radioactive materials and irradiated materials as low-level wastes must be cut, segmented, and packed in waste containers. To avoid excess exposure dose and minimize the number of waste containers for many pieces of equipment and piping components, an automatic planning method for virtual cutting of 3D equipment objects was developed under the constraints of container sizes, maximum radioactivity, maximum weight, and maximum dose rate. Different cutting-work flows were formulated and used to generate cut objects and calculate the exposure dose for the disassembling work with various cutting sequence data. With the help of the developed system, decommissioning planning will be supported by the calculated results of required cutting length and dose-rate distribution in the working environment for various cutting sequences of large equipment.

Fourthly, a robot with a flexible arm controlled by a remotely operated water-pressure mechanism has been developed to dismantle objects heavily contaminated by radioactive materials during decommissioning of NPPs, especially for the accident plants. This research aims to create a process planning support system and method that can improve the accuracy of estimating the time required by the robot to complete its dismantling activity, support recovery from delays, and determine the feasibility of conducting a dismantling process in the reactor building. Since the flexible arm has a more complex mechanism and shapes with multiple-axis joints, unique movable arm structures were modeled with a tool for three-dimensional (3D) computer graphics (CG) technology. The 3D CG model was used to make valid operation sequences for planning the robot's motion. With the help of a prototype system, motion planning can perform to calculate the duration needed for the robot to complete its task. The estimated duration is then used for updating the planned period of a specific activity in a dismantling schedule. A simplified planning method with few virtual controllers based on a spline inverse kinematics (IK) with a non-uniform rational B-spline (NURBS) curve for an arm to prepare the robot behaviors for complex dismantling processes comprised of the pistons and cylinders pressurized by water was studied. A prototype system for planning the robot's behaviors was evaluated. It was confirmed that the movement trajectory of the robot and the three-dimensional isometric display could be visualized using the mesh model generated from point cloud data which was used to make the environment model for the robot. It was also confirmed that the operations involved in a specific robot activity could be completed within the duration determined in the simulation.

The above-mentioned standard information model can be commonly applied to decommission existing NPPs and the accident plant. However, the viewpoint of risks, such as removing fuel debris, retrieving emitted hydrogen gases, and controlling wastes under conditions of criticality reactions of fuel elements, should be carefully considered. Therefore, the accident plant needs to apply the fourth scope of this research for operating robots remotely. At the same time, the second and the third scope of the study, such as mapping the radioactive waste inventory to the plant components and the automatic planning, are applied to the decommissioning project for all existing NPPs.

Table of Contents

1 Introduction

1.1 Background

In the engineering activities during the lifecycle, which consists of design, construction, operation&maintenance, and decommissioning of nuclear power plants (NPPs), many sections in an engineering company are conducting partial engineering work concurrently. In breakpoints, engineers in a particular team check the consistency among the work results of other departments. Hence, checking the consistency between the upper and the lower design results is crucial.

A common semantic model expression to realize this integration is discussed in data integration to integrate more extensive deliverables from partial engineering deliverables. Related to the data integration, the standard semantic model's effectiveness, applicability, and cost reductions have been studied in process engineering [1]. Based on the effective data integration technologies with the standard semantic model, the lifecycle of NPPs should be managed well regarding qualities, efficiencies, and costs.

There are many cases in which it is reasonable to decommission NPPs in Japan and overseas concerning balances between investment costs of heavy safety measures and speculated profits by operating plants, as shown in Figure 1.1[2]. After the big earthquake in the east of Japan and the resulting severe accident in Fukushima Daiichi Nuclear Station, rigorous safety assessments of existing power plants have been applied for all the existing NPPs in Japan. Based on the assessed results, many NPPs were evaluated as not continuing to be operated based on comparing the costs between profits until its plant life and investments for safety measures. Hence, owners and operators of such NPPs declared decommissioning of the plants. As of 2022, 25 NPPs are facing decommissioning phase, including the number 1 to 4 plants of Fukushima Daiichi Nuclear Station, which occurred in Japan.

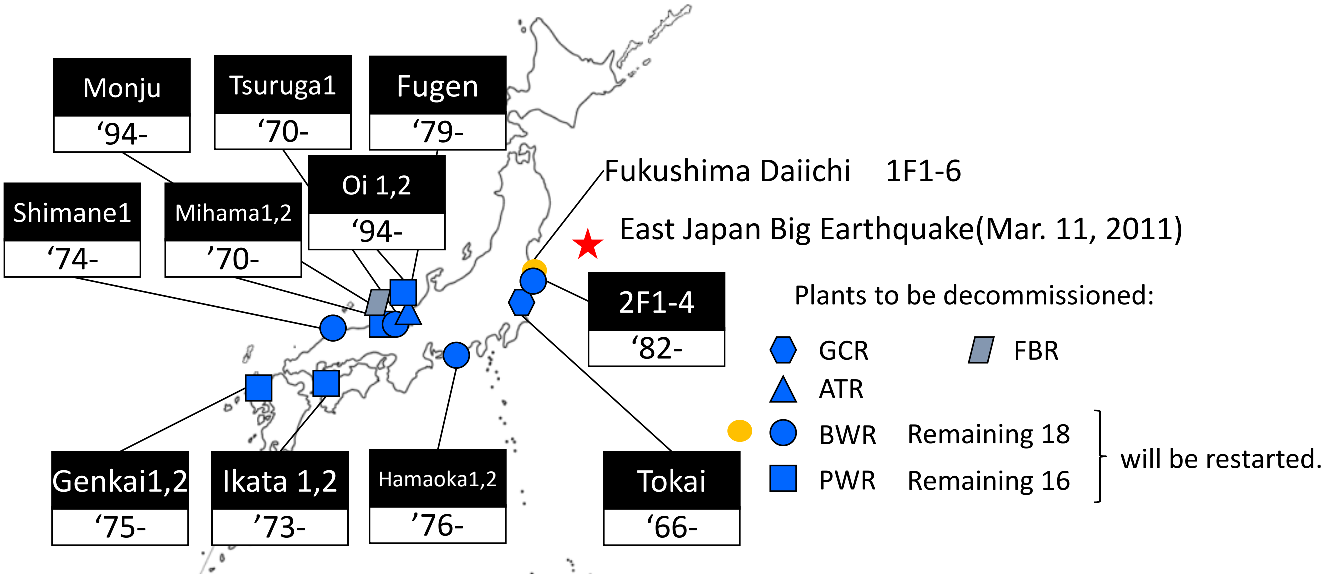

Figure 1. 1 Nuclear power plants to be decommissioned and operated in Japan.

Additionally, it is necessary to estimate costs for decommissioning projects of NPPs precisely because the cost overrun should be avoided, especially for the final phase of the plant life cycle [3][4]. Conventionally, waste quantities produced in a decommissioning project are calculated based on weights per system piping components and equipment in the NPP. To avoid cost overruns for the decommissioning project, plant operators or owners should estimate the detailed cost precisely. It is essential to evaluate the weights of large equipment, the internal structures of a reactor, and waste volumes because it includes contaminated radioactive materials.

Furthermore, we should remove melted fuel debris safely and steadily in the decommissioning work of Tokyo Electric Power Company Holdings, Incorporated (TEPCO) Fukushima Daiichi Nuclear Power Station (FDNPS). In the middle and long-range road map defined by the Nuclear Damage Compensation and Decommissioning Facilitation Corporation (NDF), the target year of starting the removal of fuel debris was set in the year 2021, and it is speculated to be suspended until 2022 due to the COVID-19 spread [5]. The most challenging issue for removing debris is an extraordinarily high dose rate area, such as 10 to 100 Gy/h in the Primary Containment Vessel (PCV) and the Reactor Pressure Vessel (RPV). Hence, we should do the remote removal work thoroughly. The removal devices or robots should be highly resistive in a high dose rate area.

Generally, conventional nuclear power plants are regulated to be decommissioned after 40 years since their startup. The NPP must be dismantled safely and economically in a decommissioning project. There are many actual cases of dismantling and removing wastes for research reactors in the US, European countries, and Japan. Hence, data on waste quantities, person-hours, exposure dose, and costs can be available [6]. Based on these results, we can precisely study the safety and economy of the decommissioning of NPPs.

The decommissioning of NPPs is classified into three types sealed controlling, shielded controlling, and immediate dismantling, based on the classification by International Atomic Energy Agency (IAEA) [7][8]. A similar type of decommissioning of NPPs is expressed, and they are often used as safe storage (SAFSTOR), entombment (ENTOMB), and decontamination (DECON). The standard decommissioning method of 1100MWe class commercial NPPs in Japan is "the sealed controlling and immediate dismantling." The relationships of those decommissioning classifications between Japan, the IAEA, and the US are shown in Table 1.1.

Table 1.1 Classification of a decommissioning project

	Japan	IAEA	U.S.
Classification	Sealed controlling	Stage 1 (Controlled storage)	SAFSTOR (Safe storage)
	Shielded controlling	Stage 2 (Conditional site release)	ENTOMB (Entombment)
	Immediate dismantling	Stage 3 (Unconditional site release)	DECON (Decontamination)

The Federation of Electric Power Companies of Japan (FEPC) has defined an overview of the standard decommissioning schedule as shown in Figure 1.1 [9]. After shutting down an NPP permanently, the spent fuel assemblies are removed from reactors. Then the piping components and equipment are decontaminated to decrease exposure in the working environment. The decommissioning plant remains for five to ten years, called the safe storage to reduce the radioactivity of piping components and equipment in the facility, and then the dismantling is started. Finally, the radioactive wastes are stored in containers, then the containers are stored in storage areas or underground to release and reuse the site. FEPC has estimated that the duration of the decommissioning takes 30 years. The OECD/NEA has estimated the cost of decommissioning all types of reactors [10]. The decommissioning costs for typical reactors in Japan, such as Pressurized Water Reactor (PWR) and Boiling Water Reactor (BWR), are 320 USD/kWe and 420 USD/kWe, respectively. After the accident of FDNPS, the cost of decommissioning is speculated to be increased because the regulation of the contaminated wastes by radioactive materials has been changed to strict directions, and no final disposal sites are yet confirmed. However, the pressure to suppress the cost of decommissioning will be increased because of tendencies for high electricity prices even though the existing nuclear power plants are not restarted as planned.

The typical configuration of a boiling water reactor (BWR) type NPP is shown in Figure 1.2 [11]. The NPP consists of a reactor building and a turbine building. The steam generated in the reactor core by controlled chain reactions of nuclear fission with recirculating water by pumps and control rods is supplied to turbines. By rotating turbines, electricity is generated at the generator and provided to the demand sides via the switchyard. The steam is condensed to water with a condenser by exchanging heat using cooling water from a reservoir or seawater. The condensed water is filtrated to remove impurity and fed into the reactor with feedwater pumps. For the safety measure, the reactor pressure vessel (RPV) is installed in the primary containment vessel (PCV), and a torus shape suppression chamber is installed to decrease pressure inside the PCV in an emergency. After long years of plant operation, radioactive materials, Cobalt-60 (Co-60, from now on), are circulated in the piping components and equipment. Therefore, we must consider that such radioactive materials should be managed appropriately and discriminated against with non-radioactive materials during the decommissioning phase of an NPP.

As for the accident plant, such as the number 1 through 3 of the FDNPS, the PCV, and explosions broke the reactor buildings. Moreover, the fuels were melted because of hot temperatures due to the loss of cooling functions, and the melted fuels were dropped underneath the PCV and eroded to the suppression chambers. Those melted fuels are called fuel debris, emitting harmful radiation to humans. Thus, we must work remotely to remove such fuel debris.

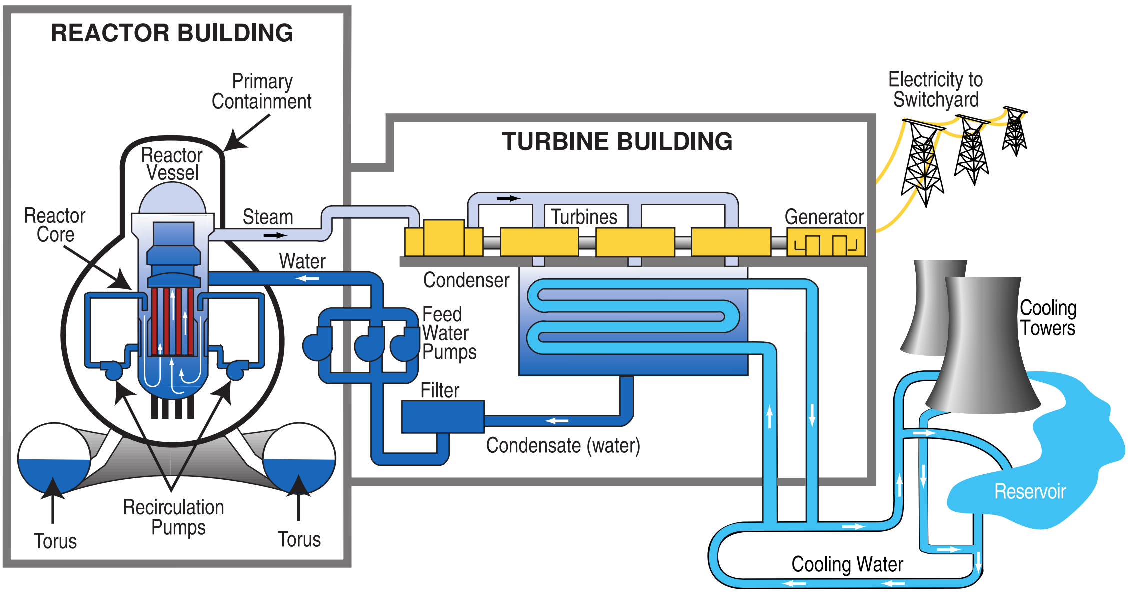

Figure 1.2 A typical configuration of the boiling water reactor (BWR) for an NPP.

Figure 1.3 shows a typical and standard schedule of a decommissioning project. After shutting down an NPP permanently, it is decommissioned within 30 years. Before the decommissioning project, planning for the 30 years project must be done well to control its duration and cost rigorously. At the beginning of the project, the spent fuel is transported to other facilities, and the radiation-controlled areas inside the buildings are surveyed for preparing for the dismantling work. Based on observed results, highly contaminated piping components and equipment are decontaminated chemically and mechanically. The primary radiation source in the NPP is Co-60, and its half-life is about five years. Therefore, the dismantling work starts five years after the plant's permanent shutdown, called the safe storage phase. After the safe storage, internal components of reactor and turbine buildings are dismantled, and radioactive waste is stored in the controlled radioactive facility. Finally, buildings are dismantled, and the site is recovered into a green field and reused for appropriate purposes.

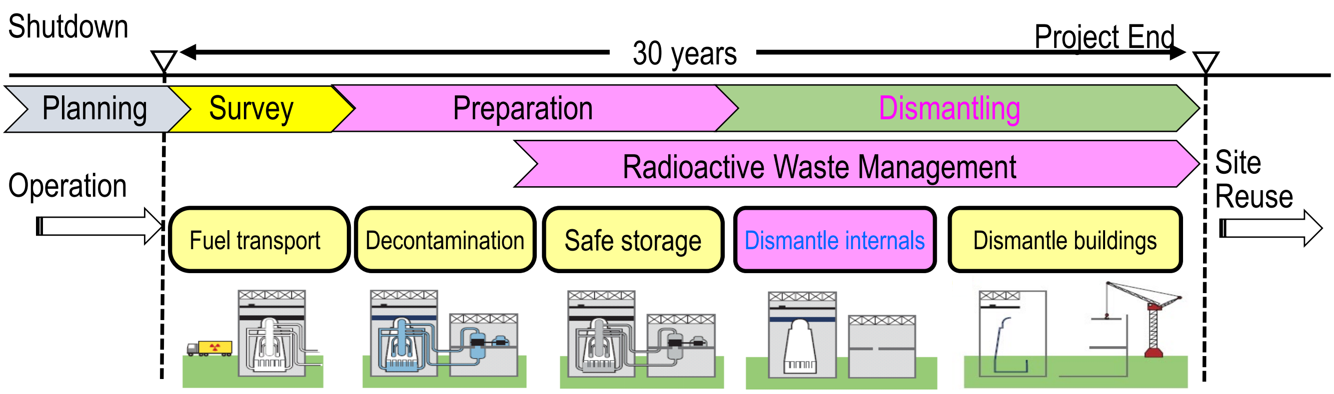

Figure 1.3 Standard schedule for a decommissioning project [12]**.**

Previously, Japanese nuclear regulation stipulated that the use of an NPP should be limited to 40 years of operation. The number of the decommissioning projects can be calculated based on this assumption, including Fukushima's number 1 to 4 NPPs, as shown in Figure 1.4. With this calculation, the peak number of projects will be almost 10 for BWRs and Pressurized Water Reactors (PWRs) in the 2030s. Recently, the Japanese government decided the utilization ratio of nuclear power for electricity generation to 20 to 22 percent in 2030. So, some of the decommissioning projects might be delayed. However, 20 NPPs will be decommissioned simultaneously in the 2030s. We never had experience conveying such parallel decommissioning projects, so we had to develop technologies to overcome this difficulty.

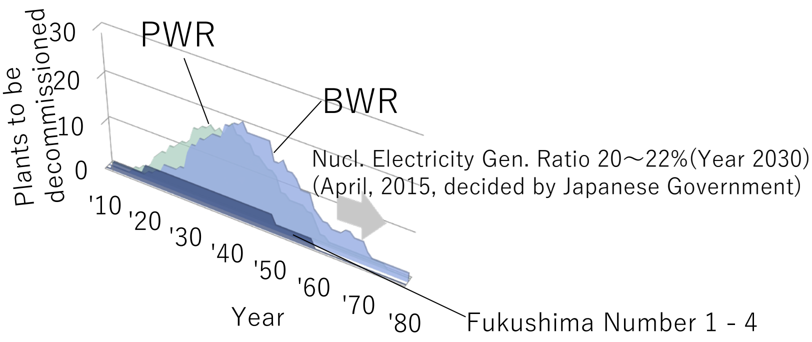

Figure 1.4 Number of decommissioning projects in Japan.

As for details of waste, some initial analyses have been done before for the Japanese NPPs [13]. The constituents of waste are shown in Figure 1.5. Non-radioactive waste is 93% (495,000 tons) is estimated for the waste quantity of an 1100 MWe BWR plant. The remaining 7% consists of 2% (13,000 tons) low-level waste (LLW) and 5% (28,000tons) clearance waste (CL) which is under the criteria of very low-level radioactivity, such as 0.01Bq/g of Co-60. NR and CL waste can be reused in building new NPPs or waste containers at dismantling sites. If the waste is decomposed or melted materials that include negligible radioactivity, that material can also be reused in other industries, such as constructing roads, transmission towers, etc. The remaining 2% of waste, which is radioactive, is stored in LLW storage containers, and the containers are stored in interim storage facilities if the final disposal sites are not prepared.

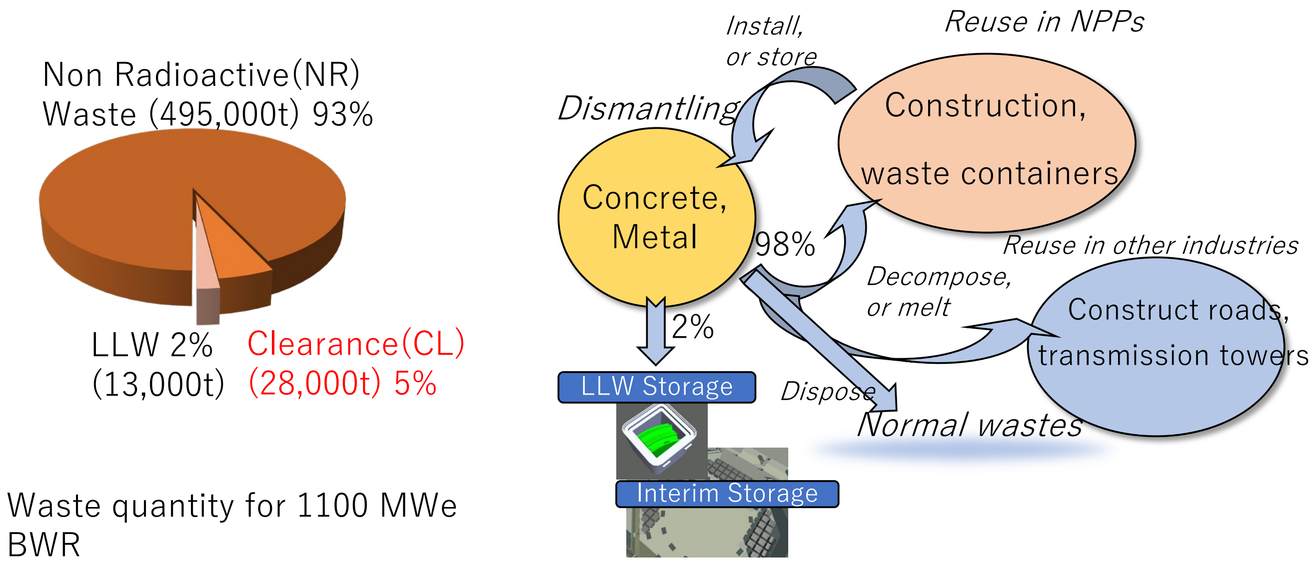

Figure 1.5 Amount of waste from decommissioned nuclear power plants and their usage in industries.

Among the electricity power generation companies that have BWR, Chubu electric company in Japan has decided to decommission Hamaoka-1 and Hamaoka-2 due to the cost of additional installments of seismic resistance components in 2008 [14]. The remaining radioactive waste has been estimated, as shown in Figure 1.6. After removing assemblies of spent fuels from the reactor pressure vessel (RPV), the waste is classified as radioactive waste and non-radioactive waste. All the radioactive waste for decommissioning NPPs is low radioactive level. High-level radioactive waste over $1x10^{12}$ Bq/t is called L1 waste, low-level radioactive waste between $8.1x10^{8}$ Bq/t and $1x10^{12}$ Bq/t is called L2 waste, and very low-level radioactive between 0.1 Bq/g and $8.1x10^{8}$ Bq/t waste is called L3 waste. The radioactive level of waste under 0.1 Bq/g, called clearance regulated waste (CL), is treated equally as industrial waste. We must reuse the CL waste to construct buildings and manufacture as much as possible.

On the other hand, L1 waste must be buried in the ground under 50 to 100 m from the ground level, we must bury L2 waste in concrete pits under 10 m from the ground level, and both L1 and L2 waste are needed to be managed for 300 years. We must bury L3 waste in the shallow underground trench for 30 to 50 years. Hence, the cost of managing radioactive waste can be reduced by decreasing the amount of higher-level radioactive waste.

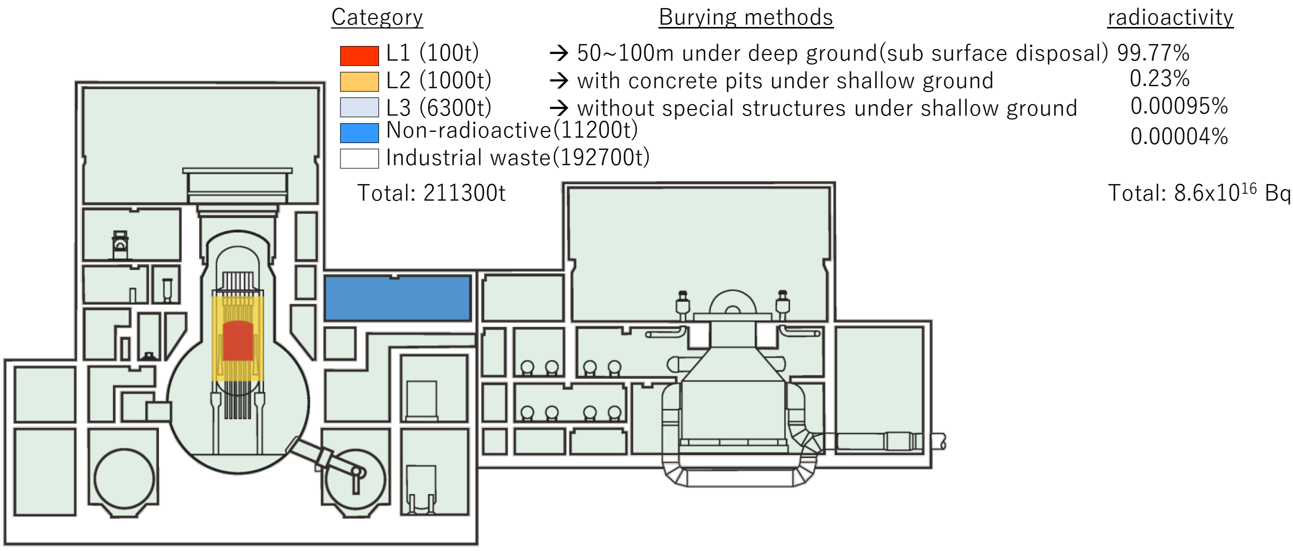

Figure 1.6 Quantities of radioactive waste.

Based on the estimation for Hamaoka-1 and 2, quantities of L1 waste are less than 0.1 % of destruction, and the sum of L1+L2 waste is minor than only 4 % of complete waste. As for L1 waste, remote dismantling methods have been verified for the research reactor in Japan, such as the Japan Power Demonstration Reactor (JPDR) of the Japan Atomic Energy Agency (JAEA). Then, other improved methods have been studied in the joint research among electricity companies. Although the amount of L2+L3 waste becomes almost 100 times larger than that of L1 waste, human workers assume that piping components and equipment are dismantled. To realize dismantling by human workers requires dismantling methods and planning to suppress occupational exposure. Additionally, since 90 % of waste is CL waste, efficient estimation, measurement, carrying out the site, and reuse of the CL waste are crucial issues.

As for the accident plant, such as FDNPS, must safely and steadily remove the solidified melt fuel distributed in and out of the reactor pressure vessel, called fuel debris. The Nuclear Damage Compensation and Decommissioning Facilitation Corporation (NDF) has defined the middle and long-term roadmap for decommissioning Fukushima Daiichi 1-4 [15]. In the roadmap, the fuel debris removal has been said to be started within 2021, but it is speculated to be formed in 2022 due to the pandemic of COVID-19. As for the removal methods for debris, it is explained in "the technical strategic plan 2021 for decommissioning of the Fukushima Daiichi Nuclear Power Station of Tokyo Electric Power Company Holdings, Inc. [16]" The conceptual studies of removing the fuel debris, the applicability of the developed methods to the actual field, and the scenarios of removing the fuel debris per each plant are described in the report. As for the conceptual studies of removing the fuel debris, the report also describes the gradual planning expansions of the scale of removing the fuel debris, the analyses of transferring and storage containers of fuel debris, principles of securing safety, etc. As for the applicability of the developed methods to the actual field. From these considerations, the most challenging thing is that areas with an extraordinarily high dose rate, such as 10 to 100 Gy/h, for the Reactor Pressure Vessel (RPV) and the Primary Containment Vessel (PCV), and the whole dismantling work must be done remotely. Moreover, the related devices must have high durability for such a high dose rate.

The Collaborative Laboratories summarize the structure of issues related to the decommissioning project for FDNPS for Advanced Decommissioning Science (CLADS) [17]. Above mentioned issues are included in this map, and the removal of fuel debris is one of the critical issues for the decommissioning of FDNPS. In the fundamental research of technologies, standardization, risk assessment, and knowledge management are crucial issues.

Common issues for the decommissioning between commercial NPPs and FDNPS are necessities of remote operations for dismantling high dose rate areas inside RPV. After decreasing the dose rate in dismantling areas, a more efficient dismantling method can be applied for both plants. As for FDNPS, there are many areas that human workers cannot enter because of heavy contamination by fuel debris. On the other hand, as for commercial NPPs, human workers can dismantle most places. Hence, the decommissioning of the conventional commercial NPPs must be done at a low cost because the permanent shutdown plants do not generate power and profits.

EPRI and IAEA report the Plant Information Model (PIM) that retrieves plant lifecycle information efficiently and contributes to the lifecycle cost, including the decommissioning phase [18]. Examples of data integrated by PIM are a 3D model, process, and instrumentation diagrams (P&ID), attribute data (weights, dimensions, dose rates, etc.), equipment design drawing, and NPP components. Each data is mutually connected with the standardized PIM.

In the latter half of the 1990s, data exchanges for 3D models between different systems and organizations based on ISO 10303-227 [19] were verified and validated. In ISO 10303-227, the plant item corresponding to an NPP component is retrieved as the essential information entity. The plant items are piping components, mechanical components (i.e., equipment), HVAC, and cableway components. They are represented as item shapes and connected via connectors with connection specifications, as shown in Figure 1.7. Plant items are aggregated to a plant system, and plant systems are aggregated to a plant. Corresponding to a plant system, a schematic representation of the functional drawing, such as P&ID, is defined. However, schematic representations are standardized in ISO 10303-221 [20]. The coverage activities for the lifecycle of process plants in ISO 10303-227, as shown in Figure 1.8, express the standardization's main objective is placed on the phase of plant design and construction and piping fabrication. The decommissioning phase is not supported so much at that time.

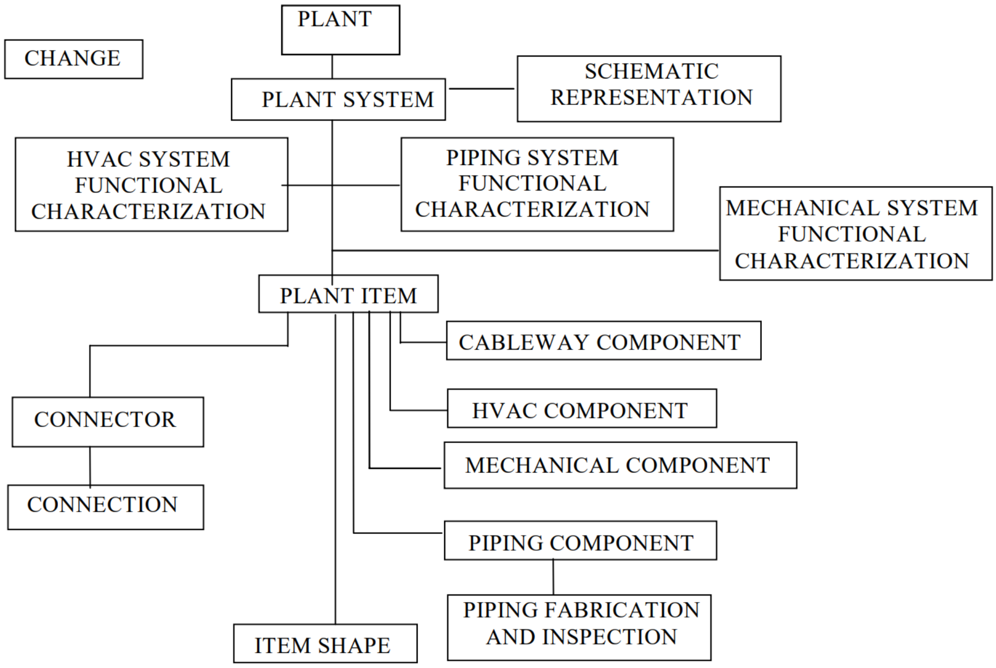

Figure 1.7 Data model represented in industrial automation systems and integration — Product data representation and exchange — part 227: application protocol: plant spatial configuration (ISO 10303-227).

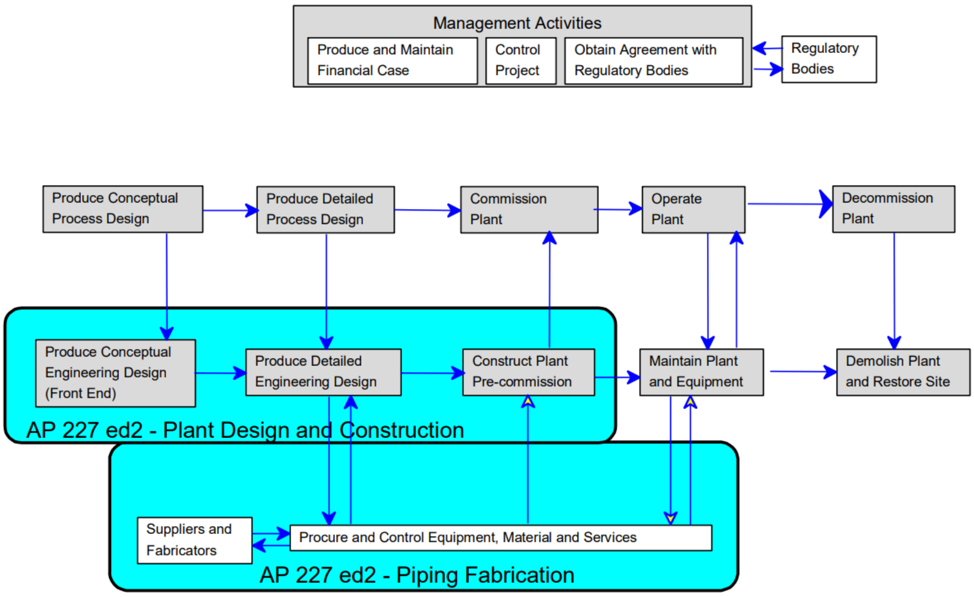

Figure 1.8 Coverage for activities of lifecycle process plants in ISO 10303-227.

After the demonstration of data exchange for a 3D model, a Generic Product Model (GPM), which consists of binary relationships of objects and associations, has been developed in IMS/VIPNET project. Within the international IMS/VIPNET project, we have developed a methodology for integrating construction data based on GPM [21]. The essential class combination of GPM for integrating plant data is defined. Although most of the classes used in GPM have referenced ISO 10303-227, GPM is focused on implementing the applications for data integrations and exchange with its XML expression and database structure.

The GPM core model expresses the semantic data model with a binary relationship between an object, an association, and an object, i.e., the S-V-O structure. Based on the GPM core model, the class library is made with generic classes, such as a plant *is_assembled_from* plant_system. The product data as instance data is expressed for a specific product, such as A_plant *is_assembled_from* A_00_sytem, and A_plant *is_assembled_from* A_01_system. Although these two sentences are written in different sentences, if the instance for the subject is the same, we can write the relationship diagram in a gathered form. Moreover, these relationships are written with a description method by GPM-XML for machine-readable expression.

The data integration layer retrieves the class library and instances based on GPM. The data mining layer supports creation processes, such as design and engineering, and is used for safety assessment. The processed data is shown in spreadsheets with attributes, 2D drawings, and 3D models with thin clients, such as web browser-based viewers.

Bi-directional translators have been made for exchanging data for CAD/CAE/CAM, PDM, ERP, and so on according to the plant lifecycle to apply this system with existing systems. Based on this conceptual development, the effectiveness and efficiencies of data integrations and exchanges have been demonstrated [22].

In the International Standard Organization, those activities related to data integrations and exchanges have continued in ISO 15926. ISO 15926 integrates lifecycle data for process plants, including oil and gas production facilities [23]. Recently the scope of the standards has been expanded to include the nuclear power plant industries. ISO 15926 inherits concepts of the ISO 10303 (STEP). It raises the idea that the standard retrieves time-changing objects through a plant lifecycle from the early planning, design, engineering, construction, operation, maintenance, and decommissioning. And it has also expanded representation methods for engineering information using first-order logic. And hence ISO 15926 can be represented using RDF/OWL [24]. It has been applied to the information management for a research reactor in the Netherland, as shown in Figure 1.9 [25]. Even if organizations use various tools and other databases, each data element can be mapped to ISO 15926 core model with Reference Data Library (RDL). RDL represents standard terms used for nuclear power plants here. The data can be exchanged and integrated into Common Data Environment (CDE).

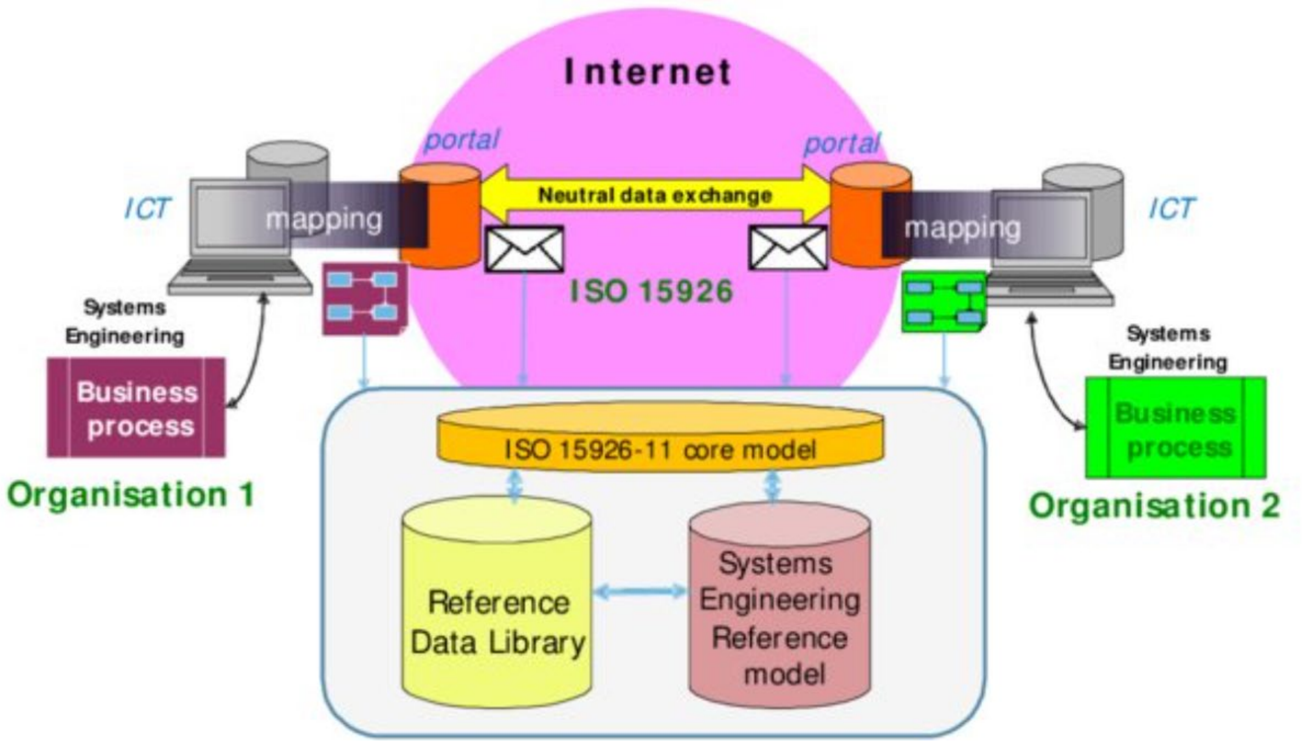

Figure 1.9 An information exchange architecture based on ISO 15926-11 using the information models as reference models to validate exchanged data between organizations [25]**.**

In this research, based on an integrated information model for the lifecycle of an NPP, precise estimation of waste quantities for decommissioning, dismantling planning for large equipment, and planning of remote operations of robots are simulated and verified.

1.2 Significance, scope, and definitions

In this research, methods for data integrations and exchanges are studied for long lifecycles of NPPs over a hundred years, including the phase after the decommissioning of NPPs. Then, a support system for decommissioning engineering processes based on a 3D CAD model for a whole NPP and technologies for planning and estimating occupational exposure dose for workers related to cutting and dismantling large equipment are studied. As for the accident plant, work planning with remotely operated robots with water pressure controls can resist extraordinarily high dose rate areas.

In this research, there are four unique features. At first, core elements of information representation are extracted as a standard information model based on International Standards, such as STEP, ISO 15296, and so on. Then practical technologies for maintaining consistencies for engineering information related to plant lifecycles of an NPP have been evaluated. The link structures for objects with associations have been used for representing piping components and equipment for the NPP here, and it has been expressed with an original markup language. Following the network shape information, which consists of objects and associations, we can identify impacts by changing engineering information. With a design change, we can apply the data to maintain consistency between design data and actual project data. Hence, the resulting technologies have academic significance.

Secondly, based on the above information model, the radioactive waste inventory of an NPP is mapped to piping components and equipment as engineering attribute information with the 3D spatial distribution. The dose rates in the surrounding area are calculated automatically. With these functions, the economy, and the safety indexes of the decommissioning, such as waste quantities and occupational exposure dose, can be evaluated. Therefore, the developed technologies are applied to decommissioning engineering processes rationally and effectively.

Thirdly, based on 3D models for large equipment to be decommissioned, an automatic planning method for cutting virtually in the 3D space and formulating cutting procedures that consist of cutting sequence data based on multiple dismantling scenarios have been studied in this research. With the help of the study, the cutting sequence data can be used not only for generating segmented objects of equipment but also for calculating occupational exposure dose during dismantling work. Because of the evaluated results, workers at the dismantling site can avoid excessive exposure doses. We can minimize the number of containers for piping components and equipment waste. With these results, it is significant to do rational, detailed planning for the decommissioning project.

And fourthly, as for the accident plant, technologies for detailed planning with robots with flexible arms controlled by water pressure in a virtual environment have been studied. The water pressure control is suitable for operating remotely in an extraordinarily high dose rate space. This research has developed simplified operation methods with a few virtual controllers for the complicated constraints of moving flexible arms. Then, a prototype system was designed to make moving sequences for planning robot operations. With the help of this research, the accuracy for dismantling work hours is calculated for dismantling tasks, and it supports recoveries from delays in the planned schedule. Consequently, the developed methods provide a significant work planning support system to judge feasible dismantling processes from an actual search space.

The above-mentioned standard information model can be applied to decommissioning existing nuclear power plants and accident plants, such as FDNPS. However, the viewpoint of risks, such as removal of fuel debris, retrieval of emitted hydrogen gases, and controlling wastes under criticality reactions of debris, should be carefully considered. Therefore, the accident plant needs to apply the fourth scope of this research for operating robots remotely. At the same time, the second and the third scope of the study, such as mapping the radioactive waste inventory to the plant components and the automatic planning, are applied to the decommissioning project for existing NPPs.

1.3 Review of literature

1.3.1 Industrial data model

Applied products and services related to plant lifecycle management (PLM) are commercially realized and widely used in many industries. Among such industries, engineers need to integrate and exchange data. For ISO 10303 [26], Standard for the Exchange of Product model data, called STEP, even if the applied scopes are different, such as plant and manufacturing, the standard is known as applicable Application Protocols (APs), can be applied to each area. Several APs can be combined into one Application Module (AM), which we can use for efficient data integrations and exchanges [27]. And there is another example of sharing manufacturing information based on a virtual enterprise environment [28]. These two cases have been realized for integrating and exchanging data based on STEP.

On the other hand, an added information representation method and a markup language have been made in Virtual Enterprise Network (VIPNET) international projects to simplify data integrations and exchanges [29]. All users can ideally use these results' original data at the design phase, called provenance. It can be effective in reducing duplicate inputs or avoiding input errors. Recently, the reference mentioned above models has been being discussed intensively by International Organization for Standardization (ISO) and International Electrotechnical Commission (IEC), and the discussed contents are related to Industry 4.0, Smart Manufacturing, and Digital Twins [30]. International Standards (IS) related to information sharing for product lifecycles are authorized in ISO TC 184/SC 4 [31]. And the information management for NPPs in conjunction with ISO 15926 is discussed in the WG3 under ISO TC 184/SC 4. The author of this dissertation is developing IS and reviewing related Standards.

ISO 15926 is a set of standards for “industrial automation systems and integration — Integration of life-cycle data for process plants including oil and gas production facilities [23].” ISO 15926 has a long history since the 1970s, and its origin is ISO 10303 (STEP), as shown in Figure 1.10. Semantic expressions, usage patterns, and interfaces have been developed in European Process Industries STEP Technical Liaison (EPISTLE) [32], Fully Integrated Automation Technology Project (FIATECH) [33], and Construction Industry Institute (CII) [34]. Then ISO 15926 expands knowledge to process industries based on the Project Management Body of Knowledge (PMBOK) [35]. On the other hand, Shell and other industries are interested in data interoperability between companies. Therefore, they have created a Handover Guide (HOG) [36]. Recently, they formed a consortium called Capital Facilities Information Handover Specification (CFIHOS) to create forum standards so that they can realize better interoperability between companies [37]. Common concepts are also standardized in Automation systems and integration based on the developed standards — Oil and gas interoperability — Part 1: Overview and fundamental principles (ISO/TS 18101-1) [38]. The developed standards are also applied to Industrie 4.0, which initially originated in Germany, and the concept is spread globally. Industrie 4.0, also called the Fourth Industrial

Revolution and is named for the idea of automation and the digitalization of manufacturing industries. It includes cyber-physical systems (CPS), the Internet of things (IoT), cognitive computing, and so on [39].

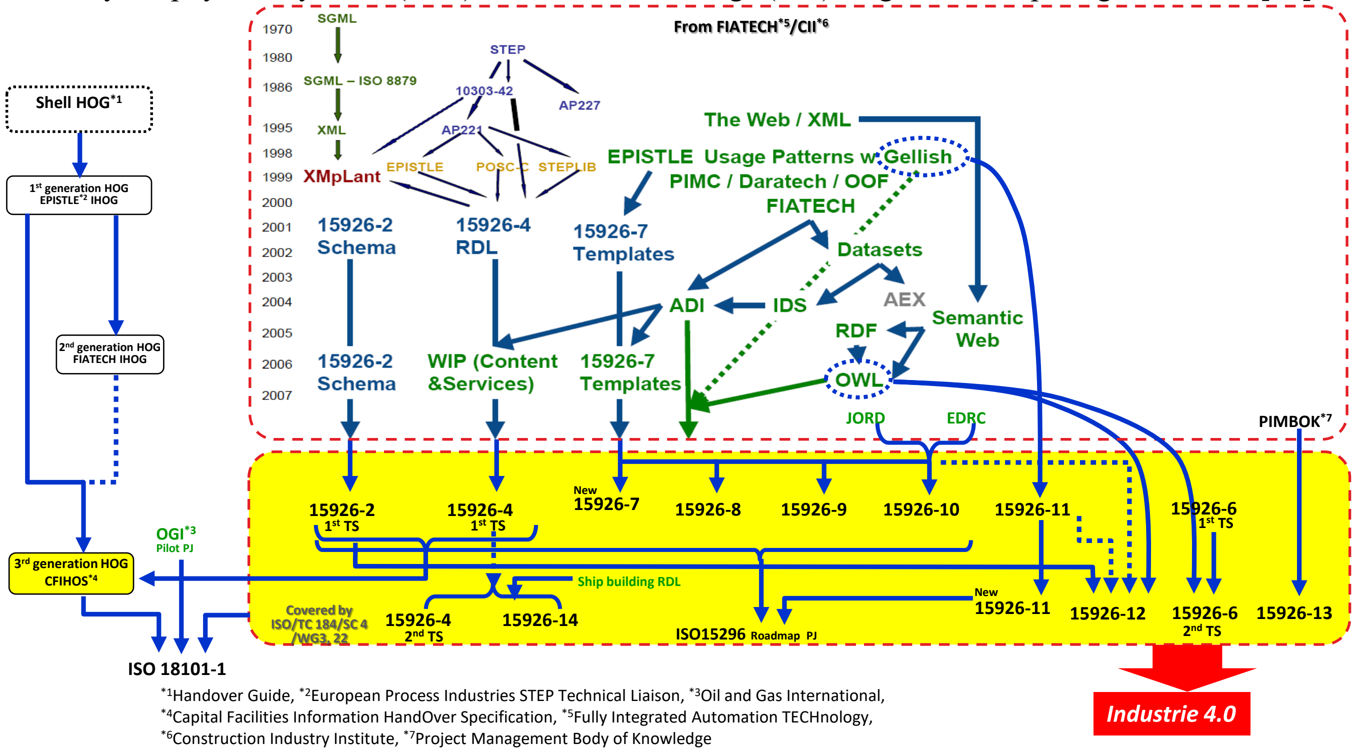

Figure 1.10 History of the developed Internationals Standards and related schemas.

The ISO 15926 consists of 13 parts, as shown in Figure 1.11. Part 5 was deleted after the proposal. Based on the data model in Part 2, ontology for geometry and topology in Part 3, and the initial reference data as a standard industrial dictionary in Part 4. Part 6 defines the rules for Part 4. Part 7 to part 14 is for the expression of the RDL and its interoperable expression methods [24]. Recently, the activities specific to nuclear industries have been started in the ad hoc group under ISO/TC 184/SC 4, called "Nuclear Digital Ecosystem Specification (AHG2) [40]." Under AHG2, they create documents for the state of the art of standardization of information management of nuclear installations over their life cycle, a survey among the nuclear stakeholders to develop a final standard for the digital ecosystem, define the business case with use cases of developing and adopting such information standards, and draft a new work item (NWI) technical report (TR) documentation.

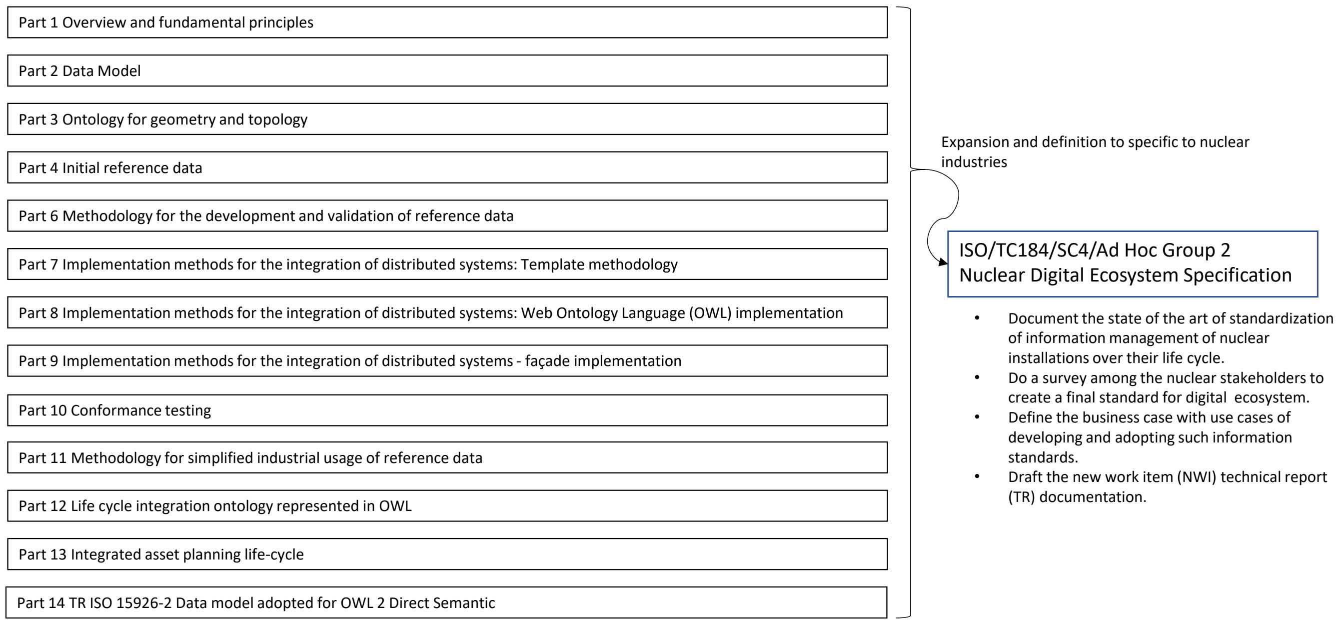

Figure 1.11 ISO 15926 and the activities related to the nuclear industries

The nuclear industry's approach to information modeling has only begun with ISO/TC 184/SC4 and ISO/TC 85/SC6, but in the past, the IAEA has been trying to use Plant Information Model [18]. By using online information such as Web search, the IAEA Report is being used as an initiative to organize by using semantic technology as a more efficient and large-scale knowledge [41]. The IAEA Report is written as follows: one of the many vital benefits of using semantic technology is that it improves the organization of data and information – by linking various sources so they can be shared and reused across sectors, organizations, and scientific communities. Through this improved knowledge, information, and data organization, nuclear safety standards, recommendations, experiences, best practices, and previous research can become more widely available.

1.3.2 Estimation of waste quantities of decommissioning nuclear power plants

At the decommissioning of the first NPP for generating electricity, Japan Power Demonstration Reactor (JPDR), the system engineering for dismantling, work hours, exposure dose, and waste weight were evaluated systematically. A project management system for dismantling processes has been integrated and operated with the system, called COSMARD [3]. And then, research institutes in Japan and Norway developed the decommissioning engineering support system, DEXUS. It has been used for supporting judgments for optimized dismantling planning in the decommissioning project [4].

An overview of simulation technologies for decommissioning projects is shown in Figure 1.12 [42]. Some intelligent databases must be calculated by diversifying activities, waste quantities, removal routing for large equipment, decontamination, and many processes. 3D CAD data and as-built models from the point cloud data measured by laser scanning and photogrammetry are populated to an intelligent database as a base for integrating engineering data required for decommissioning projects. Environmental information, such as radioactivity, decontamination efficiency, dismantling specification, and dose rate, is allocated to appropriate component information as property data to support engineering, planning, and decommissioning projects.

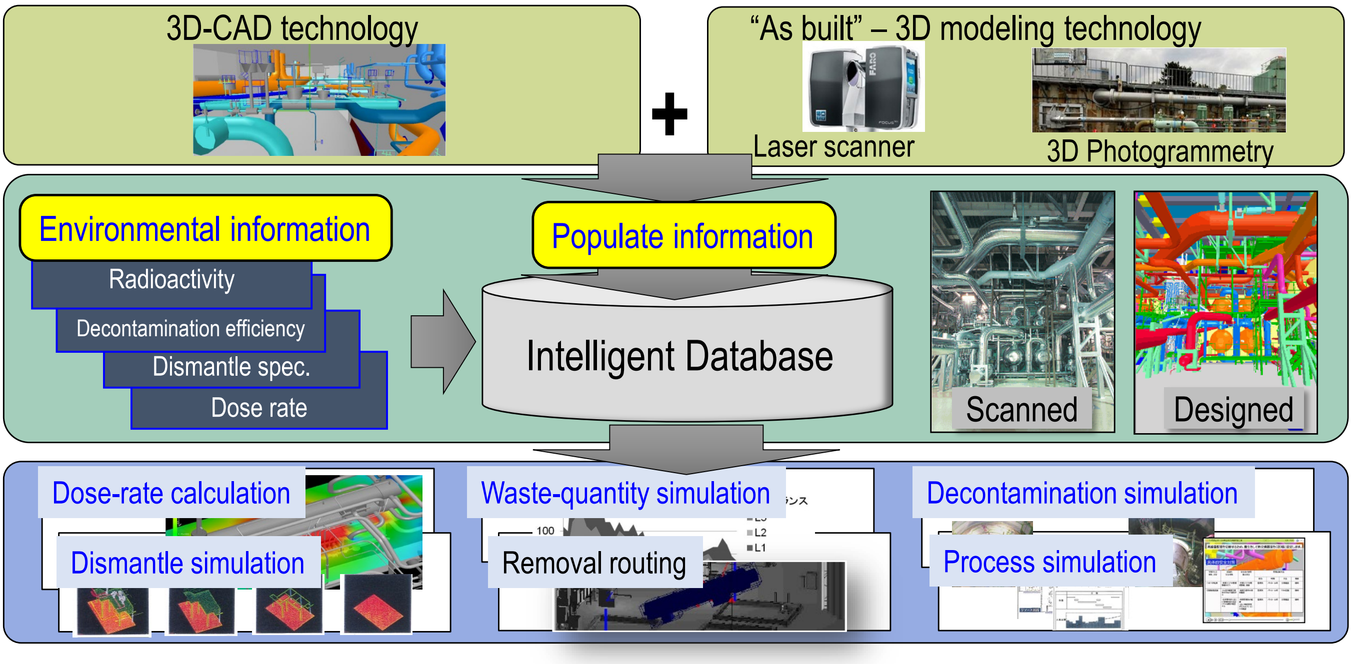

Figure 1.12 An overview of simulation technologies for decommissioning projects [42].

1.3.3 Detailed planning of decommissioning nuclear power plants

In the decommissioning phase, the last stage of the NPP lifecycle, a dismantling simulation and planning for the decommissioning project under a radiation environment, has been supported by virtual reality visualization methods (VR). The developed system was called the developed system VRDOSE [43]. Similar methods calculate the 3D spatial distribution of dose rates based on the number of nuclides as radiation sources, their distribution, geometric shapes of the dismantling work environment, and material information of piping components and equipment [44]–[46]. Moreover, the dismantling and cutting simulation for piping components and equipment has been developed in a virtual environment [47].

Compliance with the waste hierarchy defined by the European waste framework is a critical concept to minimize costs and impacts on the environment, as shown in Figure 1.13 [48]. As shown in the figure, a top priority is given to preventing waste generation in the first place. When waste is created, priority is given to re-use, recycling, recovery, and disposal. Moving up the hierarchy saves waste producers money, minimizes raw material consumption, saves waste disposal capacity, enables early solutions to be identified and delivered, and reduces overall environmental impact.

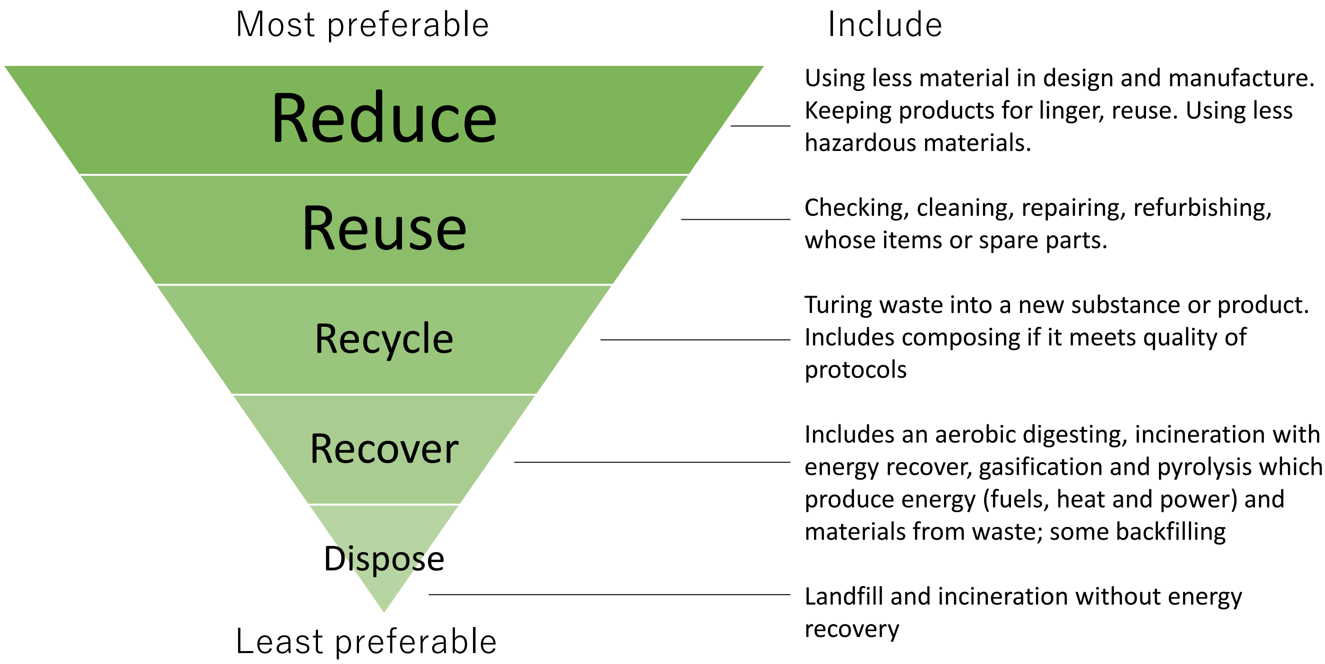

Figure 1.13 The waste hierarchy.

1.3.4 Supporting technologies for remotely operated robots in nuclear power plants

Dismantling should be done with remotely operated robots to avoid excessive occupational exposure doses in reactor internals or damaged NPPs. We should remove radioactive waste safely and economically during dismantling work. The percentage of radioactive waste is 3.6 % for the commercial NPPs and enormous volumes for the accident plant [49]. From the estimated costs of the decommissioning for NPPs, substantial portions of the fee are for activities of cutting and dismantling [50]. The developed system has visualized the dose rates calculated with a virtual reality (VR) environment under high dose rates in an NPP [51]. The most challenging robot operation is entirely operated remotely in the Primary Containment Vessel (PCV) and Reactor Pressure Vessel (RPV), which humans cannot access. The resistance of high dose rate radiation is another issue for the robot hardware. We can use water pressure-controlled robots to resist high dose rate radiation. If the robot is controlled by water pressure, we can remove the electric parts from the robot. Thus, the robots can resist high dose rates [52]. Similar soft robots are investigated and analyzed as multiple axis arms or manipulators with redundant structures [53].

Some agent-based robotic systems have been developed in the UK for sorting, segregating, and disrupting waste materials [54]. The systems were highly automated and helped with less human supervision. The proposed method has been demonstrated with a small-scale robotic arm, a time-of-flight camera, and a high-level rational agent-based decision-making and control framework.

As for using digital twins, feasibilities for some scenarios of complex tasks in a decommissioning project have been studied with improved 3D modeling and thermal and radiation images [55].

1.4 The Objectives

This research aims to generate and manage waste quantities, dismantling planning, and related engineering documents needed in a decommissioning project based on an integrated model for piping components and equipment installed in a nuclear power plant. Especially for accident plants, such as Fukushima Daiichi Nuclear Power Station, the research object is developing the method to reflect the detailed task sequences of remotely operated robots and resulting from work into preplanning schedule with environmental 3D models generated from measured point cloud data.

The objectives of this research for the conventional decommissioning of NPPs are developing technologies for estimating waste quantities and planning to dismantle against various scenarios automatically based on an integrated model for piping components and equipment.

Another objective of this research for the accident NPP was to develop technologies for reflecting the preplanned schedule based on detailed work sequences and estimated work hours for remotely operated robots in an environment 3D model made from measured point cloud data.

Technical issues for maintaining consistencies for engineering attributes, estimating detailed waste quantities and work hours, and utilizing a 3D CAD model for generating valid remote operation sequences are considered to realize these objectives. As for the verification and validation of the developed technologies, calculation methods of an appropriate number of waste containers for dismantling inside one room surrounded by reinforced concrete structures have been confirmed. The goal of this research has been set to estimate work durations per minute. Details of objectives are described in the following sections respectively.

1.4.1 Drawing Data Refining System According to Plant Product Life Cycle)

The methods for associating engineering data have been developed for a plant lifecycle which consists of construction and inspection based on standard model expression from related 2D drawings and 3D models. This research aims to update and check consistencies for a 2D drawing of piping and instrumentation (P&ID) drawing concurrently based on the association of data used in various phases of the plant lifecycle.

1.4.2 Evaluation System of Waste Quantities for Decommissioning Planning of Nuclear Power Plants

As for evaluating waste quantities for the decommission of NPPs, radioactive inventory for amounts of contamination per radioactive nuclides is mapped to piping components and equipment, and dose rates for a surrounding environment are calculated. Then the waste container models have generated automatically. This research aims to estimate waste quantities for the decommissioning work based on generated models and calculated carrying-out paths for large equipment and waste containers.

1.4.3 Evaluating Precise Quantity of Decommissioning Waste by Cutting Virtual 3D Models of Large Equipment

This research aims to develop methods for planning by virtual cutting procedures with 3D equipment models that have upper limitations for sizes of waste containers, weights, radioactivity, and surface dose rate. This research uses multiple cutting procedures with cutting sequences based on numerous dismantling scenarios. The cutting sequence data generates cut objects automatically and calculates occupational exposure dose during dismantling work.

1.4.4 Real-Time Simulation Methods for Robots with Flexible Arms Based on Computer Graphics Technology

This research aims to calculate moving durations for robots controlled by water pressure to plan complicated dismantling processes. Virtual controllers based on spline inverse kinematics (IK) with NURBS curves are introduced to simplify the robots with arms controlled by water pressure.

1.5 The research processes

1.5.1 Drawing data refining system according to a plant lifecycle

A technology for engineering data management has been developed to realize data integrations and exchanges for the NPP lifecycle. In this research, translators and viewers for CAD data used to exchange and share attributes for 2D drawing and 3D models based on a standard information model have been built. A system updates process and instrumentation drawings continuously have been constructed and verified [56]. This development discusses methods to maintain consistency between design data and actual project data in this dissertation.

1.5.2 The evaluation system of waste quantities for decommissioning planning of nuclear power plants

Based on the integrated 3D model for NPPs, a prototype system has been developed to support the engineering processes for decommissioning projects of NPPs. It is essential for plant owners and engineering companies to estimate durations and costs by evaluating waste quantities for radioactive or contaminated piping components and equipment and evaluating levels of difficulties for dismantling activities based on the circumstance dose rates around piping components and equipment. Calculating work hours and paths for carrying large equipment and waste containers from originally installed positions to temporary storage locations or an exit port is also necessary. The developed method has mapped radioactive inventory information to 3D objects of piping components and equipment of the decommissioning NPP. The dose rate for the surrounding area has been calculated, and models for packed waste containers have been generated automatically. Functions to calculate carrying-out paths for large equipment and waste containers with generated data have also been developed to evaluate the accumulated occupational dose. The results have shown that we can efficiently and effectively apply the developed methods to the decommissioning engineering processes [57].

1.5.3 Evaluating the precise quantity of decommissioning waste by cutting virtual 3D models of large equipment

In addition to cutting, radioactive and contaminated waste fragments should be stored to waste containers. Human workers should avoid excessive exposure to radiation in the dismantling environment. The number of containers required to keep waste fragments by cutting piping components and equipment should be minimum to suppress the decommissioning cost. In this research, automatic planning methods have been developed for cutting 3D models of equipment with constraints of sizes of containers, weights of waste, accumulation of radioactivity, and dose rate [58]. Cutting procedures, consisting of cutting sequences based on multiple dismantling scenarios, have been formulated to evaluate the developed method. The cutting sequences have been used for generating cut objects and calculating occupational exposure dose during dismantling work. Required cutting length and dose rate distributions have been calculated so that the developed system is adequate for planning the decommissioning. Both weights and volumes are estimated to enable traceability for radioactive waste to decommission an NPP. To allow traceability, we should identify specific equipment before cutting from the 3D models of cut waste fragments. The number of pieces with volumes and the required number of waste containers are calculated here. Moreover, the method for cutting 3D equipment objects with constraints has been developed to evaluate the occupational dose and the total quantities of waste. The cut sequence data is used to formulate different cutting workflows, generate cut geometric objectives, and calculate occupational dose from disassembling durations.

1.5.4 Real-time simulation methods for robots with flexible arms based on computer graphics technology

Remote operating robots controlled by water pressure have been developed to remove highly contaminated materials at the decommissioning project for the accident NPPs. This research aims to improve the accuracy of the estimated duration of dismantling and a method for supporting work planning by generating work sequences of robots, keeping recoveries from delaying the dismantling work, and judging feasibilities of dismantling processes from an ample searching space. Since flexible arms with water pressure control have more complicated mechanisms than multiple axis arms, the robot in a virtual environment has been modeled with 3D computer graphics (CG) tools to simplify the geometric shapes and complicated relationships of constraints between objects. With the help of the 3D CG model, work sequences can be automatically generated so that planning for moving robots is done efficiently. Based on these models and methods, a prototype system has been developed to automatically calculate the robot's moving durations. The calculated work durations have been reflected in the time of a specific activity for a dismantling schedule expressed as a Gantt chart. To plan a robot movement for complicated dismantling processes, a simplified method for preparing robot movements, including a few virtual controllers, has been developed based on a spline inverse kinematics (IK) with NURBS curves for the arm consisting of pistons operated with water pressure [59].

1.6 Dissertation structure

This dissertation consists of six chapters. Chapter 1 describes the overview of this dissertation. Then Chapter 2 illustrates an integrated semantic model for plant lifecycle management that can be applied NPPs and its applicability to checking consistencies for engineering drawings among different sections. Chapter 3 studies a method that evaluates the quantity of waste for decommissioning an NPP. The procedure is verified with a whole 3D model of the NPP. In Chapter 4, an exact amount of dismantled fragments by cutting virtual 3D models of large equipment is described for examining and verifying the automatic generation of cut objects with a 3D model and its applicability for exposure dose evaluation; in Chapter 5, real-time simulation methods for robots with flexible arms based on computer graphics technology to support the planning of remote operations in a severe environment inside NPPs. Finally, in the last Chapter 6, the dissertation is concluded.

For this dissertation, the following definitions apply.

1.7 Terms, definitions, and abbreviations

1.7.1 Terms and definitions

For this dissertation, the following definitions apply.

1.7.1.1 data mining

a process of extracting and discovering patterns in large data sets involving methods at the intersection of machine learning, statistics, and database systems.

1.7.1.2 decommissioning

the process whereby a nuclear facility is dismantled to the point that it no longer requires measures for radiation protection.

1.7.1.3 metadata

the type of data that describes and provides information on the primary resource.

1.7.1.4 ontology

encompasses a representation, formal naming, and definition of the categories, properties, and relations between the concepts, data, and entities that substantiate one, many, or all domains of discourse.

1.7.1.5 plant lifecycle management

the process of managing a facility's data and information throughout its lifetime. Plant lifecycle management differs from product lifecycle management by integrating logical, physical, and technical data into a combined plant model.

1.7.1.6 provenance

chronology of the ownership, custody, or location of a historical object.

1.7.1.7 semantic data model

a high-level semantics-based database description and structuring formalism for databases.

1.7.1.8 semantic technology

defines and links data on the Web (or within an enterprise) by developing languages to express rich, self-describing data interrelations in a form that machines can process.

1.7.1.9 TECHNOINFRA

a new unique model and modeling method to describe technical information and knowledge to a semantic level.

1.7.2 Abbreviated terms

ABWR	Advanced Boiling Water Reactor
AM	Application Module
AP	Application Protocol
BWR	Boiling Water Reactor
CAD	Computer-Aided Design
CDE	Common Data Environment
CG	Computer Graphics
CII	Construction Industry Institute
CM	Configuration Management
COSMARD	Code System for Management of JPDR Decommissioning
CPS	Cyber-Physical System
DECON	Decontamination or Immediate Dismantling
DEXUS	Decommissioning Engineering Support System
DT	Digital Twin
ENTOMB	Entombment
EPISTLE	European Process Industries STEP Technical Liaison
FDNPS	Fukushima Daiichi Nuclear Power Station
FEPC	The Federation of Electric Power Companies of Japan
FIATECH	Fully Integrated Automation Technology Project
IAEA	International Atomic Energy Agency
IEC	International Electrotechnical Commission
IK	Inverse Kinematics
IMS	Intelligent Manufacturing System
IoT	Internet of Things
ISO	International Organization for Standardization
JPDR	Japan Power Demonstration Reactor

MATLAB	MATrix LABoratory, a proprietary multi-paradigm programming language and numeric computing environment developed by MathWorks
NDF	Nuclear Damage Compensation and Decommissioning Facilitation Corporation
NPP	Nuclear Power Plant
NURBS	Non-Uniform Rational B-Spline
OECD/NEA	Organisation for Economic Co-operation and Development/Nuclear Energy Agency
PCV	Primary Containment Vessel
PDWH	Plant Data WareHouse
P&ID	Piping and Instrumentation Diagram
PLM	Plant Lifecycle Model
PMBOK	Project Management Body of Knowledge
PWR	Pressurized Water Reactor
RDL	Reference Data Library
RPV	Reactor Pressure Vessel
SAFSTOR	Safe Storage
SDGs	Sustainable Development Goals
STEP	The standard for the Exchange of Product model data (ISO 10303)
TEPCO	Tokyo Electric Power Company Holdings, Incorporated
VIPNET	Virtual Enterprise Network
VR	Virtual Reality
VRDOSE	a real-time software tool for modeling and characterizing nuclear environments by the Institute for Energy Technology in Norway

2 Application of data model for a drawing data refining system according to plant lifecycles

Abstract: Engineering data warehouse has been developed to integrate and exchange data through the lifecycle of process plants. Based on a common information model, CAD data translators from 2D drawings and 3D models were built, and their browsers were also made. To adopt every task in the plant-related work with its design data, such as process and instrumentation 2D drawings, a continuous refining system for drawing data has been built. This system has considered a mechanism for maintaining consistency between actual project and design data.

Keywords: Database management systems, Data models, CAD/CAM models, Enterprise Integration

2.1 Background for an application of data model according to plant lifecycles

Product lifecycle management (PLM) technologies are attractive in many manufacturing industries, and many related products and solutions have been developed recently. Data integration and exchange are essential in this area, and much-related work is done. Especially in ISO 10303, the standard for the exchange of product model data (STEP) [60], there are different scopes and models known as application protocols (AP) if the industrial scope is different. Feeney et al. studied the integration of the APs into application modules (AM) [61]. Hardwick et al. studied and demonstrated sharing manufacturing information in a virtual enterprise environment [62]. Zha et al. studied data integration by dividing data levels into global and local levels [63]. Liang et al. proposed a consolidated data schema to integrate data with integrated databases [64]. They integrate and exchange component data based on the original STEP. In the Virtual Production Network (VIPNET) Project that has been in the scope of the Intelligent Manufacturing Systems (IMS) program [65], a new representation model and a markup language so that data integration and exchange can be done more easily were proposed. Significantly, the technical information infrastructure, called the TECHNOINFRA, was established. With the developed system, the effectiveness of TECHNOINFRA was verified and validated using actual process plant data [66]. This PLM system makes smooth data handover between different plant life cycles essential for construction companies and plant owners due to their efficient business [1]. Only design engineers could refine the 2D schematic drawing and 3D geometric data in former design tools incorporated with PLM systems. Ideally, every user, such as a design engineer, construction engineer, and maintenance engineer, should refine the original design data, and recreation of redundant data should be avoided.

The cost for processing data through the life cycles of process plants has been increasing exponentially for large capital investments. These facts are one of the motivations for standardization, such as the ISO 15926 series. For instance, Shell, one of the supermajors in the oil and gas industries, estimates the number of documents is about 30,000. The number of tags used for identifying objects or activities was about 60,000 for the LNG project in Nigeria in 1996 [67]. However, the number of documents and tags has increased to several million in Kashagan Phase II Project in 2013. Human engineers cannot manage consistency between this massive volume of documents and tags. Therefore, the cost of operation for documents and tags is exponentially increased without IT systems [68].

Satisfying the reusability of data with high quality and precision is beneficial to the economy and the safety of operating extensive capital facilities of social and life infrastructures. It is also an essential condition for us to realize a sustainable society. For instance, linked to social problems such as many fatal disasters and environmental pollution caused in the past. One of the causes of accidents and disasters is caused by "data mismatches." Its symbolic accident in the oil and gas industry is the explosion of the offshore platform "Piper Alpha," the worst accident in the history of offshore oil fields [69]. The 1988 North Sea oil field accident killed 167 employees and caused severe environmental pollution. Today, the need to match real-world "data" with real-world "things" such as IoT, Cyber-Physical Systems (CPS), and Digital Twin (DT) has been internationally understood [70]. It is also an international agreement, such as Configuration Management (CM), a requirement in the nuclear industry [71]. CM requires that requirements, documents, and assets be closely aligned throughout its lifecycle. Similar ideas are beginning to be recognized in many other industrial sectors. Similar ideas are starting to be recognized in many different industrial sectors. At the core of this is the idea that dictionaries and rules for "matching data with those" are essential requirements for the proper operation of assets and, consequently, the sustainability of society. This is a requirement to support the SDGs as a framework for the entire world.

In section 2.2 of this paper, the TECHNOINFRA, which realizes the data integration framework, its implementation, and some application results, is described first. Problems of current work processes for data handover between different product life cycle phases are described. Section 2.3 is an effective measure for continuous usage of original 2D drawings as the center of engineering knowledge, such as a drawing data refining system. Sections 2.4 and 2.5 review the results of the developed system, and its conclusions are discussed.

2.2 IMS/VIPNET project and its results

2.2.1 TECHNOINFRA in IMS/VIPNET project

IMS/VIPNET project has been done for almost five years since 2000 as a Japanese domestic project. This project is designed to develop a TECHNOINFRA incorporating a new unique model and modeling method to describe technical information and knowledge to a semantic level to overcome the shortcomings commonly found among the conventional information sharing systems. In 2005, the VIPNET project was endorsed as an international project by the International IMS Steering Committee. The international VIPNET project comprises 12 organizations in four regions: Canada, Japan, South Korea, and Switzerland.

2.2.2 Objectives of the VIPNET Project

The objectives of this project are efficient integration and reuse of data over the exceptionally long range of product lifecycles. Eventually, we must keep tracking the history of components and storing their data over 100 years for a nuclear power plant. We have developed TECHNOINFRA composed of four layers based on these objectives, as shown in Figure 2.1.

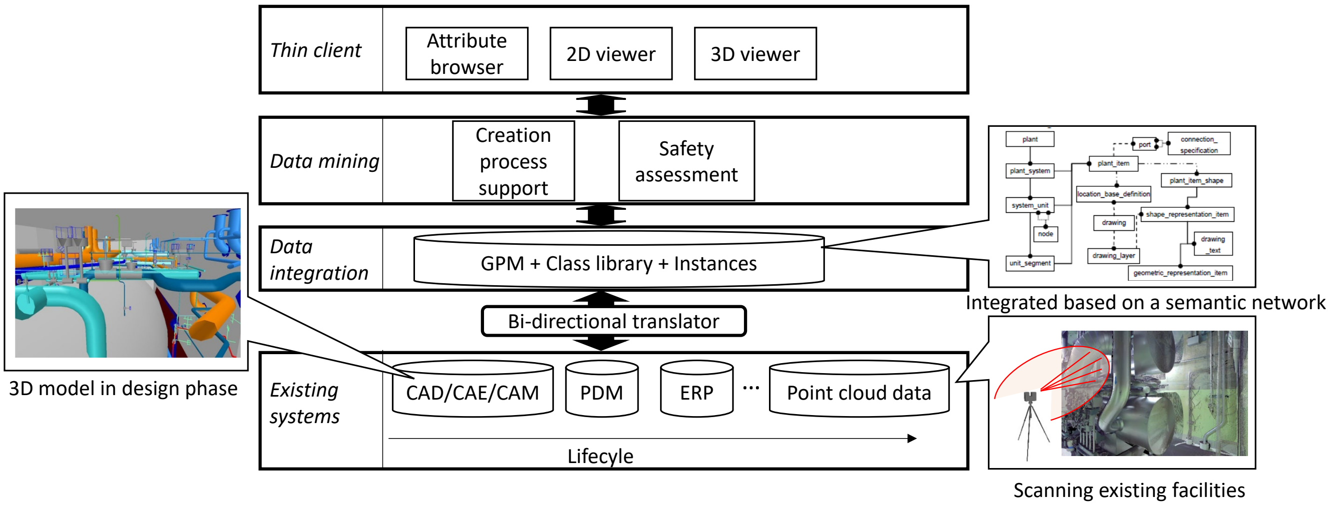

Figure 2.1 System configuration of TECHNOINFRA.

The layers are the followings: the layer for connecting between legacy existing systems and an integrated plant data warehouse (PDWH) systems (layer 1) to manage vast volumes of complex data; the data integration layer with a data integration network model, called a generic product model (GPM) [9], [10] [60], [72] (layer 2); the data mining layer (layer 3); and the user presentation layer with thin client viewers based on Java programs (browsers for attributes, documents and 2D / 3D information via the Internet or Intranet) (layer 4). With the help of translators and thin client viewers, the engineering data, such as CAD/CAE/CAM, PDM, ERP, and so on, can be translated and integrated under the 2D and 3D geometric representation. Furthermore, stored data in PDWH can be utilized for application technologies, such as data mining, safety assessments, and environmental impact assessments. The stored 2D / 3D CAD and engineering data can easily be viewed with the Web browser. Therefore, TECHNOINFRA provides an open environment for users and bi-directional translation capabilities for legacy systems as a connecting and data reusing mechanism.

Many objects, such as piping components, HVAC ducts, and cable trays, are connected to many components for long distances. Each terminal point of the components is connected to the nozzles of equipment or electrical terminals. The designed 3D model is used for analyzing earthquake resistivity, procuring equipment, controlling welding points, planning a decommissioning project, and so on. To perform the engineering work mentioned above efficiently, the connection information between parts is essential. Therefore, this kind of connection can be managed by a semantic network inherently realized by GPM. If the designated NPP is too old and there is no 3D model for it, we need to scan the existing facility with laser scanners or photogrammetry to acquire the point cloud data, which is the base of the 3D model. Once point cloud data is acquired, it can be a base of an as-built 3D model, and the geometric shapes can be decomposed to plant items for plant engineering. After integrating the decomposed plant items based on a semantic network model, those plant items are reused within applications in the data mining layer and the thin client layer. This kind of research has been done since the 1970s and reviewed recently in the context of realizing digital twins and a digital ecosystem to integrate and reuse data efficiently.

2.2.3 Generic product model (GPM)

Information modeling technologies are required for systematic description on a computer to accumulate, share, utilize, and create them. We defined a data expression model, generic product model (GPM), and description formats that are not dependent on a particular software, hardware, or other systems. Figure 2.2 shows the concept of data integration with the GPM. This model consists of essential elements extracted from various data structures, such as objects and associations. In all its complexity, the GPM attempts to describe the real world by combining these essential elements with the object-association network model. The GPM is like a verb-focused semantic network model; one of its most critical features is that it can also accept natural language syntaxes, such as a subject, verb, and object or predicate sentence order. Objects are connected via associations in the essential GPM expression, called a GPM core model. This core model came from the EPISTLE core model [73], but we modified the original model so that multiple relationships can be written to make data expression concise [74].

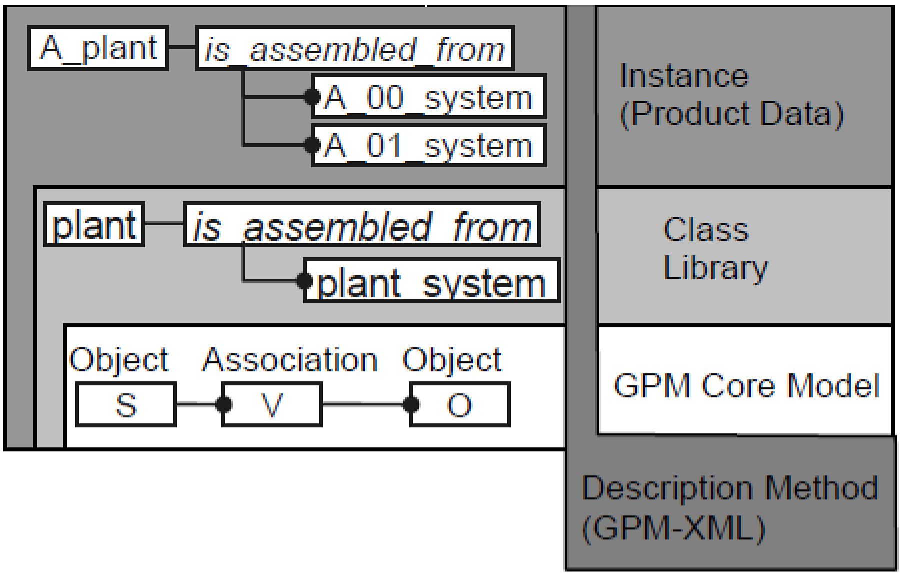

Figure 2.2 Data integration with GPM

Class connectivity with other classes is defined in the class library. However, the primary class combinations in the process plant area should be shown. Figure 2.3 shows the essential GPM class combination for the plant_item class. Plant_item is the class corresponding to things in the real world. Plant, plant_system, system_unit, and unit_segment classes are connected to the plant_item class via "*is_assembled_from*" associations, and this group constructs stratified logical connectivity for plant data elements. Namely, these classes are used for tree-like information about a particular plant.

Based on this core model, plant system configurations, classifications, and so on are described as connections of classes, such as "plant *is_assembled_from* plant_system." In this case, "plant" and "plant_system" are classes and "*is_assembled_from*" is an association. Such class definitions are aggregated as a class library and used as the actual plant data description dictionary.

Actual plant product data defined by CAD systems or other engineering systems are treated as instances, such as "A_plant *is_assembled_from* A_00_system and A_01_system". From these expressions, instance configurations and their belonging classes could be easily found and integrated systems using semantic information governed by the GPM core model and the class library. The class library is used for the validation of instance data configuration.

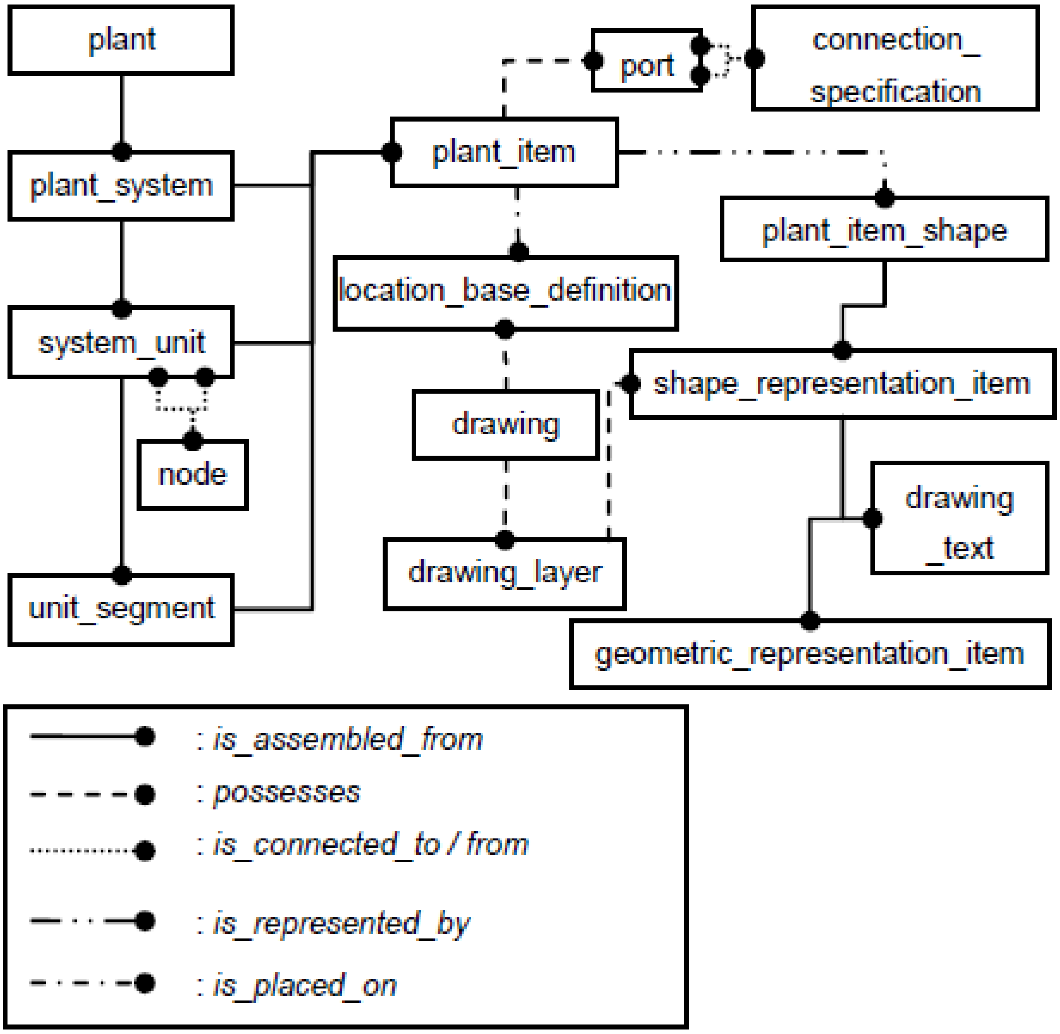

Figure 2.3 **Basic GPM class combination.**

2D and 3D geometric shapes are expressed by plant_item_shape, shape_representaion_item, and geometric_representation_item classes. Geometric_representation_item classes correspond to basic primitive shapes, such as solid, wireframe, and surface elements, which cannot be further divided. Therefore, shapes for plant products are decomposed to geometric primitives and stored in the database in the form of geometric primitive granularity. Shape_representation_item is the class that expresses a group of basic geometric primitives (geometric_representation_item). Plant_item_shape is the class that represents a group of items (shape_representation_item), and this class corresponds to the shape of a specific plant_item, and plant_item is connected to "plant_item_shape" via the "*is_represented_by*" association.

Connecting terminals for a certain plant_item is expressed by port classes. The port expression is like functional and physical connectivity in the related work. A port instance for a plant_item instance is connected to the other port for another plant_item. For example, a port for a straight pipe is connected to a port for a specific valve with "*is_connected_to*" or "*is_connected_from*" associations via a connection_specification class. The connection_specification is the class that expresses a connection type, such as butt-welded, socket-welded, etc.

Placement locations and directions for the plant_item instances are expressed by a location_base_definition class "with "*is_placed_on*" associations. For 2D drawings, such as a process and instrumentation diagram (P&ID), drawing and drawing_layer classes are prepared. A drawing instance also includes location_base_definition instances with "possesses" associations.

Thus, with the help of the basic GPM class configuration, we can express logical combinations of plant parts, shapes, connectivity, locations, and drawings as an integrated data model. Based on these concepts, about 3000 classes are defined as the class library for data handling of actual nuclear power plants. The tools check those class consistencies, which find errors from looped inheritances, assemblies, etc.

2.2.4 Current work processes and bottleneck

Recently, the design of the process plant has been done using 2D and 3D CAD systems for long years. These CAD systems generate a visualized image of things and add some engineering features as attributes. With the help of TECHNOINFRA, product primitive data, such as plant_item instances, is stored in the engineering data warehouse, including whole-part relations in plant systems, location information, connection information, geometry, etc. As engineering data in a process design phase, 2D and 3D data are integrated into the engineering data warehouse that uses the GPM class library as a plant semantic model. Related information on the procurement process, project control for the construction, and so on can also be stored in this data warehouse.

Usually, the unit of work processes in the different lifecycle of plants, such as between design and construction, are additional. Therefore, the granularity of drawing data should be changed according to the plant life cycle. However, such data refining has never been done within the information system. Inspection or maintenance workers write their markup or annotations on the printed-out sheet to use previous design results. Or they write such annotations on image data using simple drawing application programs. However, this work performance will be drastically improved if data handover is done smoothly.

With the features of TECHNOINFRA, the system uses Web-based Java technology and the GPM, which is especially effective for the integration of plant data semantically. Namely, engineering data created in the previous phase can be handed over smoothly and effectively to the next plant life cycle phase.

Specifically, process and instrumentation drawings are used as original data. Then the data is copied to other layers of the drawing. The piping components are divided by separator symbols. The separated piping components can be mapped to other related drawings, inspection results, and testing conditions for quality assurances. And the 3D spatial model can be shown by a 3D viewer corresponding to the area in the 2D viewer. Furthermore, data transfer from the GPM data warehouse to legacy systems or gathering actual process results to the GPM data warehouse can be done by dividing functionality for piping components. The system with this functionality is called a drawing data refining system.

2.3 Drawing data refining system

2.3.1 System configuration

As mentioned in the introduction, the TECHNOINFRA has already been developed for a data integration system using a GPM-based data warehouse, as shown in Figure 2.4.

The capability of TECHNOINFRA is verified using 2D CAD data, such as process and instrumentation drawings, and 3D CAD data, such as 3D spatial configuration model data in a process plant design. These 2D and 3D data are integrated into the engineering data warehouse with the help of GPM. The visualized data can be shown by a 2D, 3D browser delivered to client PCs by the Java Web Start mechanism via the intranet. Documents and estimation of piping component materials can also be mapped to piping instance data and managed in the data warehouse.

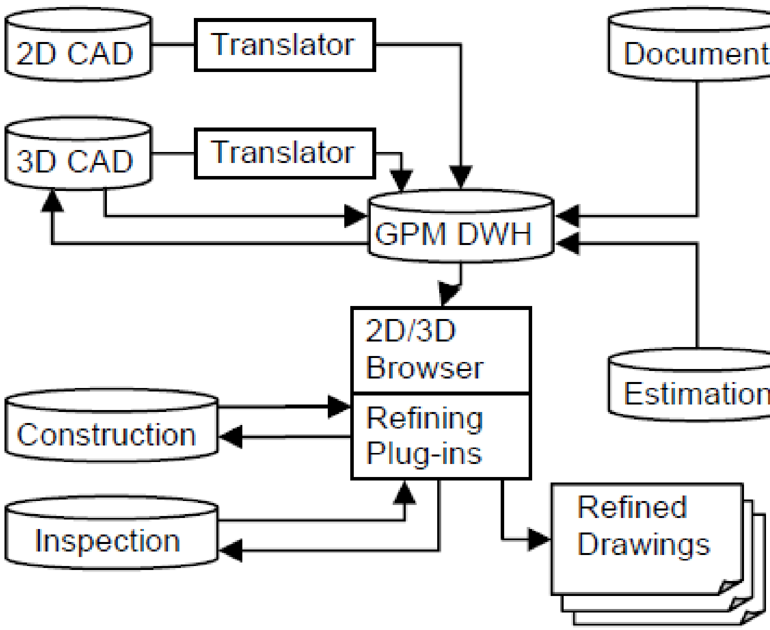

Figure 2.4 System configuration

A plug-in for the drawing refining system was added to use this system for handing over the data between different plant life cycles. With this addition, the design data, such as P&ID, which was made in the previous design phase, can be used effectively and efficiently in successive steps, such as making construction plans or startup experiment phases. In such consecutive phases, each progress of the work phase can also be stored in the same engineering data warehouse via a newly added plug-in.

2.3.2 Methods for dividing piping components

This section explains methods to make drawing data using the previously mentioned drawing data refining system. As shown in Figure 2.5, layer copying from original drawing data is used for creating another drawing data for each objective of different work phases in the plant lifecycle.

The newly created drawing data will be the work planning data for the maximum pressure testing on some piping lines and mapping drawings to the installation drawing data. The original drawing layer becomes reference managed layers in the copied drawing data. Then some specific purpose layers are added to each managed layer. These specific purpose layers are layers for separators, reference drawings, and special symbols. The layer for the reference drawing is copied from the parent-managed layer. The layer for the separators is used for the division of piping lines, and the layer for the special symbols is used for the newly added symbols which users want to add for their purposes. The layers of separators, reference drawings, and special symbols are created to use the drawing data for different purposes and workflow steps. Newly added attributes used in specific work phases are gathered in table form. Then this table form object can be treated as an additional table on the newly made refined drawing data so that users can visually understand the unique conditions in some work steps on the drawing.

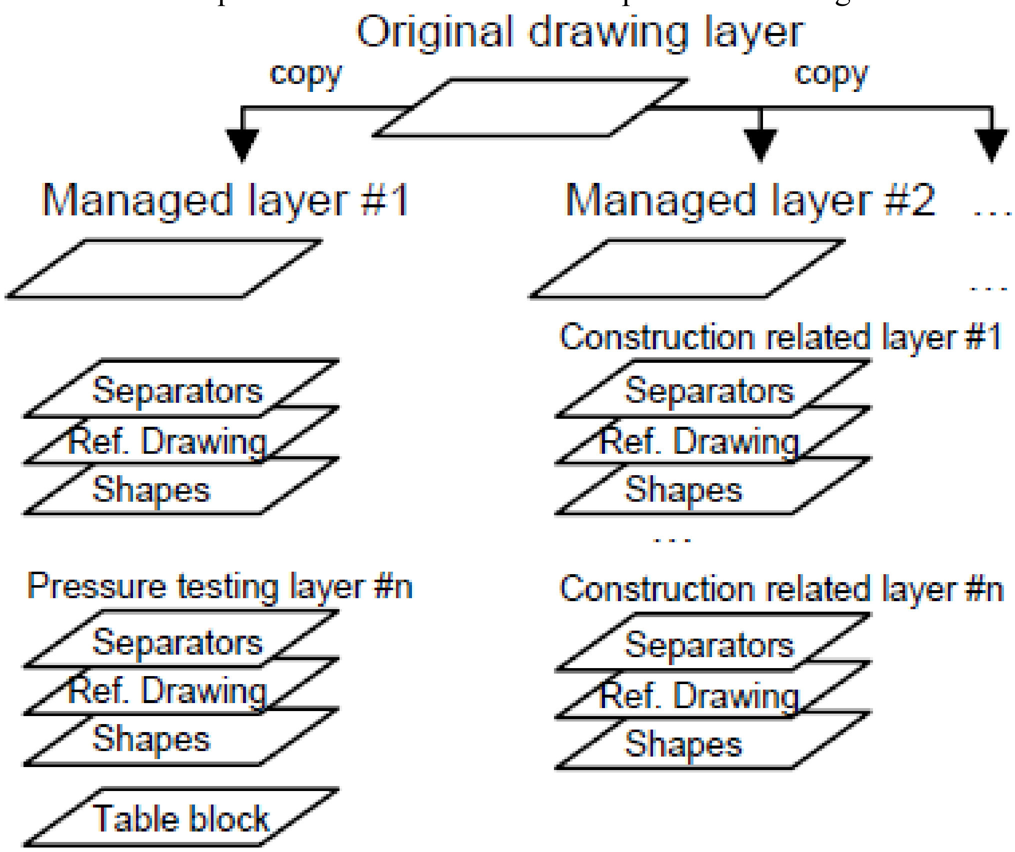

Figure 2.5 Layer copying from original drawing data.

To explain dividing piping lines, using separators and related information are shown in Figure 2.6. As an original line state, a piping line named an instance N_1 is surrounded by two valves composed of three straight lines, E_1, E_2, and E_3, as shown in Figure 2.6 (a).

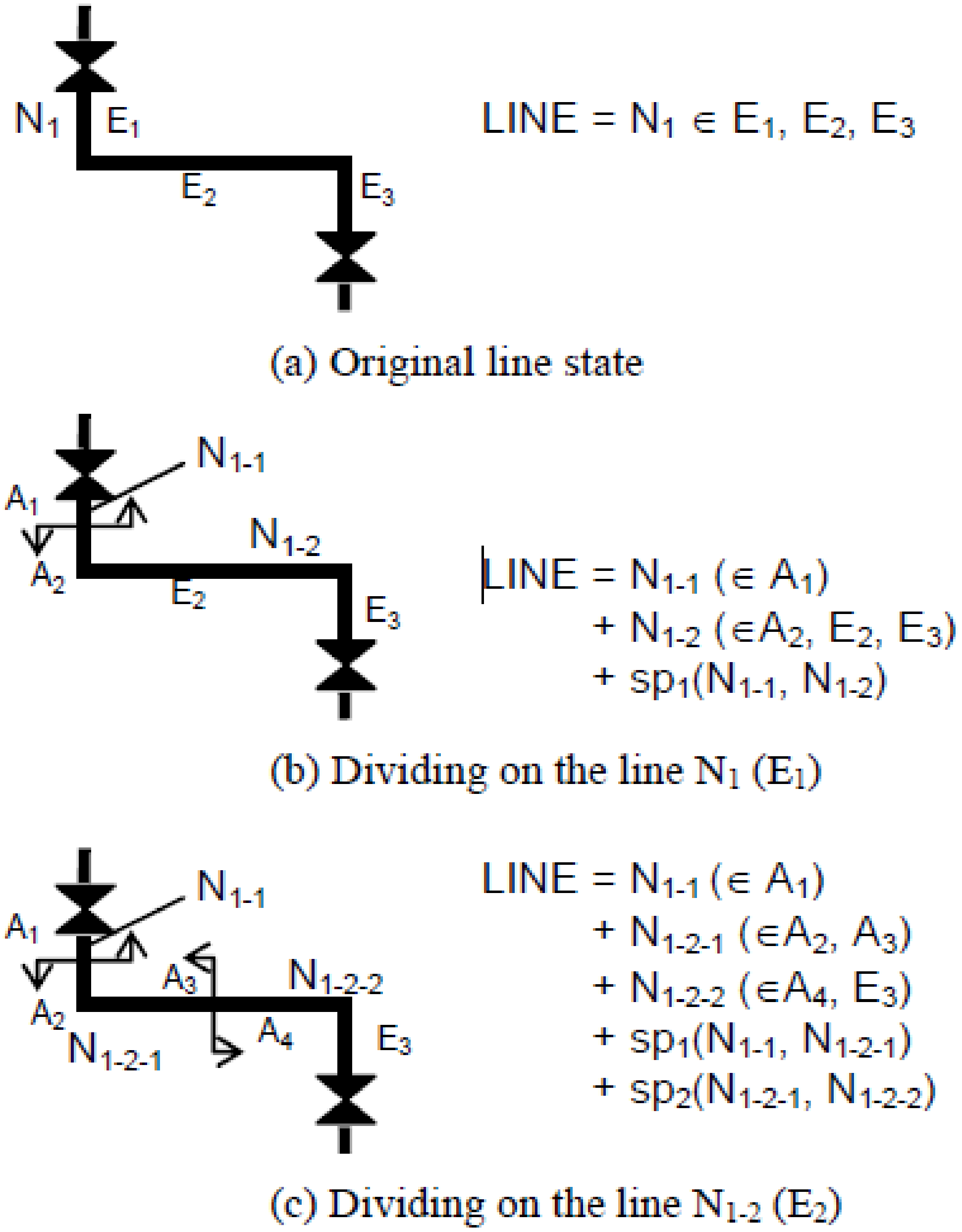

Figure 2.6 Methods for dividing lines.

The instance N_1 corresponds to the plant_item class, and E_1, E_2, and E_3 correspond to geometric_representation_item in GPM classes, and these are used for plant component and shape recognition. In this figure, let us consider that E_1 is divided into two straight lines, such as A_1 and A_2 at sp_1. Then the created two lines, A_1 and (A_2, E_2 and E_3), are named as instances N_{1-1} and N_{1-2}, respectively. The sp_1 is also denoted as sp_1 (N_{1-1}, N_{1-2}) because two-line instances, N_{1-1} and N_{1-2}, share the separation point. In the following case, N_{1-2} is divided into two lines on line E_2. The piping instance N_{1-2} becomes N_{1-2-1} and N_{1-2-2} because the instance is split into two piping instances. The divided piping lines, N_{1-2-1} and N_{1-2-2} are composed of (A_2, A_3) and (A_4, E_3). The separation point of these two piping lines is sp_2 (N_{1-2-1}, N_{1-2-2}) on the line of E_2, which N_{1-2-1} and N_{1-2-2} share.

Figure 2.7 shows a recovering method for already divided piping lines. This figure shows the case of a withdrawal of the separation point sp_2. At this separation point, the included piping line instances, such as $N_{1\text{-}2\text{-}1}$ and $N_{1\text{-}2\text{-}2}$, can be acquired, and these lines are recognized as merging lines. Then the recovered merging line becomes $N_{1\text{-}2\text{-}1}$ from $N_{1\text{-}2\text{-}1}$ and $N_{1\text{-}2\text{-}2}$. The line shapes for $N_{1\text{-}2\text{-}1}$ are A_2, A_3, A_4, and E_3. The composition of line shapes and the line instance differ from the previous one. However, the visualized line shapes and meaningful instances are like these methods. The drawing data refining system must recover identical piping instances visually and semantically without a naming method. These methods for dividing and recovering piping lines depend on one previous state, so the methods do not require massive memory like stack memory allocation. This method can reverse the split lines to the original lines on the drawing.

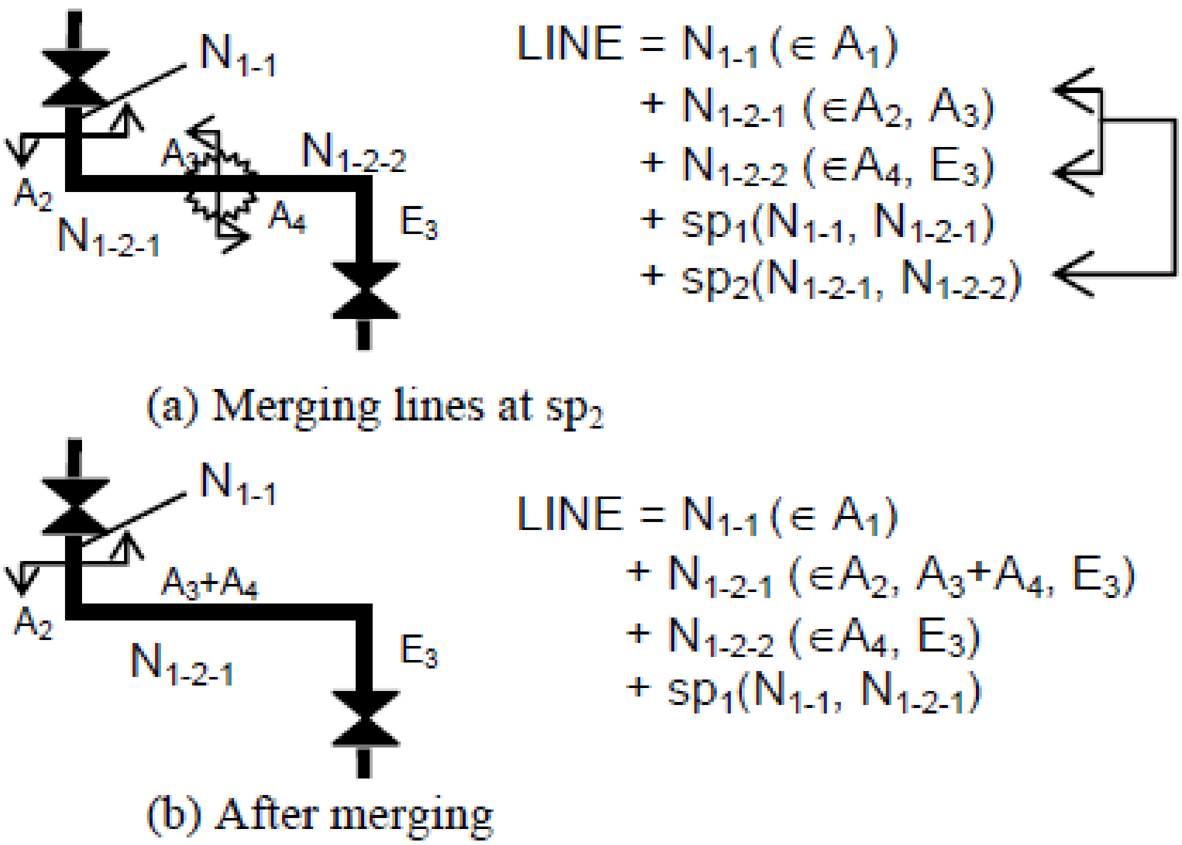

Figure 2.7 Methods for recovering the previous history.

2.4 Reviewed results

2.4.1 Created drawings from the original piping and instrumentation diagram

An example of dividing piping lines for related installation drawings is shown in Figure 2.8. This drawing is created on the piping and instrumentation drawing (P&ID), which was made at the initial design phase in the plant life cycle. Then, in the plant construction phase, installation drawings are made from 3D design data and previous knowledge about the inevitable plant construction drawings. To be consistent or acquire seamless knowledge from design data to construction knowledge, the connectivity between P&ID and installation drawings is essential for users. In this system, the separators are placed on the piping lines so that the names of corresponding installation drawings are attached with arrows, such as 'RHR-2.06-H-009' and 'RHR-13.0H-005', and so on. The lines divided with separators can have specific colors to emphasize correspondence zones.

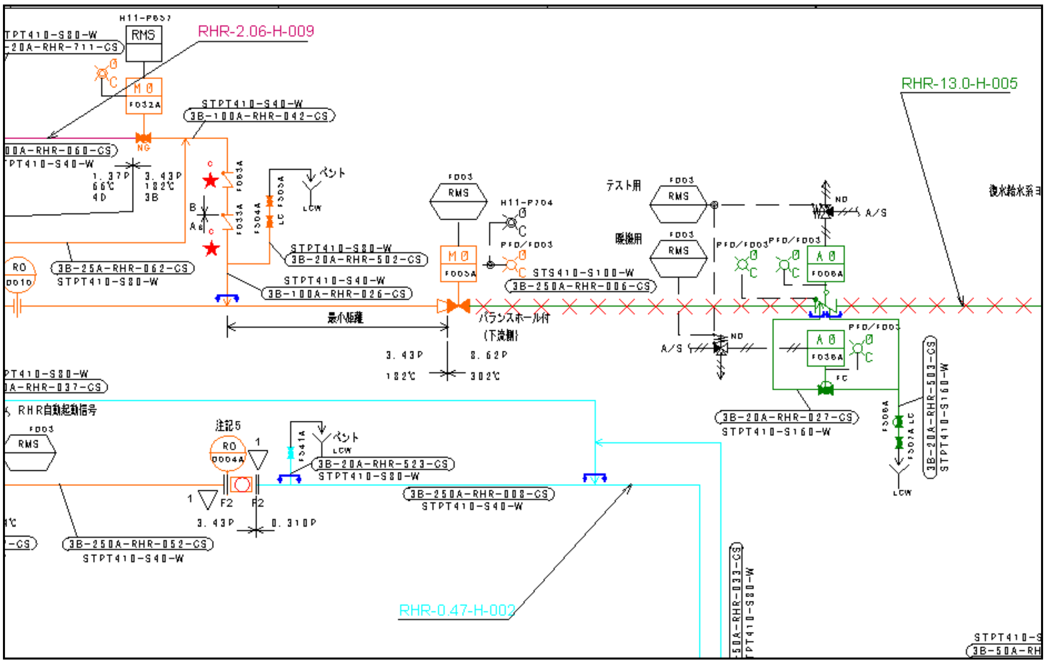

Figure 2.8 Example of dividing piping lines for related installation drawings.

Figure 2.9 shows an image of the drawing data refining system. Layer copy buttons are used to copy layers from the original P&ID or already made the refined drawing. With these buttons, users can create their refined drawings and share the drawings with the help of drawing data delivery mechanisms via networks. Users can freely place the separated lines on the copied drawing layer and put their relevance to pressure testing conditions for specific piping lines. Using the same manner, related names of installation drawings in the construction phase and associated work areas in the startup testing phase. In this system, relevance to other data about P&ID can be placed by dividing the piping lines and showing a summarized table form. This table form is automatically generated from the divided lines with related information.

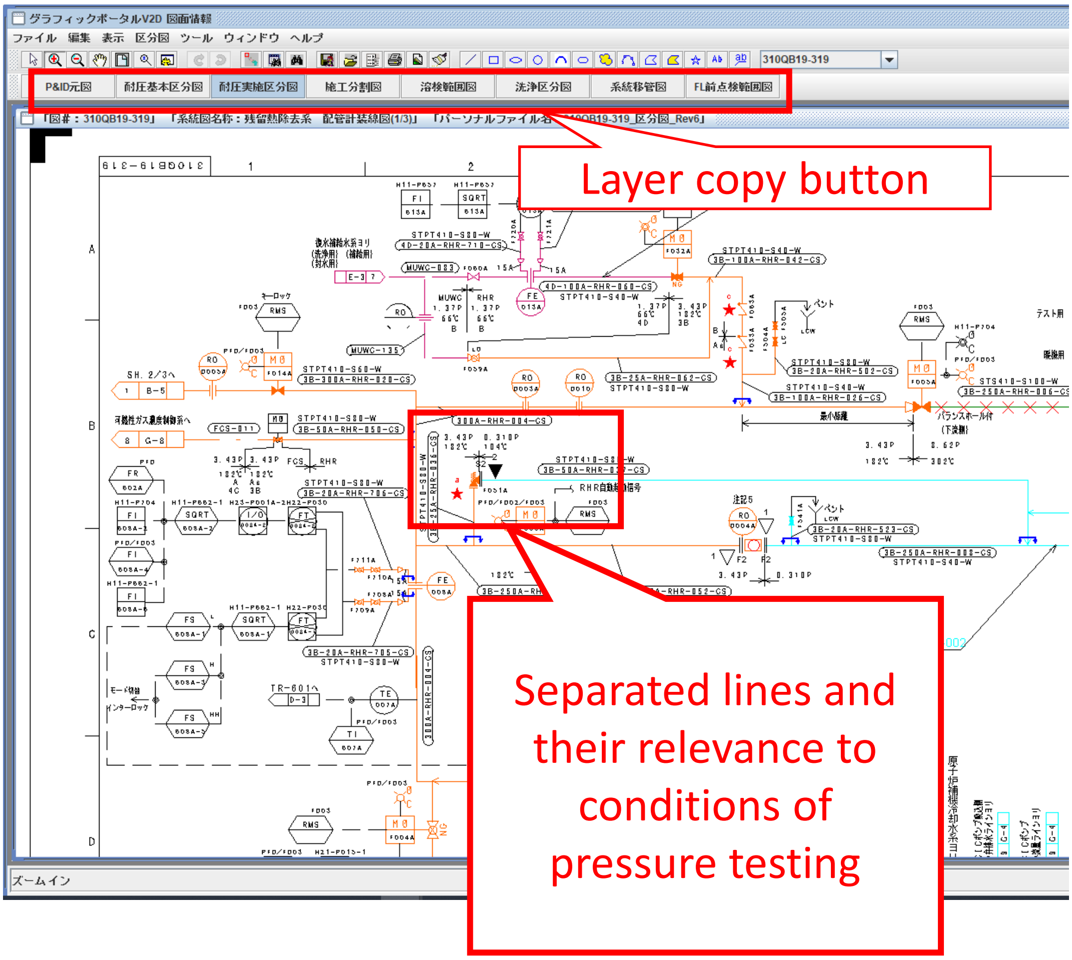

Figure 2.9 An image of a drawing data refining system.

2.4.2 Achieved functions

With the help of this drawing data refining system, it has achieved efficient drawing systems for related plant design information and effective connections of data among different plant life cycles. By sharing refined drawing data in each phase of the plant lifecycle, such as design, construction, quality assurance, and maintenance, the once-created design data can be reused and maintained correctly by each section. However, only the design section can modify drawing data in the former system. By picking up the construction status or status of testing progress from related database management systems, users can easily understand the work progress connected with visualized design data.

Figure 2.10 shows achieved function comparisons about drawing data refining based on the systematic questions to engineers. The evaluated results are for the in-house CAD, a previous client-server system, and the system built based on the TECHNOINFRA. The efficiency scale is from normalized qualitative evaluation. The connectivity of the newly developed drawing data refining system to other legacy systems, such as a document management system and engineering data management system, is superior to other systems. Reflection of the status of work progress and basic drawing functions for the system is the same between the in-house CAD system and the newly built system. The reflection functions of the previous client-server system were poor because it used the original data format. Compared with the previous system, the newly developed method can reflect the status quickly because it uses standardized information based on GPM, and some translators were already made.

Basic functions for writing lines or symbols for the previous systems are not so different because engineers are eager to use their accustomed design tools. Therefore, the usability of newly developed tools and more flexible collaboration between the legacy system and the developed system should be considered and developed.

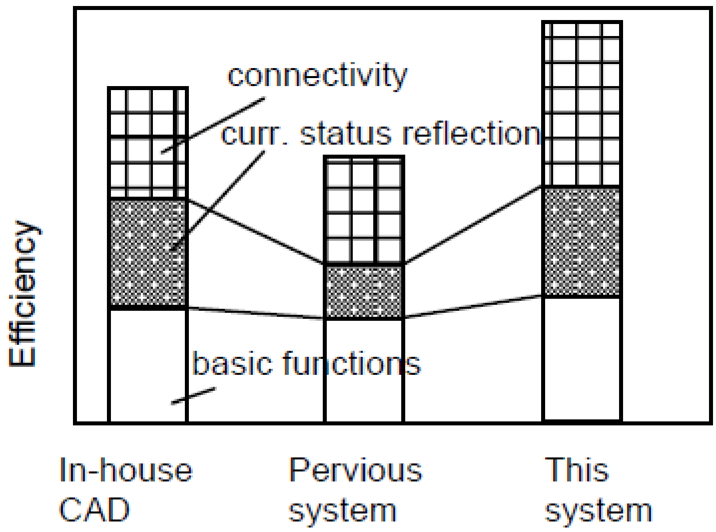

Figure 2.10 Achieved functions.

2.5 Conclusion for an application of data model according to plant lifecycles

A drawing data refining system was developed based on the technical information infrastructure (TECHNOINFRA) formed in the IMS/VIPNET project. Based on a common information model, CAD data translators from 2D drawings and 3D models were built, and their browsers were also made. A continuous drawing data refining system has been constructed to adopt every task in the plant-related work with its design data, such as process and instrumentation 2D drawings. This system verified and validated data consistency between actual project and design data. This drawing data refining system uses efficient mechanisms for piping lines with less memory. In evaluating this system, the efficiency and effectiveness of the achieved functions were shown.

In the international VIPNET project, we have developed a TECHNOINFRA incorporating a new unique model and modeling method to describe technological information and knowledge to a semantic level to overcome the shortcomings commonly found among the conventional information sharing systems. Eventually, we must keep tracking the history of components and storing their data over 100 years for a nuclear power plant. Therefore, TECHNOINFRA provides an open environment for users and bi-directional translation capabilities for legacy systems as a connecting and data reusing mechanism.

As for TECHNOINFRA, we defined a data expression model, generic product model (GPM), and description formats that are not dependent on a particular software, hardware, or other systems. In all its complexity, the GPM attempts to describe the real world by combining these essential elements with the object-association network model. Class connectivity with other classes is defined in the class library, such as the basic GPM combination for the plant_item class. Based on these concepts, about 3000 classes are defined as the class library for data handling of actual nuclear power plants.

The design data, such as P&ID, which was made in the previous design phase, can be used effectively and efficiently in the successive step, such as making the construction plan phase or startup experiment phase. In the developed method, layer copying from original drawing data is used for creating another drawing data for each objective of different work phases in the plant life cycle. To be consistent or acquire seamless knowledge from design data to construction knowledge, the connectivity between P&ID and installation drawings is important for users. Therefore, we have developed layer copy buttons to copy layers from the original P&ID or have already made the refined drawing. With the help of this drawing data refining system, it has achieved efficient drawing systems for related plant design information and effective connections of data among different plant life cycles. Based on the questionnaires to engineers, we have confirmed that the newly developed system can reflect the status quickly because it uses standardized information based on GPM, and some translators were already made.

As stated in 1.1 Background, a typical NPP is operated for 40 years or more, and the duration of decommissioning the NPP takes 30 years more. Therefore, this common standard model, independent of vendor-specific software, has been important in managing the data for almost 100 years. This research verified a typical data succession between design workflows using the developed method and confirmed that it is adequate to manage the change histories.

3 The evaluation system of waste quantities for decommissioning planning of nuclear power plants

Abstract: A decommissioning engineering support system was developed using three-dimensional models for nuclear power plants. As for the calculation of the duration for dismantling work and costs, based on the spatial distribution of the dose rate surrounding equipment and piping components, it is important to evaluate the difficulty levels of dismantling work and waste quantities consisting of radioactive and contaminated materials equipment and piping components in the decommissioning project. Furthermore, it is necessary to assess person-hours for large equipment and waste containers being conducted from the installed or packed places to designated temporary areas or removed from the building by carrying-out paths and related work. In this system, radioactive inventory data is mapped to 3D objects of equipment and piping components for a decommissioning nuclear power plant. Based on the mapped radioactive inventory data to 3D objects, the spatial dose rate distribution is automatically calculated, and waste container models are automatically generated. Using generated data, carrying out paths for large equipment and waste containers are automatically calculated. Results of an evaluation showed that the developed system could support decommissioning engineering tasks systematically and effectively.

3.1 Background on decommissioning planning of NPPs

The cases for decommissioning NPPs are increasing regarding balances of costs. The NPP should be operated further with additional safety construction. Otherwise, the NPP should be decommissioned with a permanent shutdown. Additionally, we must proceed with decommissioning projects with safety, efficiency, and economy. There are actual decommissioning projects for research and commercial reactors that can be referenced for incoming projects, especially information management systems. As for the first decommissioning project for Japan Power Demonstration Reactor (JPDR) in Japan, Japan Atomic Energy Research Institute (JAERI) at that time, currently reorganized as Japan Atomic Energy Agency (JAEA), developed an integrated information management system called COSMARD, which is the abbreviation of the Code System for Management of JPDR Decommissioning. The COSMARD has evaluated data for decommissioning system engineering information, such as work hours, occupational exposure dose, the weight of waste, and managed schedules for decommissioning processes [3]. Since then, the research institutes of Japan and Norway have collaborated and developed Decommissioning Engineering Support System (DEXUS). They have used the system to support optimized planning for dismantling NPPs in a decommissioning project [4]. As for planning based on dismantling simulation under high dose rate environments, the research institute in Norway has developed a system called VRDOSE with Virtual Reality (VR) [75]. The VRDOSE system calculates spatial distributions of dose rate based on nuclides of radiation sources, distribution shapes, geometric shapes of the dismantling work area, and material information of piping components and equipment [76]–[78]. Several organizations research the simulation technologies for the processes of dismantling and cutting piping components [79]

Above mentioned research activities were trials for planning and managing decommissioning engineering using the partial 3D model for NPPs. Contrary to those research activities, we have developed the engineering support system for decommissioning projects using a 3D CAD model for whole NPPs [80], [81]. In this system, we used the 3D geometric shapes of the designated NPP and functional connectivity of the piping components and equipment. Additionally, we stored accumulated radioactive contamination during plant operation in a database and shared the data with the developed decommissioning engineering support system.

3.2 Engineering for supporting decommissioning planning

We have developed a system for supporting decommissioning engineering based on functions that calculate radioactive waste quantity, generate objects by cutting piping components and equipment, calculate egressing paths for large equipment, and calculate accumulated occupational exposure dose, as shown in Figure 3.1. As mentioned in Chapter 2, geometric shapes based on point cloud data can be decomposed to plant items, and their relations are integrated with the GPM class library. On the other hand, residual radioactivity in the equipment and piping components is evaluated based on a history of an NPP operation. This evaluated radioactivity is called radioactive inventory, and the inventory can be mapped to each plant item and stored in an intelligent 3D model. The functions in the system use the data stored in the intelligent 3D model that retrieves the amount of radioactive inventory data a plant operator evaluates. With the developed system connecting the decommissioning schedule and the intelligent 3D model, we can improve the accuracy of calculated work hours and the duration of dismantling projects.

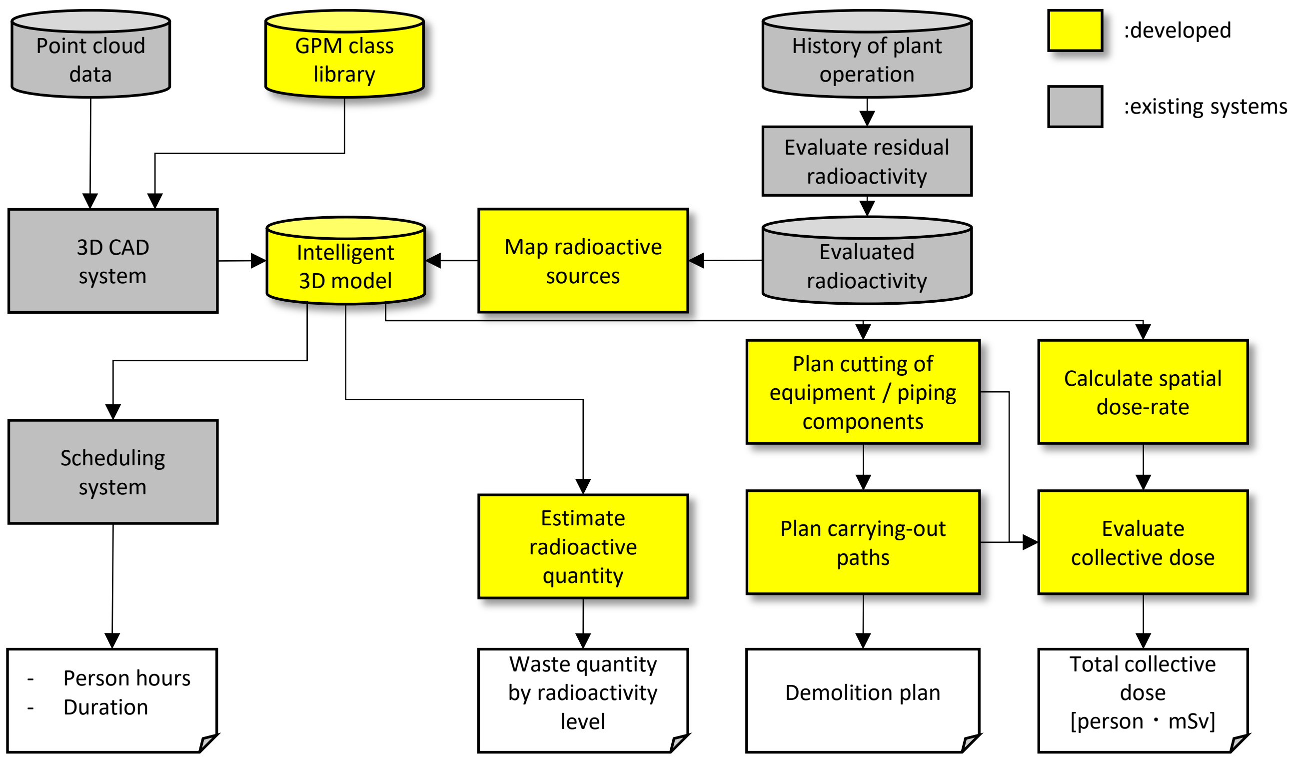

Figure 3.1 System configuration.

3.3 Visualization of environmental dose rates for dismantling areas

The developed system automatically allocates radioactivity data that is remained an NPP after a permanent shutdown to internal surfaces of piping components and equipment. All the data required to calculate dose rate and quantity is stored in the intelligent 3D model. Spatial dose rate distribution is calculated using 3D distributed radioactive source data with the Particle and Heavy Ion Transport code System (PHITS) [82]. The system can visualize the spatial distribution of dose rate based on the calculated results. The visualized distribution of dose rate is shown in Figure 3.2, which colorizes the transparent voxels based on the strengths of the dose rate in the dismantling work area.

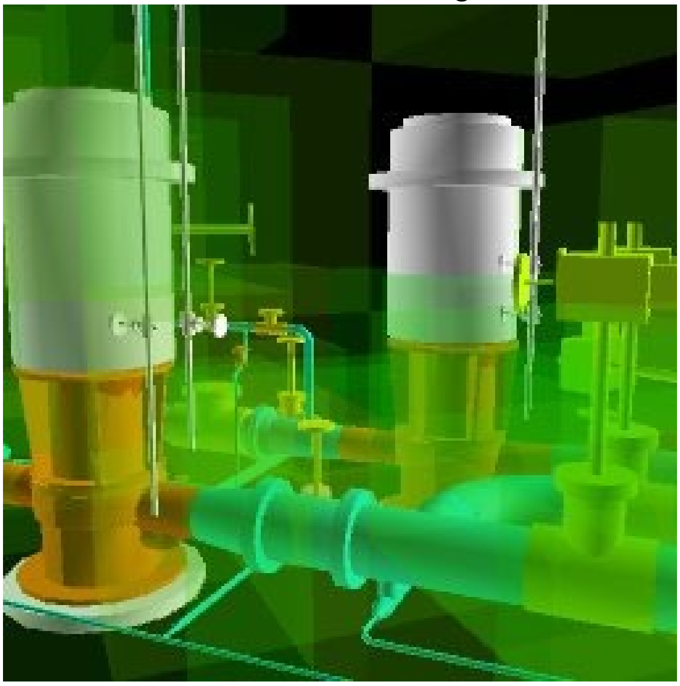

Figure 3.2 Spatial dose rate distribution around equipment and piping components.

3.4 Generation of 3D objects for waste containers

3.4.1 Methods for generating 3D waste fragments and containers

The system cuts piping components and equipment into pieces of 3D objects and uses the cut objects to store them in the model of waste containers. With this function, the system also calculates the number of pieces of cut fragments, the radioactivity, the required number of waste containers, and the weight of each waste container in dismantling work. The generated waste container model with cut fragments is shown in Figure 3.3. Figure 3.3 (a) shows the packing model of the segmented piping components, and Figure 3.3 (b) shows the packing model of the segmented equipment. Furthermore, the system can evaluate the maximum filling rate of fragments in each waste container by designating the placement directions as horizontal or vertical. With these capabilities, we can determine the optimum cut lengths of objects and the required number of waste containers.

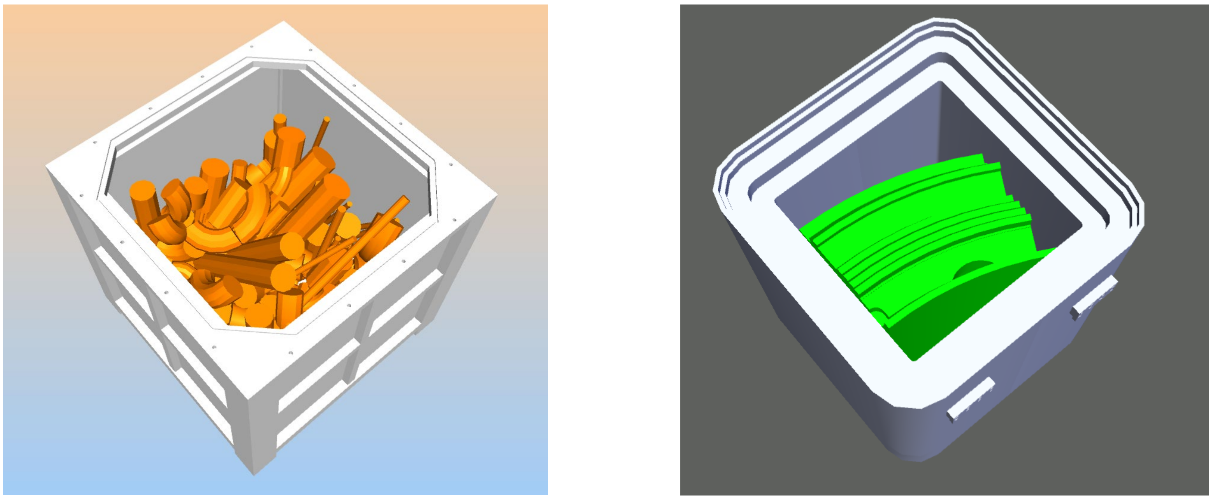

(a) Packing model of segmented piping components.

(b) Packing model of segmented equipment.

Figure 3.3 Generated waste container model.

3.4.2 Results for estimating the number of waste fragments and containers

The system automatically calculates the number of waste fragments and containers based on the 3D model. Thus, we have estimated the relationship between the number of waste fragments and the cut lengths of piping components and equipment. As the evaluation result, we found the tendency to decrease the number of waste fragments and the required number of containers if the cut lengths increase, as shown in Figure 3.4. Here, the number of waste fragments is almost stable if the cut lengths are over 500 mm. The required number of waste containers in the dismantling areas surrounded by reinforced concrete walls is two to five. To pack the waste fragments into containers with the maximum fill rate, we must store the cut piping components with short lengths and half of the cylindrical pipes toward flow directions. In this case, since the number of cutting events will be increased, the work hours related to cutting tasks are increased, affecting the occupational exposure dose to workers. Contrary to the above case, if the work hours for the dismantling and cutting tasks are decreased, the number of waste containers and the management cost increase. The trade-off between the cutting lengths and the number of waste containers should be optimized in terms of the accumulated occupational exposure dose, the total management cost of the waste containers, and the work for the egressing waste containers and large equipment.

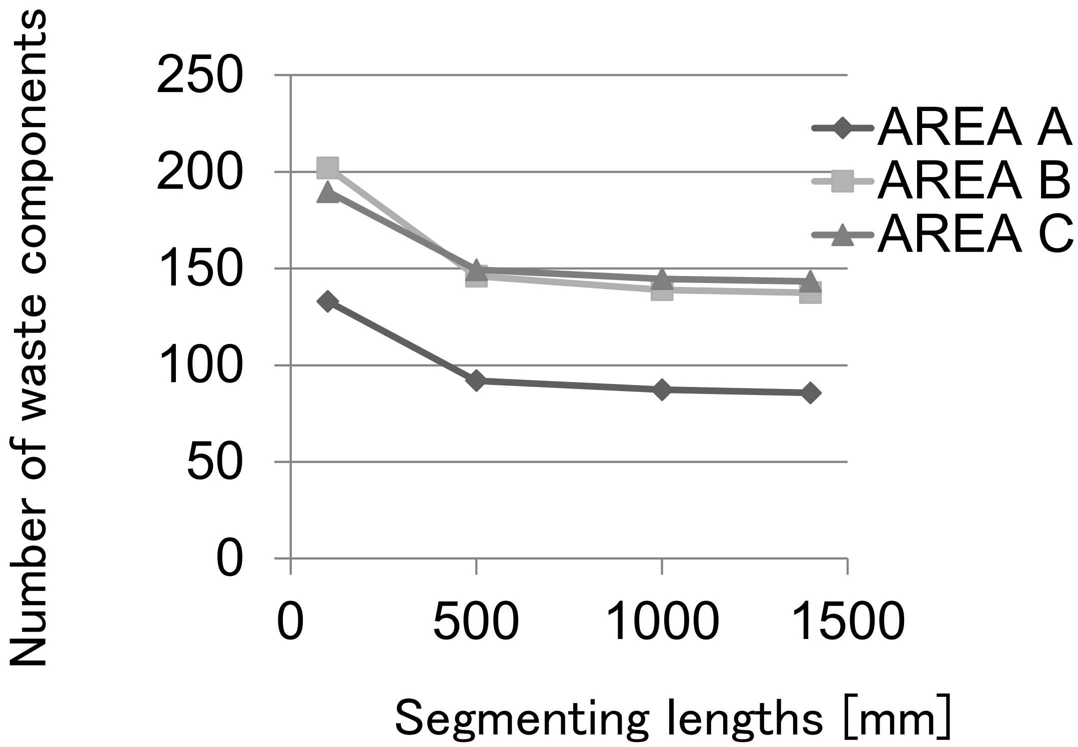

Figure 3.4 Relationship between the number of waste components and cut lengths.

As for planning the interim storage of containers for low-level piping components and equipment waste, the system can determine the required number of waste containers. Therefore, the model for the placement in the building could be generated, as shown in Figure 3.5. With this research and development, we have confirmed that the system can visualize the 3D model of the required waste containers and generate the planning for the interim storage of the containers with the automatic cutting functions for piping components and equipment.

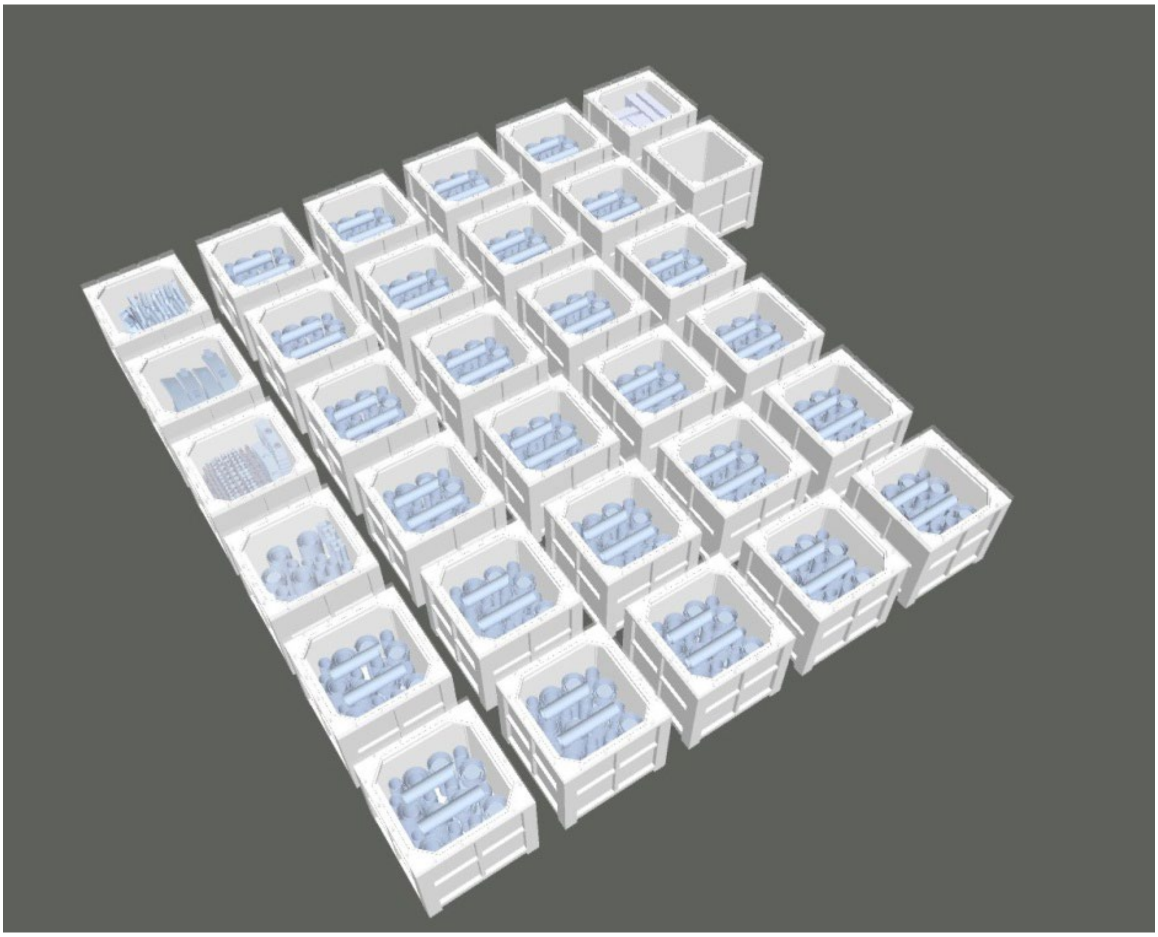

Figure 3.5 Containers required for low-level waste.

3.5 Planning for paths to carry out waste

We must plan egressing paths to avoid interferences between installed facilities and egressing objects, such as large equipment and waste containers, and decrease occupational exposure dose. In a complex and narrow space in a nuclear plant, it is not easy to consider the equipment of the length of a few meters, the route to carry out without interfering with facilities and buildings by hand on the 3D-CAD system. Furthermore, it is difficult to consider the route that the exposure dose of the operator to be received in the carrying-out operation is minimized by a manual calculation.

We have developed a system automatically to search for the optimal carrying path to this problem. This system automatically searches the way that does not interfere with buildings, etc., at least by exposure dose in 3D space of the building, crane, hanging by monorail, calculates the posture and orbit of the lead of the air caster.

3.5.1 Methods for path planning

The flow of processing of the system is shown from (a) to (e).

(a) Input data

The developed system reads the three-dimensional geometric shapes of the building and the carrying-out objects as input data, the start points, the end points, and the spatial radiation dose-rate map.

(b) 3D object decompositions and network generation

The system decomposes the 3D geometric shapes of a building model into a set of rectangular box cells (Figure 3.6). The system then leaves a rectangular parallelepiped cell with no three-dimensional shape to explore the space through which the unloading material can pass (Figure 3.7). After the process, the system generates a graph network with the remaining rectangular cells as nodes and adjacent rectangular parallelepiped cells with edges (Figure 3.8).

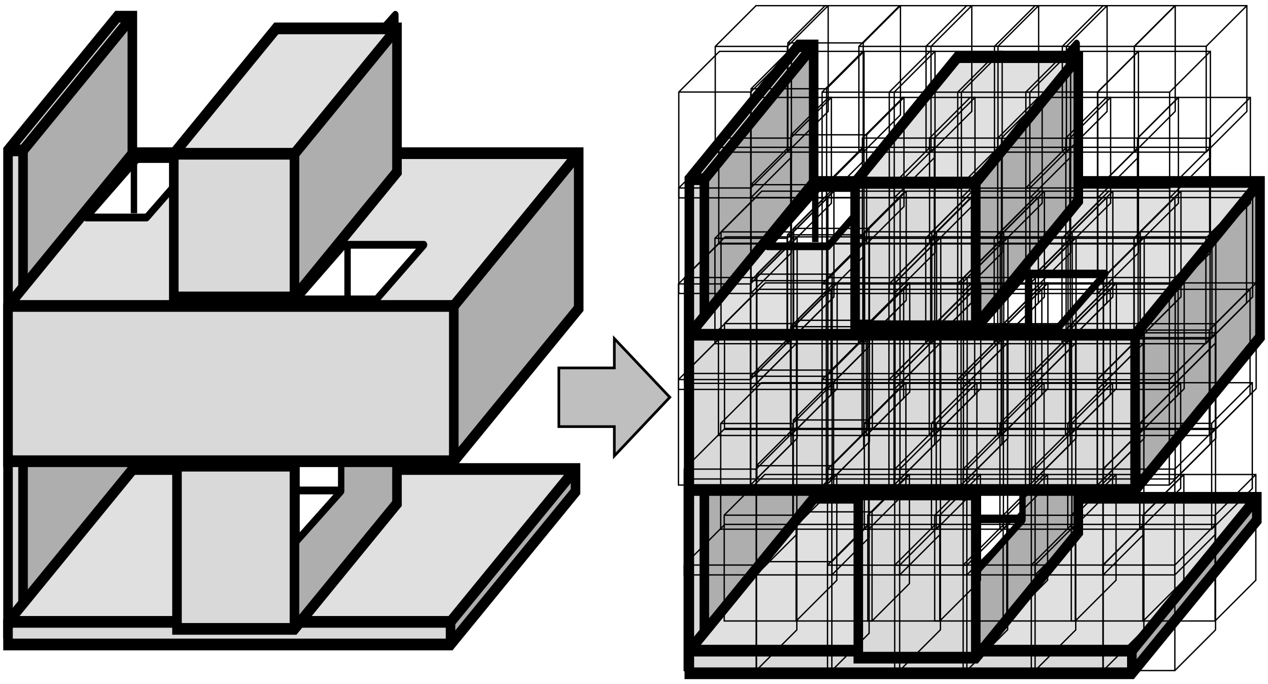

Figure 3.6 3D Building model divided into cuboid cells.

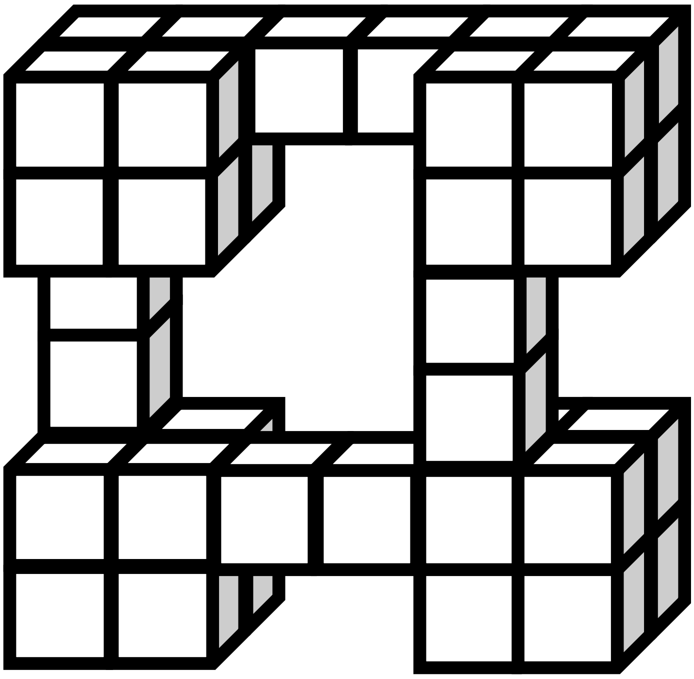

Figure 3.7 Cuboid cells containing no geometries have remained.

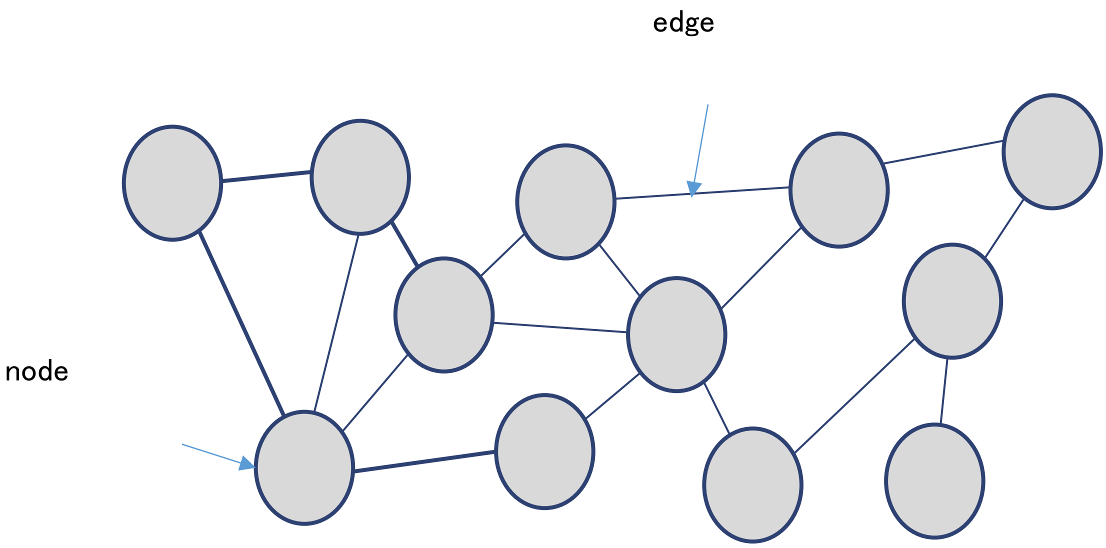

Figure 3.8 Graph network for finding optimum paths.

(c) Exploring optimized pathways

The system sets the node corresponding to the start and endpoint of the eject on the generated graph network. Then, the system selects the evaluation value for each node on the graph network, which is the objective function of the route search. Figure 3.9 results from searching for a path to minimize the radiation dose rate as a valuation value. This example shows the smallest of the three ways by searching with optimized functions.

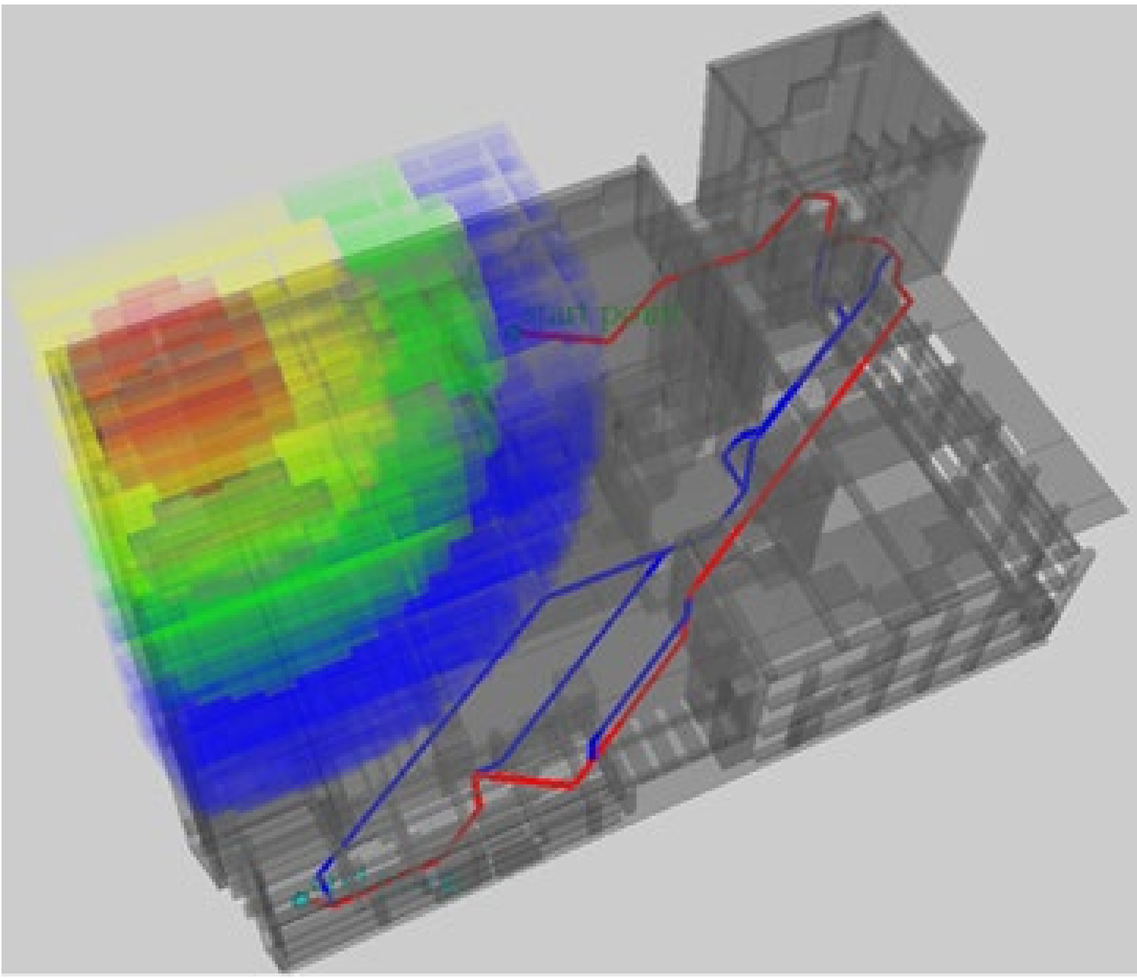

Figure 3.9 Found paths to avoid radiation exposure.

(d) Calculation of vectors for six-dimensional trajectories

The route is computed as a point-column vector group of passing points. According to the mechanism, dynamic characteristics model, the carriers or cranes' movement locus is calculated as six-dimensional trajectory vectors of the positions and posture orientations to follow the point rows of these passing points.

(e) Output data

Finally, the system outputs the 6-dimensional trajectory data vector, the conveying time, and the exposure dose of the worker from the positions and postures.

3.5.2 Objective functions

The developed system applied the shortest path calculation algorithm by the Dijkstra method [83] to the computation processing of the route search on the graph network. This system used the objective function to minimize the evaluation indexes of the following a) from c) for the path calculation.

a) Reciprocals of the carrying-out space margins,
b) Number of times to turn the carrying out materials,
c) Radiation dose of the workers.

Here, we defined the first evaluation index of the space margin by the product of the orthogonal three-axis distances from the surface of the smallest outer envelope of the conveying object at one point on the path to the obstacles (Figure 3.10).

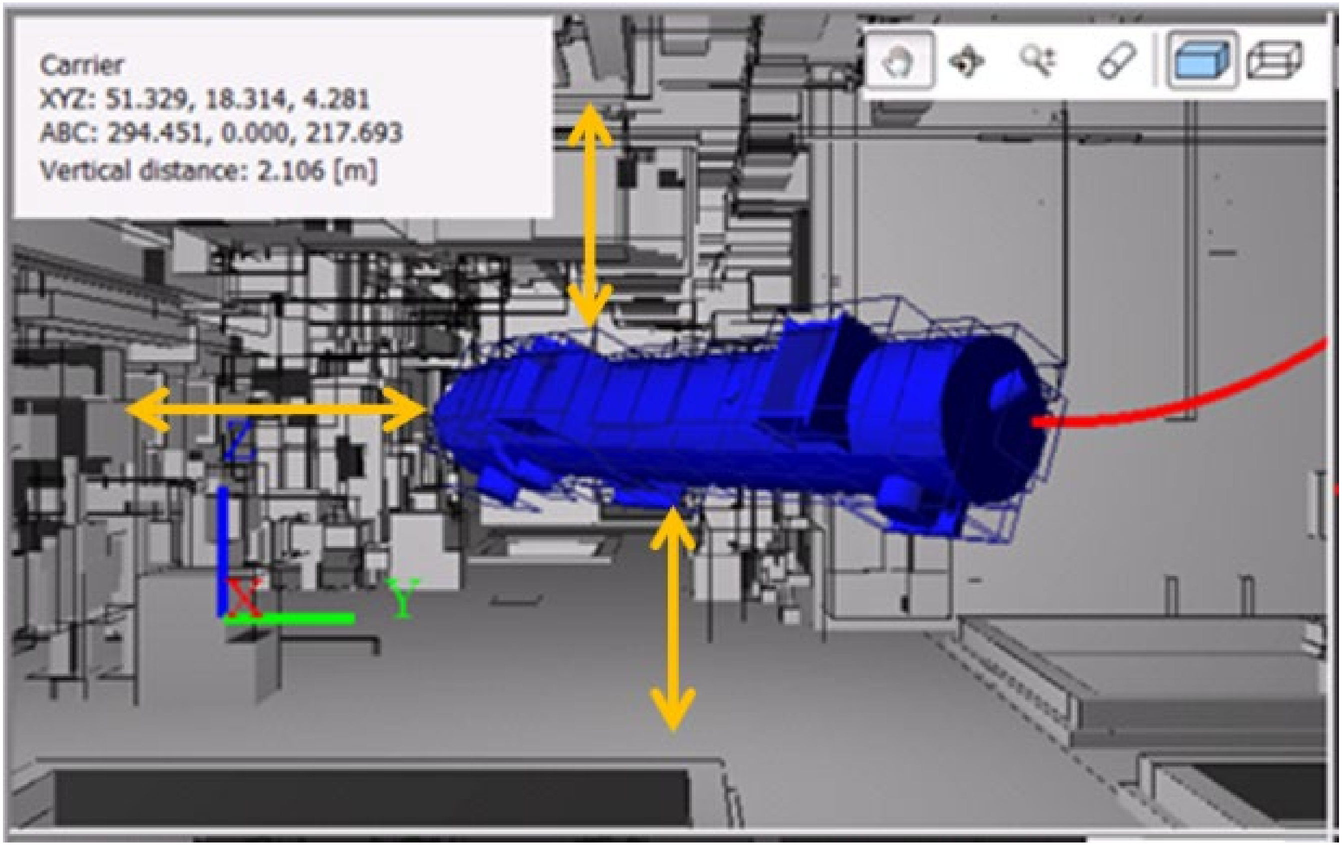

Figure 3.10 Space margins for a path of large egressing equipment.

In addition, we set the second evaluation index for the number of times turning the carrying-out object by the amount of the place where the carrying path is bent. We made the second evaluation index because the number of times the posture change increases if the number of turning times on the pathway is large because the conveying work person-hours increases. Therefore, it is desirable to minimize the number of turning times.

Then, the exposure dose is the third evaluation index. The index is calculated with the product of the shortest distance at position *v* on the carrying-out path, the dose-rate *r(v)*, and the passing time *ΔT*. And we have calculated the accumulated dose *Fr(p)* on path *p* by adding the setup time *tp* and the load changing time *n*, such as replacing the crane from the carrier, with the following Equation (3.1).

$$Fr(\mathrm{p}) = \sum_{v} \Delta t \times r(v) + \sum_{n} tp(n) \tag{3.1}$$

Thus, if there is more than one evaluation index to be minimized, it is not always possible to reduce all the evaluation indexes. As a countermeasure to such a case, commonly used is a method of the load sum of the evaluation index to be used as an objective function. However, a problem cannot determine how to allocate each evaluation index's weight. On the other hand, the evaluation index was prioritized in the development system, and the result was narrowed down from a high-priority evaluation index. If the evaluated values are the same, the system sets the objective function to assess the following index to be incrementally assessed [84]. The highest priority in the extraction path search of large equipment is ensuring the space allowance when the posture change, such as during rotation and crosscut. It is impossible to carry out itself if it cannot change posture. Therefore, we decided to set the space margin as the evaluation index of the highest priority.

Similarly, workers take much time to change postures of large equipment of a few tons of weight and replace machines from carriers to cranes for conveying means. Therefore, as the second evaluation index preferred is the number of turning times, we decided to minimize this index. Finally, we calculated the third evaluation index as an exposure dose.

3.5.3 Results for path planning

In this system, the physical model of the crane hanging mechanism is expressed by a differential algebra equation, and the function to simulate the dynamic characteristics by time integration has been developed [85]. We decided to configure the crane dynamic characteristic simulator developed by four tasks from the following (a) (d).

(a) Configuration of interference checking

The user chooses the wall, floor, ceiling, equipment, piping, etc., around the crane to check for interference during simulation from the display screen (Figure 3.11 (a)). To accelerate the computation, only the selected planes are subjected to interference checking (Figure 3.11 (b)).

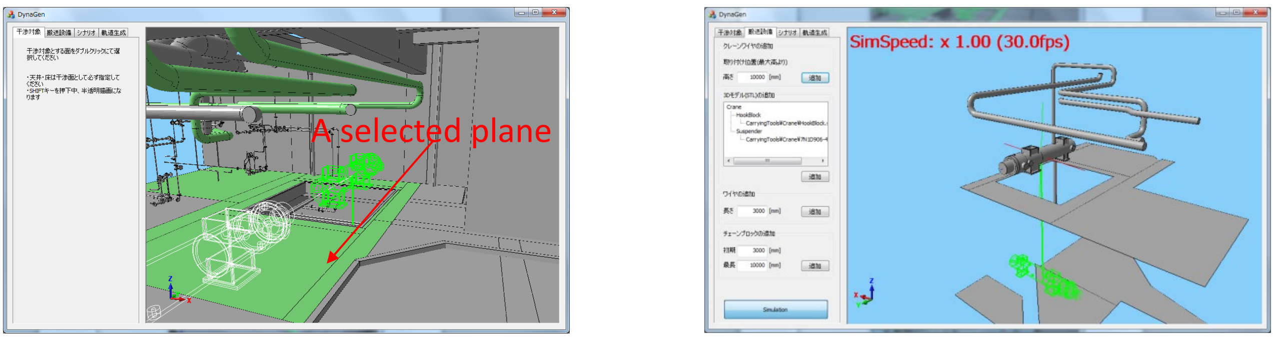

(a) Selection of planes to evaluate collision (b) Remaining planes for checking collisions

Figure 3.11 Environmental planes for collision check.

(b) Definition of a crane mechanism

This system has hooks for hanging out objects such as large-sized equipment and chain blocks that stretch in chains. It was defined on a 3D model as a crane mechanism, such as Figure 3.12. Because the load and the tension of the wire applied to the hook and the chain block are displayed on the screen, the user can judge the safety of the slinging work.

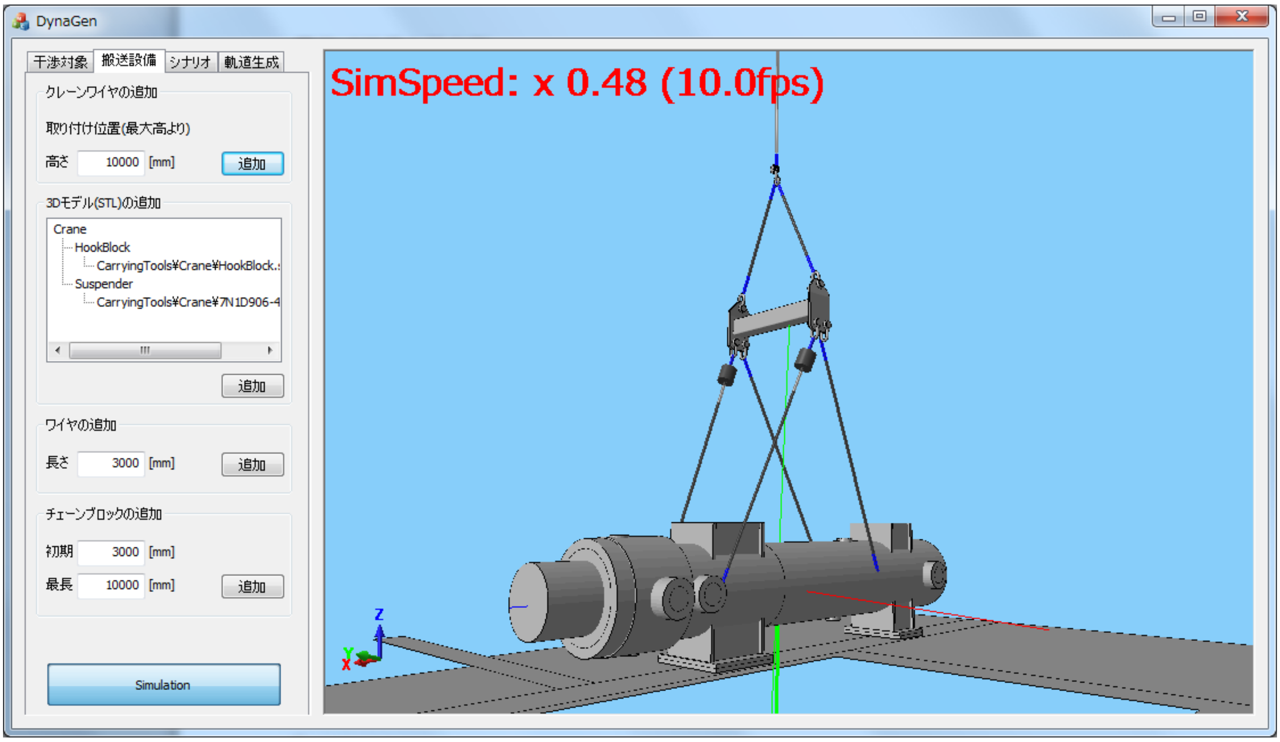

Figure 3.12 Kinematic definitions for a crane.

(c) Operation scenario

The user can operate a crane in real-time on the simulator to create an operation scenario without vibration or interference (Figure 3.13). The user adds a command to the crane lifting/hanging command and the expansion and contraction of the chain block by a button and creates a crane operation scenario. By calculating the load and the tension of the wire to the trajectory and each site to the generated command value in real-time, the user can determine the safety of the operation.

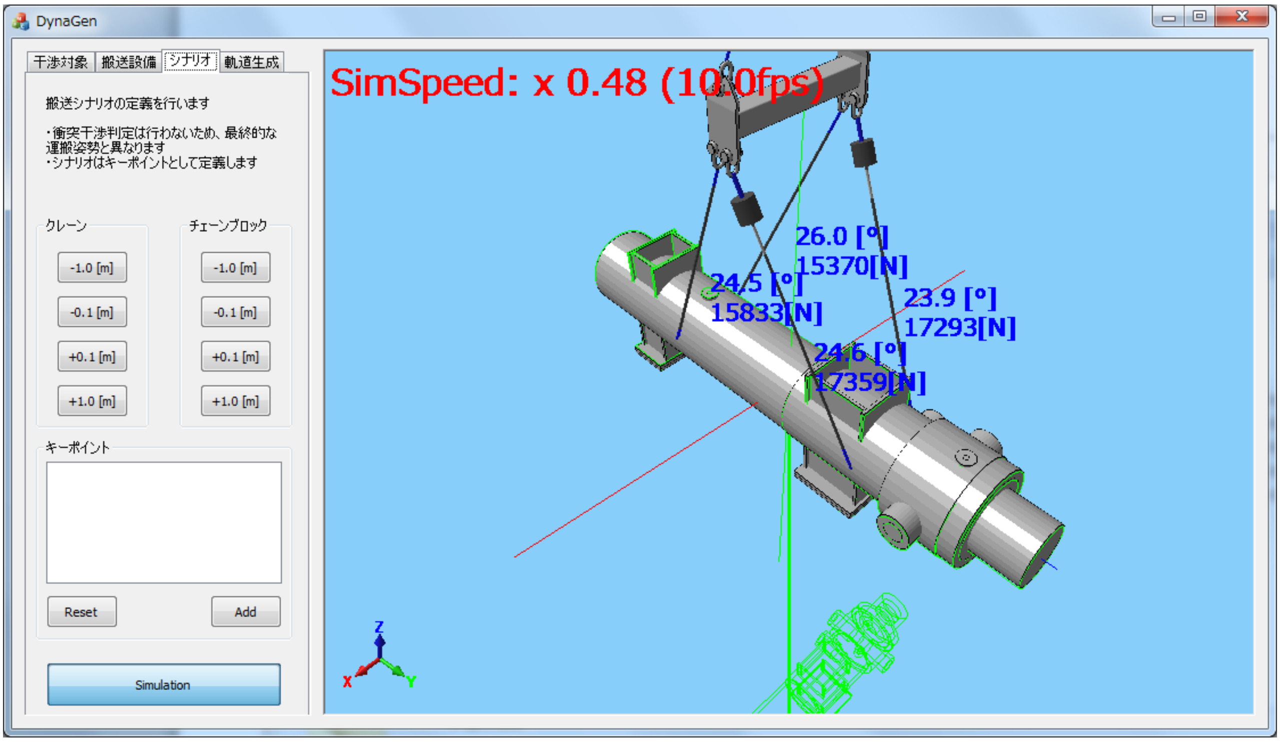

Figure 3.13 Creation of operation scenarios.

(d) Generation of trajectories

Under the conditions set in (a), the crane mechanism defined in (b), by the operation scenario created in (c), the developed system generated the trajectory of the crane by solving the dynamic characteristic differential algebra equation as shown in Figure 3.14. Thus, the user can check the series of crane trajectories in the simulation concerning the crane unloading of large equipment. And it is possible to confirm the safety of the possibility and mechanical work interference by numerical data by sharing stored in the video. Construction stakeholders can use such information to pre-examination the risk of the work.

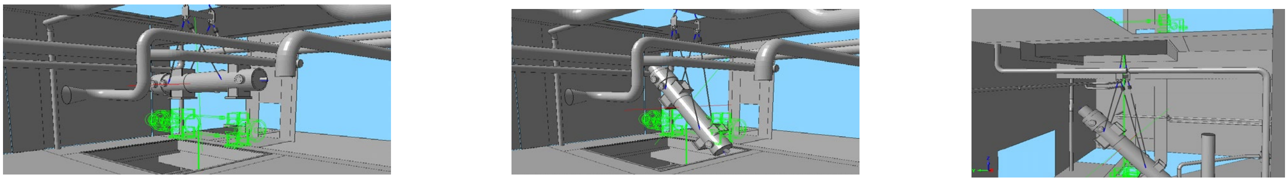

(a) Initial posture of equipment. (b) Tilting equipment. (c) Final posture of equipment.

Figure 3.14 Generation of trajectories for large equipment.

The above-described path search algorithm checks the interference point by parallel processing by a general-purpose graphics processor (GPU). We compared the calculation time on a PC with a single CPU PC and GPU, as shown in Figure 3.15. We have confirmed that GPU parallel computation can speed up the computation time by about 300 times compared to a single CPU. When the 10^{10} polygon number, about 30 minutes in a single CPU, where the path search calculation processing has taken, it is possible to finish the calculation at high speed of about 10 seconds.

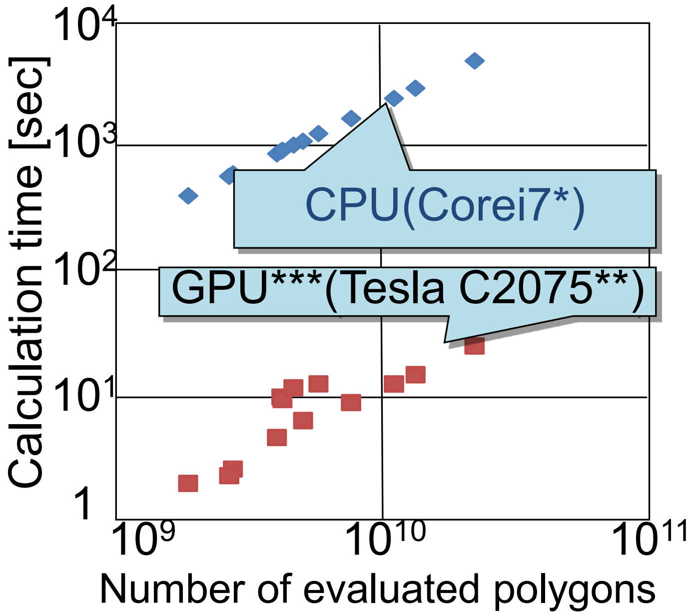

*Intel, 3.3GHz
**NVIDIA Corporation
***General Purpose computing on Graphics Processing Unit

Figure 3.15 Calculation time comparisons of a single CPU and parallel processing of GPU.

An example of the result of the carrying-out simulation, based on the scenario of carrying out a typical waste storage container using the developed system, is shown in Figure 3.16. Here, the storage container stuffed with waste fragments on the upper floor of the reactor building, once temporarily placed in the basement. Then, through the space, the main steam pipe tunnel chamber, between the reactor building and the turbine building, shows the results of searching the route to carry out the unloading port of the turbine building. This calculation specified two transit points of the torus room, the main steam piping tunnel chamber, and the start and end of the storage container. Here, the large-diameter piping and the torus chamber of the main steam piping tunnel chamber, which is known to interfere with the storage container, and suppression chamber, were removed from the building model.

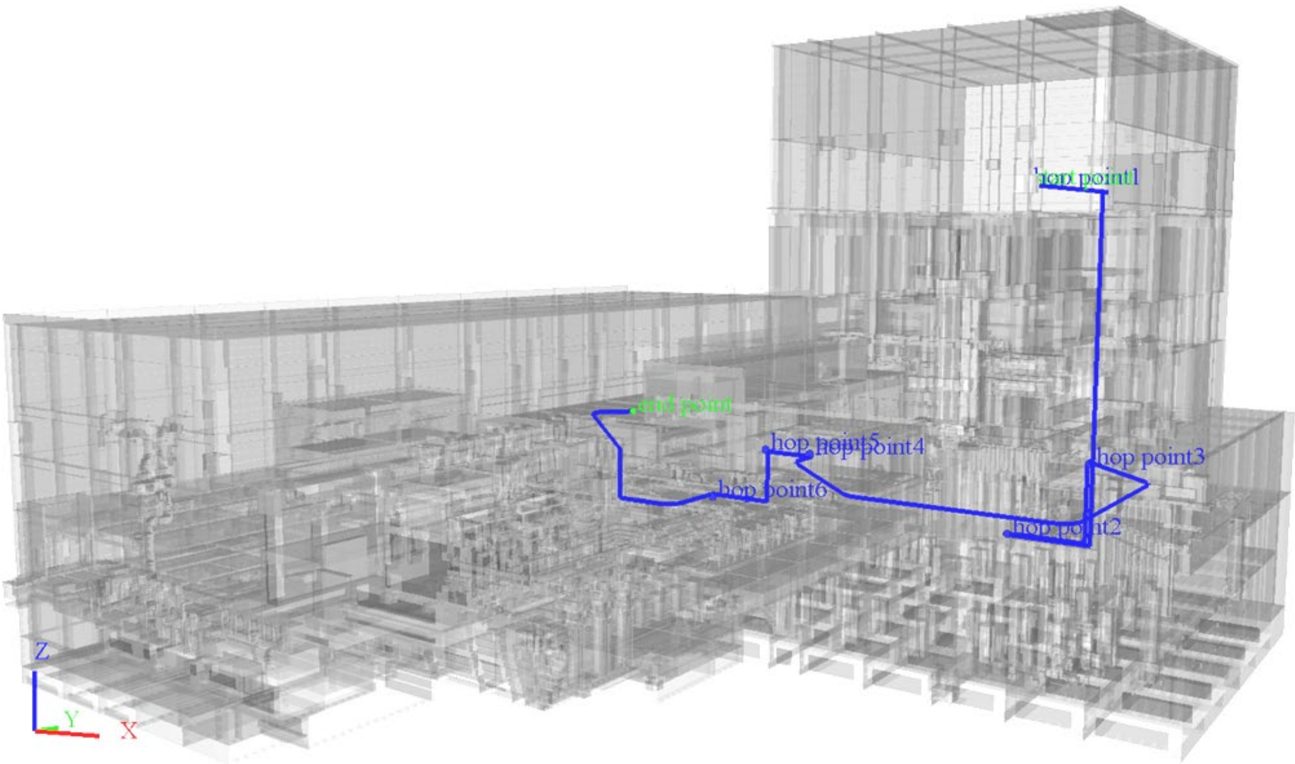

Figure 3.16 An egressing path in the plant building.

An example of the state of the carrying out of large equipment in a building model by using the trajectory of the equipment carried out and the hanging trajectory of the crane because of the calculation is shown in Figure 3.17. Using this function, users can organize the numerical data of the carrying out route in a drawing, or share it as a video, to understand the safety and work time of the fieldwork.

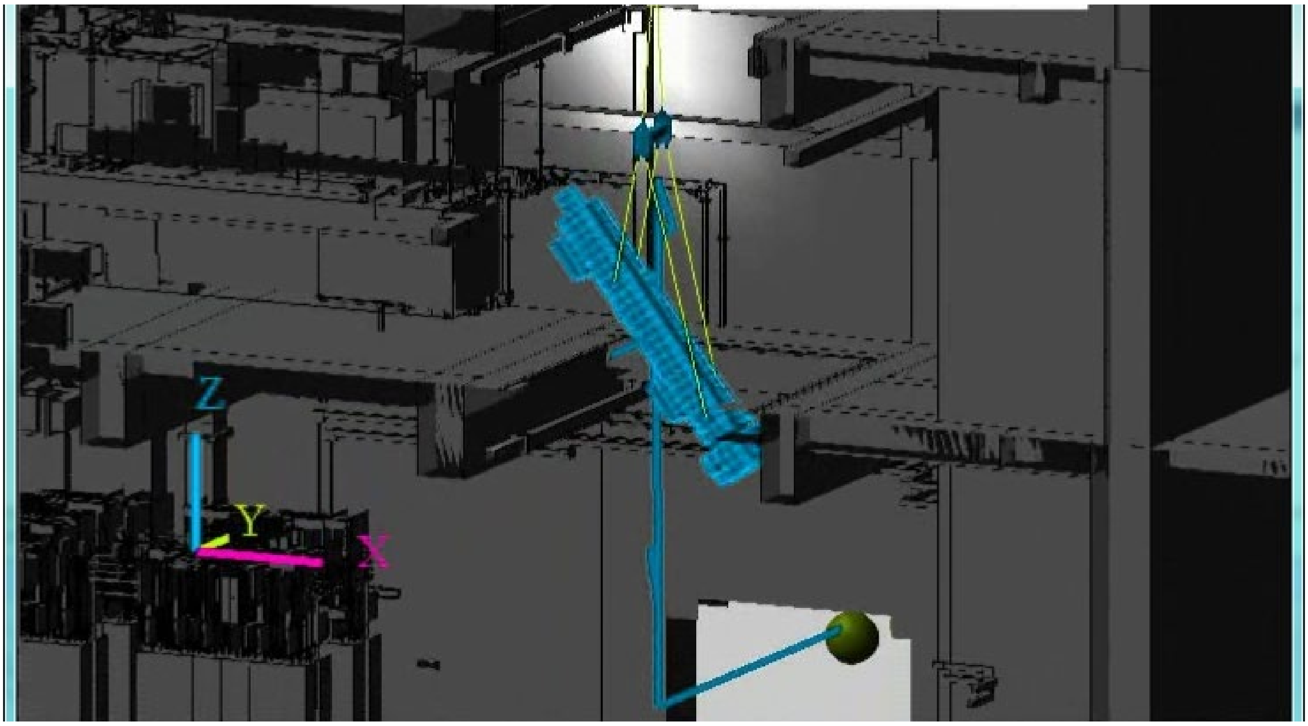

Figure 3.17 Combined results based on carrying-out path generation and crane rigging simulation.

3.6 Conclusion on an evaluation system of waste quantities for decommissioning planning of NPPs

We have developed an intelligent 3D model that assigns radioactive inventory data that is substantial amounts of data to 3D objects and the ability to automatically generate the distribution of the spatial dose rate as well as the waste containment model. This allows the appropriate cutting lengths of equipment and piping components, the number of waste inmates required, and the calculation of the accumulated exposure dose based on various dismantling scenarios and can support the judgment related to the decommissioning plan. We also confirmed that we could support the decommissioning engineering systematically and efficiently by using simulation results related to waste volume and carrying out paths. All the necessary data to calculate dose rate and quantity is stored in the intelligent 3D model.

With the developed system connecting the decommissioning schedule and the intelligent 3D model, we can improve the accuracy of calculated work hours and the duration of dismantling projects. And then, the system cuts piping components and equipment into pieces of 3D objects and uses the cut objects to store them in the model of waste containers. As a result of the evaluation, we have confirmed that the number of waste fragments is almost stable if the cut lengths are over 500 mm. The required number of waste containers in the dismantling areas surrounded by reinforced concrete walls is two to five.

We have also developed a system automatically to search for the optimal carrying path. This system automatically searches the way that does not interfere with buildings, etc., at least by exposure dose in the 3D space of the building. Hanging by cranes and monorails were used for calculating the postures and orbits of the large equipment to be carried out. We applied the shortest path calculation algorithm by the

Dijkstra method to the route search on the graph network in the developed system. This system used the objective function to minimize the evaluation indexes of a) reciprocals of the carrying-out space margins, b) the number of times to turn the carrying out materials, and c) the radiation exposure dose of the workers.

The crane rigging of heavy equipment was simulated with the functions, a) configuring interference checking, b) defining a crane mechanism, c) defining operation scenario, and d) generating trajectories. With the parallel processing by GPU, the calculation has been done about 300 times faster than a single CPU calculation.

Construction stakeholders can use such information to re-examine the work's risk with the generated trajectories. And, using the developed functions, users can organize the numerical data of the carrying out route in a drawing, or share it as a video, to understand the safety and work time of the fieldwork.

4 Evaluating the precise quantity of decommissioning waste by cutting virtual 3D models of large equipment

Abstract: Equipment and piping components contaminated by radioactive materials and irradiated materials as low-level wastes must be cut, segmented, and packed in waste containers. To avoid excess exposure dose and minimize the number of waste containers for many pieces of equipment and piping components, an automatic planning method for virtual cutting of 3D equipment objects under the constraints of container sizes, maximum radioactivity, maximum weight, and maximum dose rate was developed. Different cutting-work flows were formulated and used with cutting sequence data to generate cut objects and calculate the exposure dose for the disassembling work. With the help of the developed system, decommissioning planning will be supported by the calculated results of the required cutting length and the dose-rate distribution in the working environment for various cutting sequences of large equipment.

Keywords: decommissioning; 3D-CAD; dose-rate visualization; waste-quantity estimation; virtual cutting plane

4.1 Background on detailed planning based on virtual 3D models

Decommissioning projects are expected to increase for nuclear power plants (NPPs) operating for many years. Decommissioning projects for NPPs must be carried out safely, efficiently, and economically. Dismantled radioactive waste in the decommissioning project is estimated as 3.6% of the total waste in a commercial boiling water reactor (BWR) type nuclear power plant [86]. The total cost of dismantling processes, including cutting, processing, and removing waste materials in a decommissioning project, is 73% of the total decommissioning cost [87]. At the same time, the radiation exposure dose for dismantling work must be within the speculated value provided in safety regulations. Therefore, decommissioning projects must be planned optimally, considering work duration and exposure dose. Several decommissioning projects have been completed in the past thirty years, and related project-management systems have been developed. A database for dismantling and evaluating workload, radiation exposure dose, waste weight, as well as schedules of the dismantling processes was managed by the Code System for Management of Decommissioning (COSMARD) [3] for the Japan Demonstration Power Reactor (JPDR). Since then, research institutes in Japan and Norway have developed a Decommissioning Engineering Support System (DEXUS) for identifying an appropriate dismantling plan for a decommissioning project [4]. Virtual reality (VR) methods have been applied in conjunction with the VRDOSE software tool to simulate and plan to dismantle work in an environment contaminated by radioactivity [43], [88], [89]. The distribution dose rate can be computed with numerical calculation codes that take source types and locations, the geometry of the environment, and the materials' characteristics [76]–[78]. A cutting process simulation has been developed and tested for the waste from equipment and piping components [79].

Hitachi has been developing decommissioning engineering support systems based on 3D computer-aided design (CAD) models [80], [81], [90], [91]. Decommissioning engineering involves evaluating a residual radioactive inventory, planning for decontamination, dismantling, remotely controlling machines, managing waste processing, and measuring radiation. Decommissioning projects should proceed based on these procedures. The 3D geometric shapes of a decommissioning plant, functional system data, and residual radioactivity accumulated during plant operation should be stored in a database and shared by decommissioning support systems to integrate these procedures. Basic functions for evaluating the quantity of decommissioning waste and the worker's accumulated dose by cutting virtual 3D models of large equipment have been developed to provide the above systems with essential data.

This dissertation's problem and objective of this research are described in Section 4.2. Section 4.3 describes the method for automatically generating cutting objects using 3D models of large equipment. The simulation method for various possible cutting procedures is then described in Section 4.4, and the simulation results and discussion are presented in Section 4.5. Finally, the conclusion is given in Section 4.6.

4.2 Problem statement and objectives of the research

In Japan, funds for decommissioning are allocated while nuclear plants are still operating. Estimating the cost of decommissioning after power generation is permanently shut down is necessary to avoid running out of funds. The technologies required for decommissioning can be divided into elemental technologies and systems engineering [92]. Decommissioning projects need to integrate both to be appropriately carried out. A database containing geometric shapes, function (system) data for the decommissioning NPP, and contamination from radioactive materials accumulated during operation need to be linked to the elemental technologies and appropriate use of systems engineering.

The following problems need to be solved to utilize systems engineering in conjunction with elemental technologies:

- Both weight and volume of the waste need to be controlled so that radioactive waste for decommissioning NPPs is traceable.
- Identifying segmented equipment from a 3D model is a key to calculating the number of volumetric segmented fragments and the required number of containers.
- There are tradeoffs between avoiding overexposure to radiation and minimizing the number of waste containers with multiple scenarios for segmenting equipment and piping components.
- Different cutting workflows should be formulated for generating cut objects and calculating the exposure dose for disassembling work, particularly for cutting sequence data.

4.3 Method for automatic segmentation based on an equipment 3D model

4.3.1 System configuration for integrated cutting and dismantling simulation

We have developed an automatic method for generating 3D cut objects from equipment models with internal structures for planning the dismantling of equipment in the decommissioning phase of NPPs (Figure 4.1). Segmented 3D objects were stored with cutting conditions obtained from equipment 3D models. The equipment 3D models with the radioactivity distribution were used to calculate the environmental and interim dose rates during dismantling work. The number of person-hours and exposure doses for the dismantling work was calculated after simulating the dismantling sequences with segmented 3D objects, typical dismantling sequences, and interim dose rates at tentative cutting states. Finally, waste container models were generated with segmented 3D objects and used to automatically calculate the trajectory for removing the waste containers from their original locations, putting them in a provisional storage place, and then moving them outside the plant.

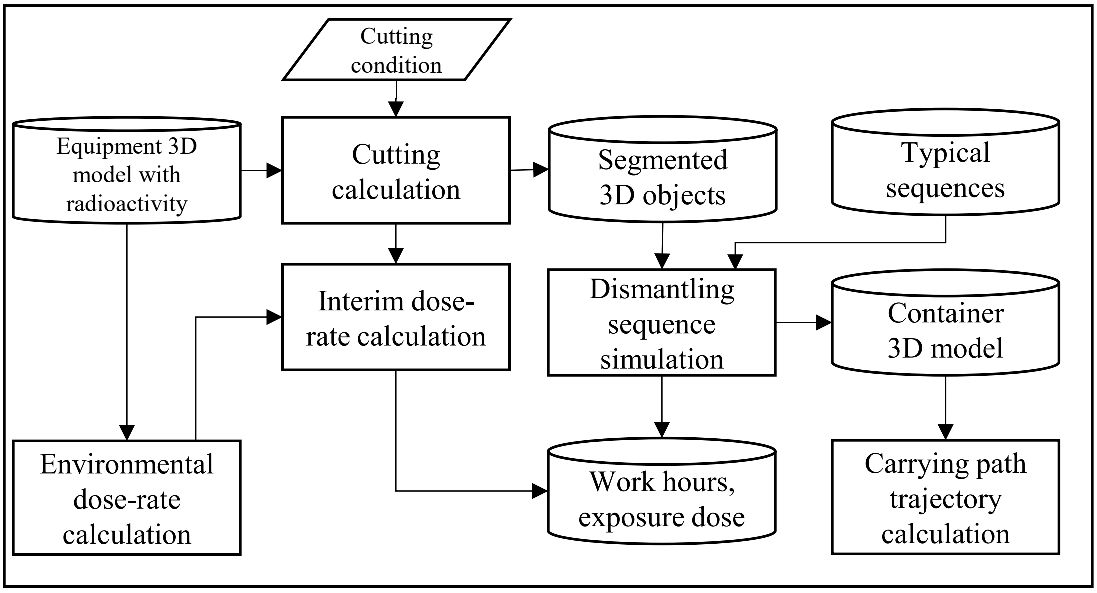

Figure 4.1 System configuration for integrated cutting and dismantling simulation.

4.3.2 Automatic segmentation of 3D model for large equipment

In this development, 3D models for large equipment such as heat exchangers, tanks, and pumps were automatically cut using the following procedure (Figure 4.2):

(1) Prepare the original equipment model with internal structures and define virtual cutting planes.
(2) Superimpose the equipment model onto the horizontal and vertical cutting planes and generate cut objects from both sides of the cutting planes. Then, uniquely identify the cut objects by the IDs of the objects.
(3) Convert the cut objects to an available 3D CAD format file that can easily be used for other tools (such as viewers), dismantling, and simulations.
(4) As for the geometric shapes of heat exchangers (i.e., cylinders), adjust the distances between the cutting planes and the cylindrical axis and the number of divisions in the circumference directions from the user interfaces.

Data on the cut objects were stored in a database, and the number of cut fragments (C0001, C0002, etc. in the case of equipment number AA-HX-13-1 for the 13-1st heat exchanger (HX) in the system AA) was calculated. The above method was used to generate fragments under various constraints during dismantling and to generate a management hierarchy of elements for traceability.

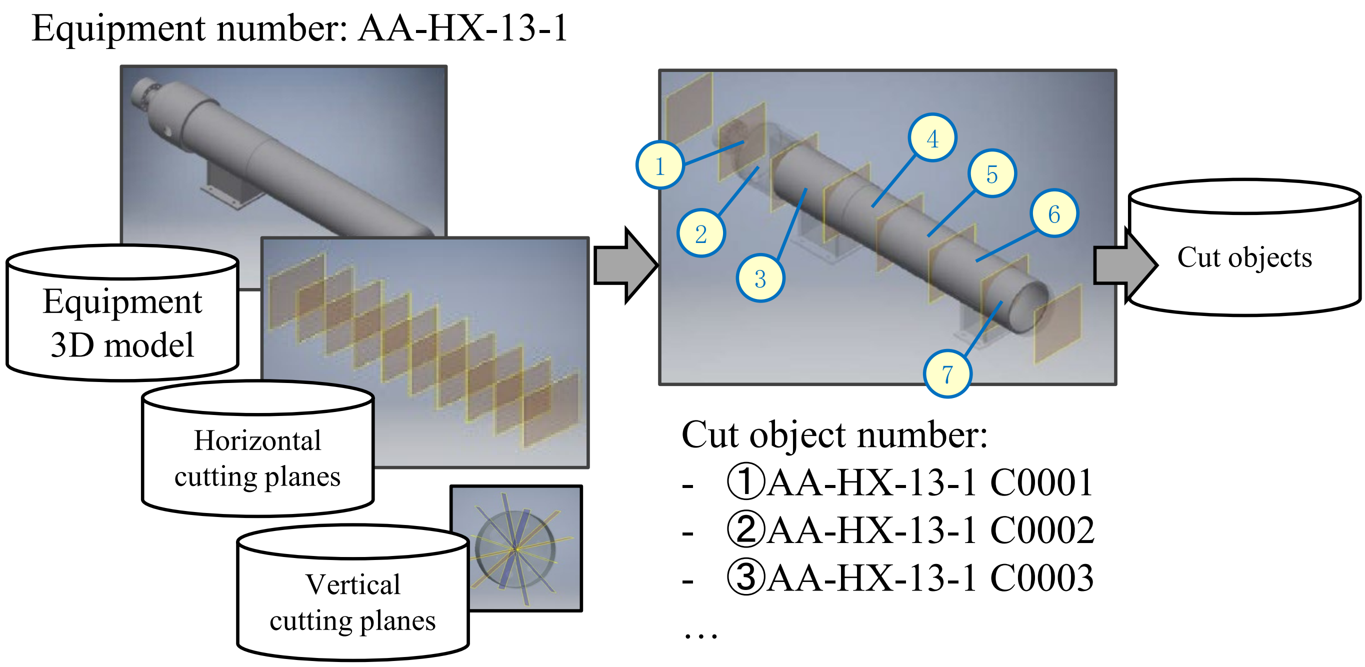

Figure 4.2 Detailed 3D model of equipment cutting based on virtual planes.

4.3.3 Optimization of cutting length

Figure 4.3 shows a flowchart for generating geometric shapes for cut fragments under the constraints of waste containers. The geometric shapes were generated in the following three steps:

(1) Step 1: Setting virtual cutting planes

Since most of the large equipment resembled cylindrical or cubic shapes, multiple virtual cutting planes were placed perpendicular to the axis in the longest direction of the equipment shape, and the intervals (lengths) between adjacent virtual cutting planes were equal. Two interval lengths correspond to the manual and automatic adjustment of virtual planes. One type of interval length was fixed groups with pre-defined cutting lengths. The other variable interval groups depended on radioactivity concentration, container size, and weight limitations.

(2) Step 2: Setting constraints for cutting dimensions

The automatic calculation method calculated the maximum interval lengths to satisfy waste container limitations. The user's designations calculated the equal interval lengths, such as the number of cutting planes and the length of intervals.

(3) Step 3: Adjusting cutting lengths

The distance intervals were determined by repeatedly calculating the cutting lengths of fragment objects in automatic mode until the requirements for the waste container, such as internal volume, maximum radioactivity concentration, maximum surface-dose rate, and maximum weight storable in the selected waste container, were satisfied.

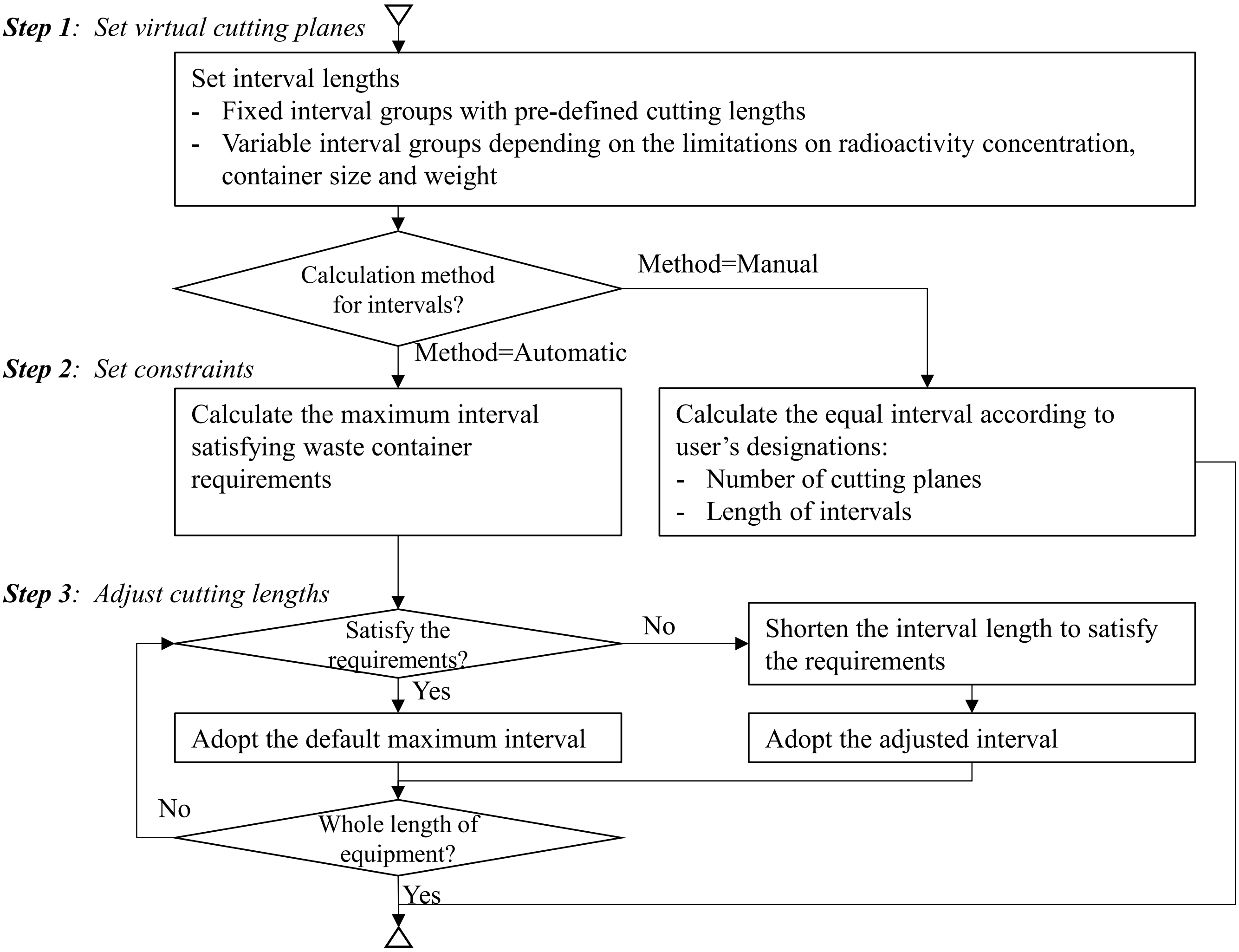

Figure 4.3 Flowchart for arranging virtual cutting planes.

The cutting-interval length and the number of divisions in the axial and circumferential directions to satisfy the constraints on waste containers were calculated for the cylindrical equipment. In this calculation, the dimensions of the cut fragments were adjusted according to the internal volume of the specific waste container. The concentration of radioactivity, maximum surface dose rate, and total weight of cut waste fragments were then evaluated to determine whether those values were under the stipulated limits when the cut fragments were packed into the waste container. If the radioactive concentration and the total weight were not within limits, the cutting interval was shortened, and the values were re-evaluated until they were within limits. The number of cutting divisions for the circumferential direction was selected from 180, 90, 60, 45, and 30 degrees to generate equal objects by cutting.

The cutting lengths were fine-tuned about the lines made by the virtual cutting planes perpendicular to the axis for the longest dimension. The cutting interval was also set by manually designating the number of cutting planes and the size of intervals between the virtual cutting planes.

The maximum dose rate was calculated using the Particle and Heavy Ion Transport code System (PHITS) [82]. Suppose the dose rate exceeds the value limit for a specific waste container. In that case, the system sounds a warning to indicate that the condition of the packed waste fragments is not within the surface-dose-rate limit.

4.3.4 Management of hierarchy for segmented components

A bill of materials (BOM) is changed regularly during disassembling processes [93]. The following rules managed the hierarchy and nodes of the BOM:

(1) According to the cutting and disassembling schedule, unique IDs must be assigned to each node on the generated fragments.
(2) The origins of the generated fragments must be represented as parent-child relationships in the hierarchy.

The changing hierarchy of the cutting objects is shown in Figure 4.4. Assembly001 depicts a cross-sectional view of a heat exchanger composed of Part001 (the outer body) and Subassembly001 (a bundle of small-bore tubes). These parts were cut along the dotted lines. The equipment labeled "Part" was treated as an object with no child components before cutting, whereas "Subassembly" was treated as an object with child components. In this example, Subassembly001 comprises Part002, Part003, Part004, etc. Information concerning the parts and components in the BOM before cutting was provided, and a BOM database was prepared so that the system could manage such information.

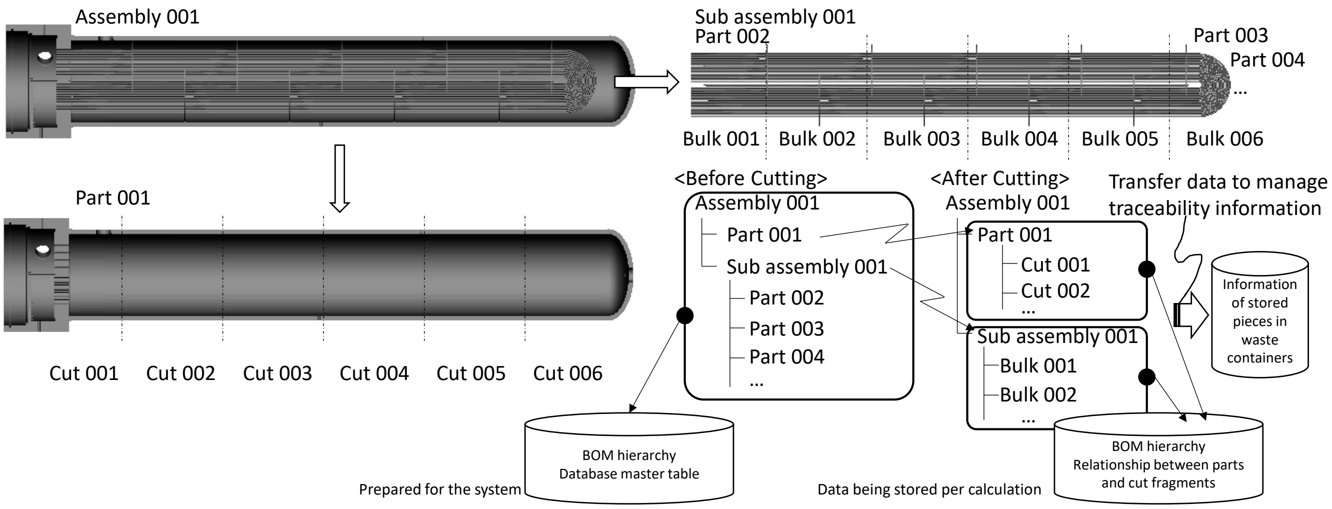

Figure 4.4 Bill of material (BOM) hierarchy for cutting objects.

After cutting, Part001 was cut into fragments Cut001, Cut002, …, and Cut006. Likewise, Subassembly001 was cut into Bulk001, Bulk002, …, and Bulk006. "Bulk" refers to a bundle of cut fragments, such as tubes, and the cut tubes in bulk could not be identified uniquely because of the efficiency of handling data. Within this process, the BOM hierarchy was used to manage the information on the cut object fragments and the origins of the parent parts. The relationships between parts and cut fragments were stored in the database every time object cutting was calculated. The cut fragment inherited the attributes of the original parts, and the concentration of radioactivity and weights were allocated according to the volume ratio between the original part and the fragment. Then "before cutting" and "after cutting" information can be linked and used for controlling the traceability information. The traceability information is stored in a database with the relationships between cut pieces and its storing waste containers. Therefore, even if the waste containers are stored in a different location from the decommissioning NPP, the total amount of radioactivity in the waste containers is calculated systematically with the database of traceability and the previously mentioned 3D intelligent model as it contains the radioactivity data allocated to each plant item.

4.4 Cutting procedure for simulation

4.4.1 **Changing dose rate depending on cutting procedure**

Multiple cutting sequences need to be considered while considering exposure dose and duration of work to estimate decommissioning costs to cut large equipment such as heat exchangers (Figure 4.5). For this purpose, the following three cases were studied.

A heat exchanger has internal structures containing a group of small-bore tubes contaminated with radioactive materials such as Co-60 with the fluid from a nuclear reactor core during plant operation. If the tubes are extracted first, the remaining body of the heat exchanger is minimally contaminated, and the radiation exposure dose rate can be suppressed. Then the body of the heat exchanger can be cut vertically and horizontally. The extracted tubes should be cut separately, taking double the cutting time. However, the exposure dose can be decreased with moderate shields. These cutting sequences are referred to as Procedure A.

The heat exchanger with the internal tubes can be cut horizontally first and then vertically, as in Procedure B. The heat exchanger can also be cut vertically and horizontally (Procedure C). Both Procedures B and C take less time than A; however, the exposure dose may increase because the shields in the cutting situation cannot be set appropriately in front of the cutting objects.

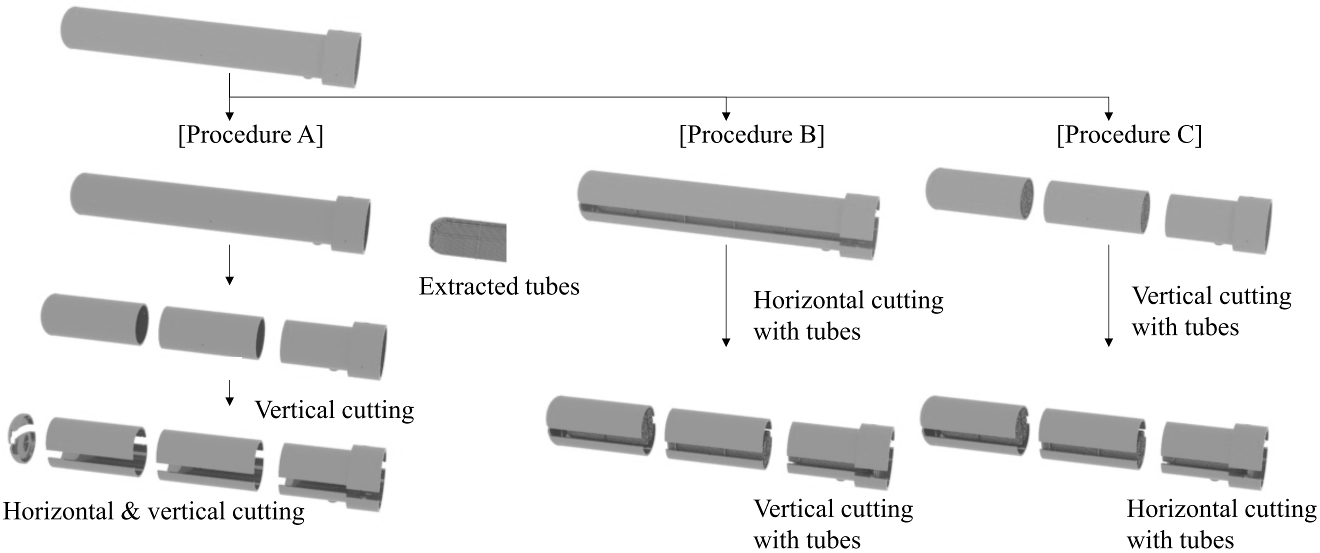

Figure 4.5 Multiple cutting sequences for heat exchanger with internal tubes.

The exposure from bare radioactive sources in extracted tubes occurs while disassembling cut fragments. The dose-rate distribution drastically changes when tools cut the equipment. However, calculating the dose rate at each cutting is impractical and time-consuming. The dose rate is based on allocating the radioactive sources in the equipment material. Although the radioactive sources are decreased linearly by removing the cut objects from the installed locations, the Monte Carlo calculation using PHITS in small intervals takes a long time. Thus, we needed to calculate dose-rate more efficiently in cutting work situations.

4.4.2 Timing of movement for cut fragment objects

In addition to cutting, removal tasks are also performed during dismantling. Radioactive fragments are moved from their original locations to provisional storage space. As a result, the dose rate in the work environment varies during the disassembling processes.

Typical work states were selected to reduce processing time to calculate the changing dose rate in the work environment. The attribute values were set to indicate the type of work as "Dose" in the parameters for multiple cutting sequences, as shown in Table 4.1. In each state of "Dose," the dose-rate distribution at the corresponding cutting, namely "procedure name" and "sequence," was calculated. The dose-rate distributions at the other sequence numbers were not calculated for the types of work such as "Cut." If the complex behaviors of workers are simulated in detail without this kind of table, many parameters and dose rate calculations need to be prepared for calculating the exposure dose. With the help of the uniform table, the exposure doses that depend on several cutting sequences can be calculated more efficiently.

Table 4.2 Parameters for multiple cutting sequences.

Procedure name	Sequence	Group name	Cutting method	Type of work	Placement coefficient				Surface coefficient	
					Place the object "as is", p_1	Transporting to another place, p_2	Transporting adjacent parts, p_3	Stacking objects, p_4	Caps on cut surfaces, s_1	Insulations on cut surfaces, s_2
Procedure A	1	G001	K001	Cut	1	3	3	3	1	1
Procedure A	2	G002	K002	Cut	1	1	1	1	1	1
Procedure A	3	Null	Null	Dose	3.52	1	1	1	1	0.92
Procedure A	…	…	…	…	…	…	…	…	…	…
Procedure B	1	G001	K002	Cut	1	1	1	1	1	1
Procedure B	2	G002	K001	Cut	1	1	1	1	1	1
Procedure B	…	…	…	…	…	…	…	…	…	…
Procedure C	1	G001	K001	Cut	1	1	1	1	1	1
Procedure C	2	Null	Null	Dose	3.52	1	1	1	1	0.92
Procedure C	…	…	…	…	….	…	…	…	…	…

The same table was used when considering both the timing of the movement for cutting fragment objects and the dependencies of cutting sequences on different paths. The column labeled "group name" was used for the cutting activities with a group of parallel virtual cutting planes. The method corresponding to the tools used for disassembling was labeled as the "cutting method."

As shown in Figure 4.5, different cutting workflows were formulated with this sequence data and used to generate cut objects and calculate the exposure dose from the disassembling work.

Placement coefficients were set for treating various situations of placing the cut fragments to calculate the factors affected by the movement of cut objects, such as placing the objects in provisional places as is (p_1), transporting objects to another location (p_2), moving adjacent parts (p_3), and stacking cut objects in temporary areas (p_4). As a safety measure, the effects of the exposure dose rates from the radioactive sources inside the cut objects were treated using the coefficients for insulation effects by placing caps on cut surfaces (s_1) and insulation on cut surfaces (s_2). These coefficients were used to calculate the maximum dose rate in working environments D_{max} as

$$D_{max} = S_{max} \times \prod_{i=1}^{4} p_i \times \prod_{j=1}^{2} s_j \qquad (4.1)$$

Where S_{max} is the maximum dose rate when there are no shields, the exposure dose can be calculated by the product of D_{max} and work hours in Equation 4.1.

Multiple cutting sequences are shown in Figure 4.5. For instance, after a bundle of small-bore tubes is extracted, the outer body can be cut horizontally and vertically in Procedure A. In Procedure B, the tubes can be cut horizontally and vertically again; in Procedure C, the tubes are vertically and horizontally cut. The exposure dose from each disassembling work sequence depends on these cutting sequences since radioactive materials exist inside the heat exchangers.

4.5 Results and discussion

4.5.1 Surface dose rate on waste containers

Figure 4.6 shows a visualization of the calculated dose-rate distribution surrounding waste fragments from a large piece of equipment. Gamma radiation penetrated the surface of the waste container, and the maximum surface dose-rate spot was calculated by comparing the dose rate values on the surface. Then, the system automatically checked whether the packed fragments and the waste container satisfied the regulations.

In this case, the radioactivity of Co-60 for the waste fragments was 9×10^8 Bq/t. This concentration of radioactivity was categorized as very low-level waste [86]. After 100 years, the Co-60 radioactivity level will decrease to about 10^{-6} since the half-life of Co-60 is 5.3 years. Then the above radioactivity will become 9×10^2 Bq/t, and the radioactive waste will be regarded as cleared materials because it is less than 0.1 Bq/g (=10^5Bq/t). This reduction of radioactivity is significant because we do not need to treat the cleared materials as radioactive waste. To do so, identifying and allocating radioactivity would help track the radioactivity of each fragment.

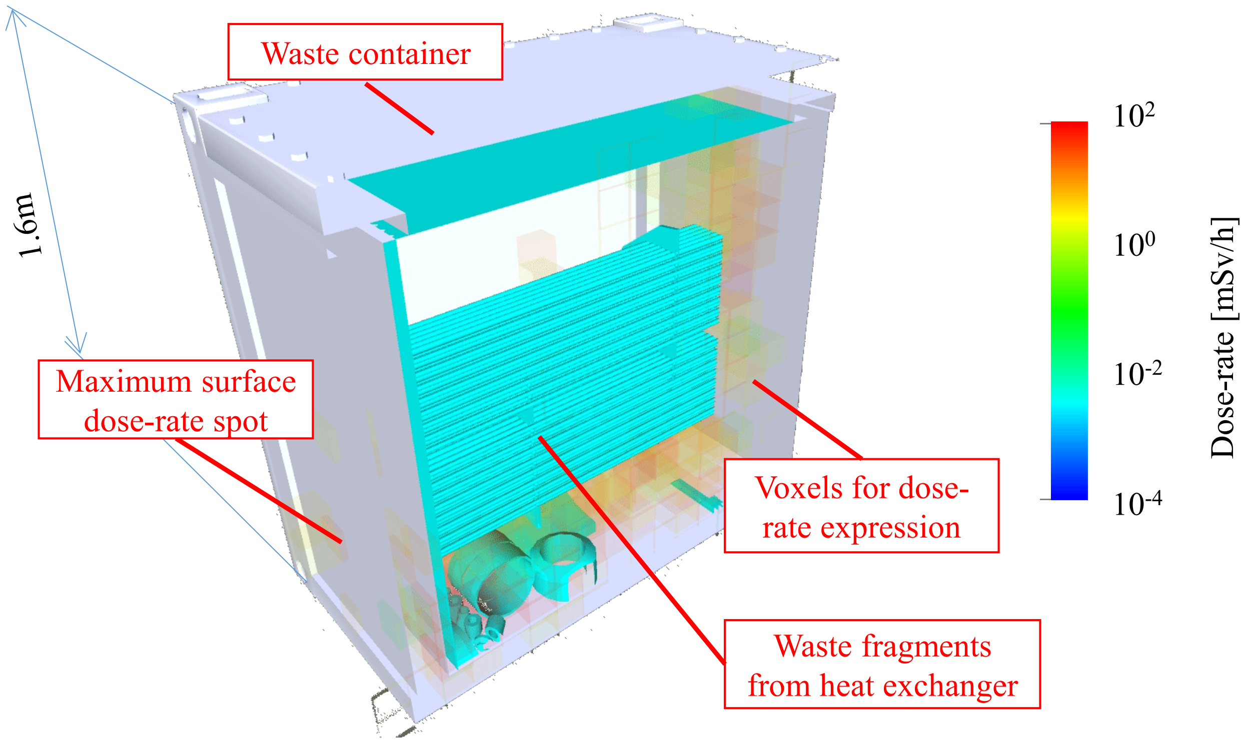

Figure 4.6 Visualization of a waste container with packed waste fragments and dose-rate distribution.

4.5.2 Dependency of accumulated dose on type of cutting procedures

The exposure dose rate depends on the cutting procedure and time. If the cutting lengths are shorter, the exposure dose tends to become higher than longer lengths because the cutting time increases, as shown in Figure 4.7. In Procedure A, the heat exchanger tubes are removed, and then the body and the tubes of the heat exchanger are cut separately. Therefore, the exposure dose of dismantling the heat exchanger with Procedure A becomes higher than that of Procedures B and C. This is due to the placement coefficients p_i, even though the surface coefficients s_j are sufficiently low. This exposure evaluation provides basic information on workers' exposure dose during dismantling tasks for equipment and piping components contaminated with radioactive materials.

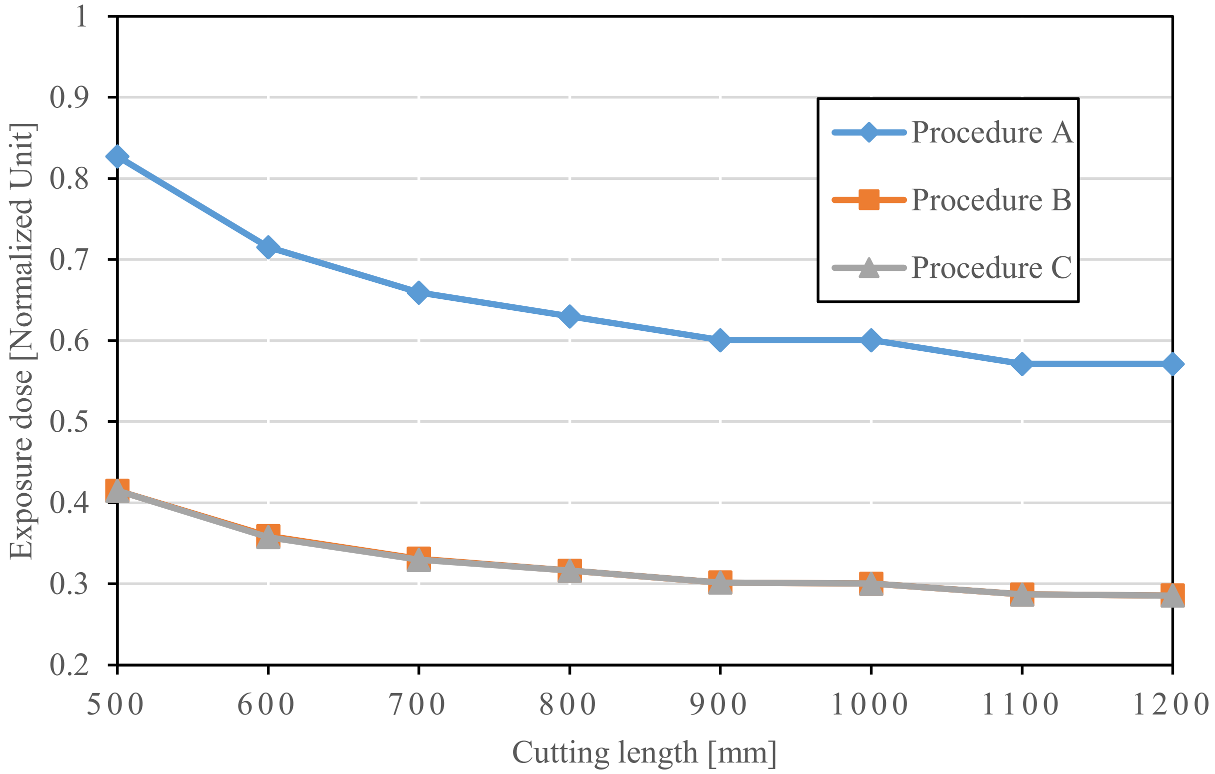

Figure 4.7 Accumulated dose dependency on cutting procedures.

4.5.3 Calculated results of waste quantities and required number of waste containers

The relationship between the number of fragments and cutting length was investigated with the developed system for the integrated cutting and dismantling simulation. As shown in Figure 4.8, the number of fragments decreases when the cutting length increases. The procedure shown in Figure 4.5 affected the number of fragments. If the internal small-bore tubes were cut together with the external body of the heat exchanger as in Procedure C, the number of fragments increased compared with those in Procedures A and B. This result indicates that similar geometric shapes should be cut within their group to reduce the number of objects comprising the waste fragments. While the number of waste fragments decreased when the cutting length was increased, the number of required waste containers increased from 10 to 14. This increase in containers was due to the complexity of the geometric shapes. The decreasing number of waste fragments was flattened between 900 mm to 1000 mm. This flattened range was affected by the remainders of the tubes and the body of the heat exchanger less than 1000 mm, which were cut 900 mm or 1000 mm each.

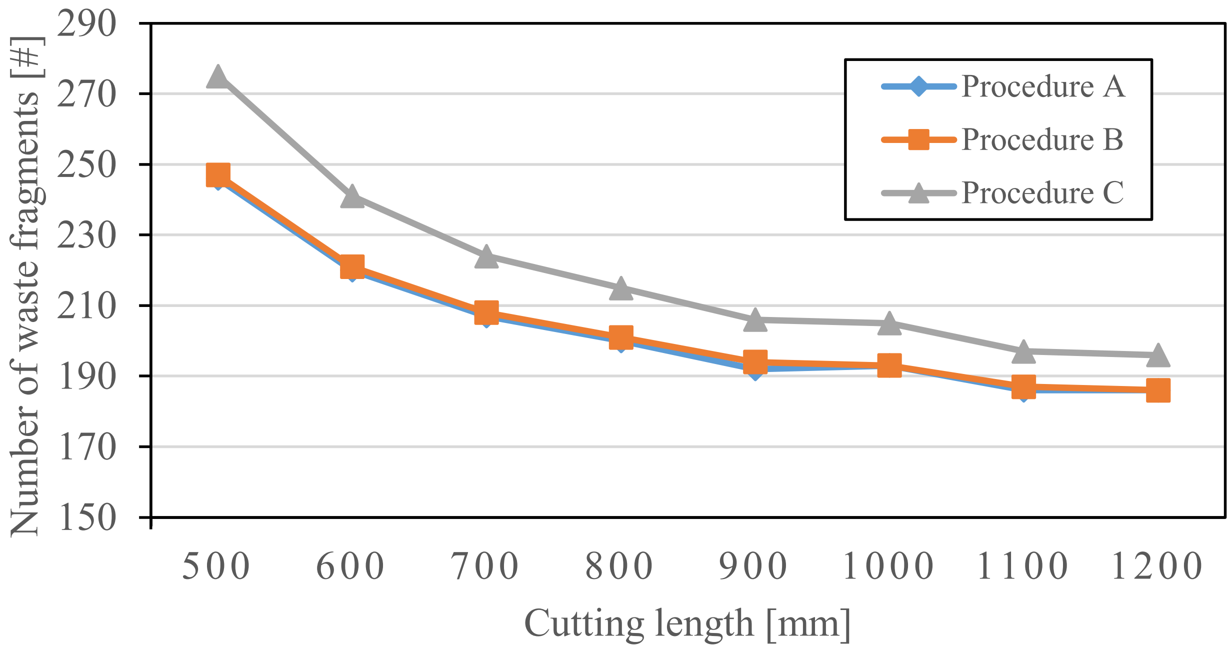

Figure 4.8 Relationship between the number of fragments and cutting length.

4.6 Conclusion on evaluating the precise quantity of decommissioning waste by cutting virtual 3D models of large equipment

This research aimed to minimize the risk of overexposure to radiation and reduce the number of waste containers needed for cutting equipment and piping components into fragments. We have developed an automatic planning method for virtually cutting 3D equipment objects given constraints on container size, radioactivity, weight, and dose rate to evaluate exposure and amount of waste. Cutting sequence data was used to formulate different cutting workflows, generate cut objects, and calculate the exposure dose from disassembling work.

Simulation results were shown for surface dose rate on waste containers, accumulated dose dependency on types of cutting procedures, and calculated results of waste quantities. If the cutting lengths are shorter, the exposure dose tends to become higher than longer lengths because the cutting time increases. This applies to highly contaminated components with radioactive materials as it takes time to complete disassembling. For the waste quantities and required number of waste containers, fragments decrease if the cutting length increases. Further, we verified that similar geometric shapes should be cut within their group to reduce the number of objects comprising the waste fragments. In contrast, the required number of waste containers was unchanged. This was due to the complexity of the geometric shapes.

By calculating the results of the required cutting length and dose-rate distribution for various cutting sequences of large equipment, the developed system is expected to support engineering planning. Using the method developed to estimate the amount of waste, we determined that the system can systematically and effectively support decommissioning engineering. Its ability to map radioactive inventory data to 3D objects enables the automatic dose rate calculation and waste container model generation.

Since the decommissioning projects themselves do not create profits and should be done within a saved budget during the previous plant operation, we must simulate the project's feasibility can be accomplished within budgets. As mentioned in the background, the dismantling processes such as cutting and removing work occupy the more significant portions of the cost for the decommissioning processes. Therefore, the evaluation of durations and waste quantities for cutting work in this research is an especially notable feature of the decommissioning simulation.

5 Real-time simulation methods for Robots with a flexible arm based on computer graphics technology

Abstract: A robot with a flexible arm controlled by a remotely operated water-pressure mechanism has been developed to dismantle objects heavily contaminated by radioactive materials during decommissioning of nuclear power plants. This research aims to create a process planning support system and method that can improve the accuracy of estimating the time required by the robot to complete its dismantling activity, support recovery from delays, and determine the feasibility of conducting a dismantling process in the reactor building. Unique movable arm structures were modeled using a three-dimensional (3D) computer graphics (CG) technology tool. The flexible arm has a more complex mechanism and shapes those of multi-axis robots. The 3D CG model was used to make valid operation sequences for planning the robot's motion. With the help of a prototype system, motion planning can perform to calculate the duration needed for the robot to complete its operation. The estimated time is then used for updating the planned duration of a specific activity in a dismantling schedule. A simplified planning method with few virtual controllers based on a spline inverse kinematics (IK) with a non-uniform rational B-spline (NURBS) curve for an arm comprised of the piston and cylinders pressurized by water was studied to plan the robot behaviors for complex dismantling processes. A prototype system for planning the robot's behaviors was evaluated. It was confirmed that the movement trajectory of the robot and the three-dimensional isometric display could be visualized using the mesh model generated from point-cloud data used to make the environment model of the robot. It was also confirmed that the operations involved in a specific robot activity could be completed within the duration determined in the simulation.

Keywords: Decommissioning, Computer Graphics, Forward Kinematics, Inverse Kinematics, Non-Uniform Rational B-Spline (NURBS) Curve

5.1 Background on real-time simulation methods for robots

In current decommissioning projects for high dose-rate areas in nuclear power plants (NPPs), workers must reduce occupational exposure; thus, dismantling parts must be done with remotely operated robots. It is necessary to dismantle radioactive waste safely and economically: amounts of such waste are estimated to be 3.6% by weight in commercial reactors [86]. Since the number of NPP decommissioning projects is likely to increase, the development of robotic dismantling technology is becoming more critical. A cost analysis of NPP decommissioning projects shows that cutting and dismantling account for a substantial portion of the cost [50]. So far, a system that visualizes calculated radiation dose rates in a virtual reality (VR) environment has been developed for mitigating high dose-rate environments inside an NPP [88]. Dose-rate distributions can be calculated with high accuracy based on the geometry of the facility, materials, and radioactive sources [76]. Moreover, computer simulations of the processes of cutting equipment and waste generation have been developed [77], [79]. In particular, the amount of waste generated can be predicted accurately on a volumetric basis using 3D CAD models [80], [94].

The radiation resistance of the devices making up the robot is a critical issue. To address this issue, we have developed a robot arm with a flexible structure and a hydraulic drive mechanism. Since the flexible arm does not have an electronic controlling mechanism in the robot’s body, it has high resistance to radiation [95]. This robot was described in a survey paper on soft robotic manipulators, which analyzed structures ranging from multi-axis arms to redundant multi-axis arms and arms with many joints and arms that can bend continuously like living organisms [96]. The flexible arm developed by Hitachi is positioned between a redundant multi-axis arm and an arm with many joints.

Autonomous and teleoperated control of robots in a particular environment was simulated with Unity 3D virtual reality software and MATLAB using shared memory for real-time feedback [97]. A dual-manipulator mobile robotic system was developed for nuclear decommissioning, and inverse kinematics controlled the system [98]. A multi-objective genetic algorithm was used to stabilize the motion of robots through inverse kinematics [99]. Visualizations of robots' movements were simulated by the automated generation of the kinematics equations of the robots and analytical solving of their motion planning equations subject to time-varying constraints, behavioral objectives, and modular configuration [100].

Section 2 below describes the issues to be resolved and the objectives of this research. Section 3 describes a CG robot model suitable for the visualization of kinematics. The methods for simulating robots with flexible arms in real-time are described in section 4, and the results of simulations are discussed in section 5. Section 6 is the conclusion.

5.2 Issues to be resolved and objectives of the research

The high dose rates encountered during decommissioning of NPPs have made it essential to deploy remotely operated robots. Hence, it is necessary to plan how long it will take for a robot to perform the desired actions, such as cutting and removing obstacles or operating a manual valve handle on behalf of a human in an environment like the worksite. In addition, when working in the field, it is necessary to check whether the robot works without collisions in an environmental 3D model created before its operation. The following functions are studied for a real-time robot simulation to meet these requirements (Figure 5.1 depicts them as a system configuration):

- A function to import designed 3D models and point cloud data measured in the field and incorporate them in an environmental model for a VR simulator,
- Simulation of kinematics to calculate the coordinates of the robot's crawler and the rotation angles of arm joints by the operation commands in the VR environment, or a function to visualize the posture and motion of the actual robot in real-time,
- Based on VR simulation results, calculate the duration needed to complete an activity on a schedule.

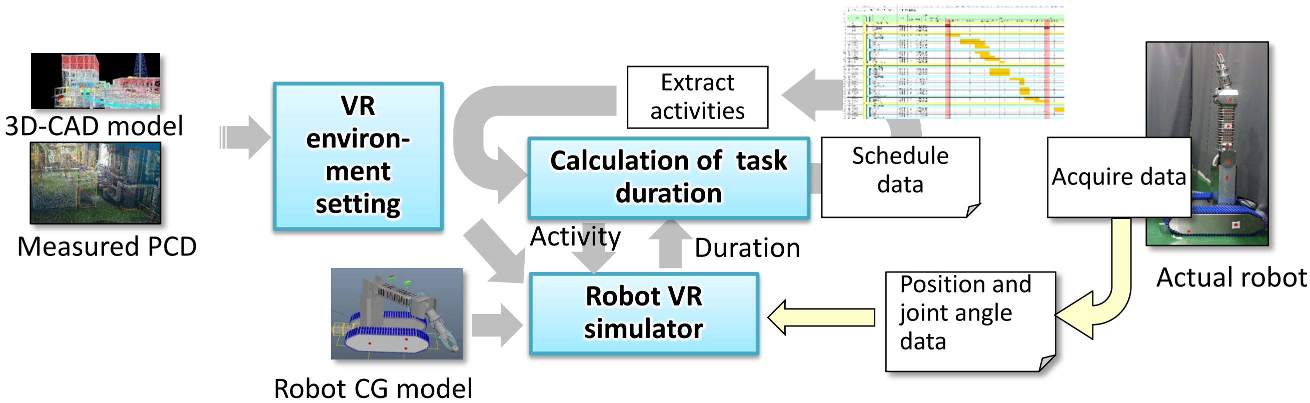

Figure 5.1 System configuration of real-time robot simulation.

5.3 Building a robot CG model suitable for visualization of kinematics

5.3.1 Requirements for real-time robot simulation

This paper describes the research and development of an execution-time calculation of a single task using the VR environment described in (a) and the robot VR simulation described in (b) above. For the VR environment, it is necessary to address an efficient and rapid method for generating shape models that accurately reproduce in-situ 3D measurement data.

Determination of the usage conditions under which the models are generated and the screen is updated about the complexity of the model, which depends on the upper limit of the number of constituent polygon meshes so that the robot can be used interactively in a VR environment without a time delay. In addition, there is the following technical issue regarding the robot VR simulation function. Developing a simple method is necessary to determine the robot's movable space and operation time. Previous studies have investigated these issues and have set forth a development strategy [101]. When decommissioning an NPP, there are places where equipment and piping are not modeled in 3D CAD data. It is not always possible to prepare a VR environment that matches the on-site conditions in advance.

As for the geometric shape model, (i) can create mesh models from 3D measured point cloud data. The 3D point cloud data contain errors, and a method called corner-aware neighborhood (CAN) is used to generate a smoothed mesh shape in which the errors are suppressed by taking the normal vectors near the corners of the object [102]. However, this method cannot be used for plant and piping components whose shapes change significantly. In this research, we developed a way to connect meshes based on the similarity of normal vectors to mesh planes generated from neighboring point-cloud data to reproduce equipment and piping shapes.

The real-time usage conditions of the VR environment in (ii) are described using Unity, a widely used VR software development tool [103]. A mobile device can handle a mesh model with no more than 10^5 vertices, while a PC can take a model with no more than 10^6 vertices.

We decided to express the geometric shape with fewer meshes than the upper limit for PCs so that we could use real-time processing.

A previous study examined a simple method of evaluating the robot's operational space and operation time (iii); in particular, it studied how to automatically plan the movement route of the robot based on a self-position estimation on a 3D map [104]. However, the resulting plans of that method cannot account for complex operations such as removing obstructing objects or opening and closing valves. Hence, we devised a real-time collision checking process to ensure that the robot is operated in a way that conforms to the physical constraints of its environment.

5.3.2 Controlling postures of flexible arms with a spline IK method

It is necessary to recreate the detailed motions of each part of the robot to check collisions operation in the confined three-dimensional environment of a plant. Figure 5.2 is an enlarged picture of the flexible arm parts of the robot. The arm parts are supported by plate springs made of metal and are reinforced so that the initial state is a posture on a straight line. Inside the plate spring, pistons are attached to the joints. The direction in which the piston is compressed or expanded is controlled by the pressure of the water in the cylinder, and the movements of the individual pistons affect the flexible posture of the entire arm. A virtual joint structure called a rig was created to estimate the pose of the individual parts from the overall movement, and the states of components such as pistons were calculated and visualized.

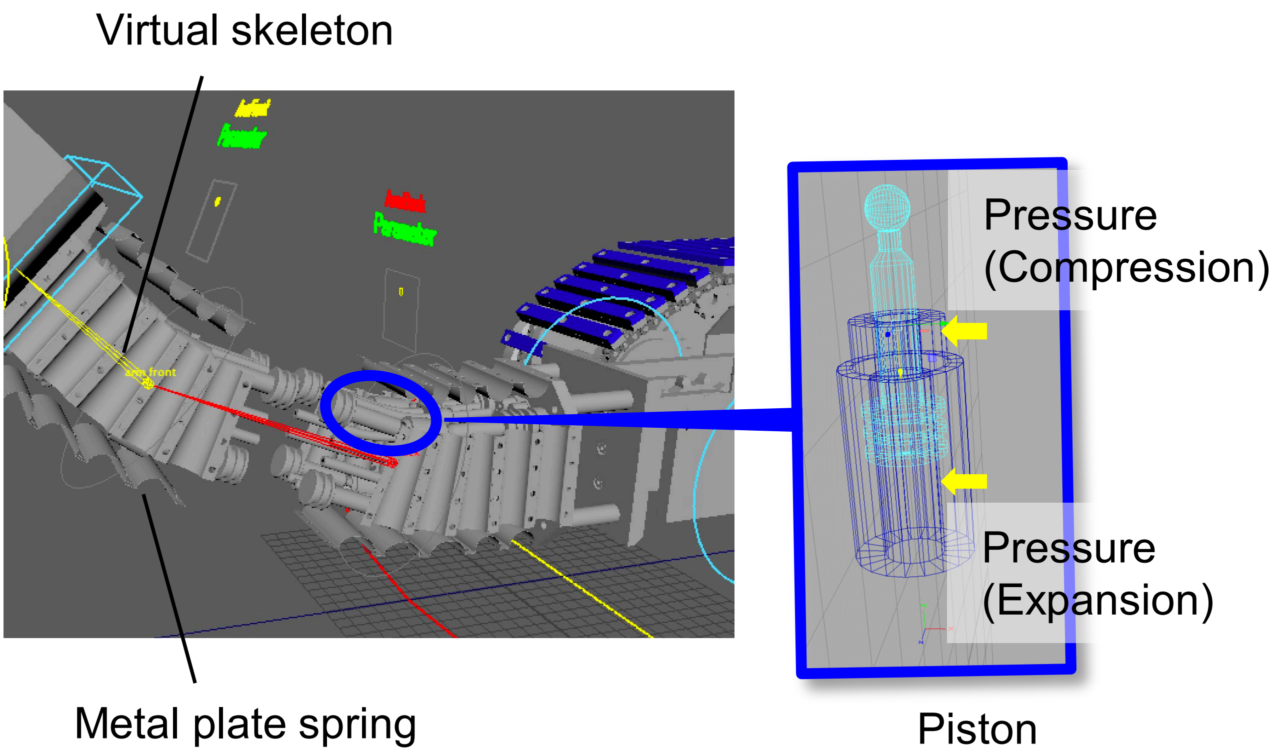

Figure 5.2 Image of a robot with piston movements enabled by water pressure.

Inverse kinematics (IK) was used to simulate the robot's behavior and make it easy to operate. To simplify the discussion of the problem, a case where the behavior of each joint is simulated in a two-dimensional plane by calculating backward from the target position of the robot's hand in the case of a joint arm is shown in Figure 5.3.

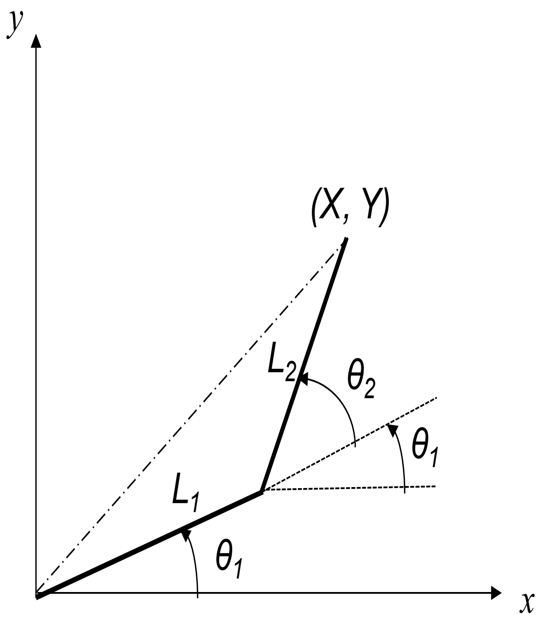

Figure 5.3 Determination of angles from the location of the end-effector of an arm composed of two links.

We assume that an arm has two links of length L_1 and L_2 and that the links are connected at angles θ_1 and $\theta_1 + \theta_2$ to the X-axis. The relationship between the time variation of the hand coordinates (X, Y) and the rotation angles of each joint (θ_1, θ_2) can be expressed as in Equation (5.1), where the time derivatives of the individual coordinates are represented as dots.

$$\begin{pmatrix} \dot{X} \\ \dot{Y} \end{pmatrix} = \begin{pmatrix} L_1 \cos\theta_1 + L_2 \cos(\theta_1 + \theta_2) & L_2 \cos(\theta_1 + \theta_2) \\ L_1 \sin\theta_1 + L_2 \sin(\theta_1 + \theta_2) & L_2 \sin(\theta_1 + \theta_2) \end{pmatrix} \begin{pmatrix} \dot{\theta}_1 \\ \dot{\theta}_2 \end{pmatrix} \quad (5.1)$$

If $\begin{pmatrix} \dot{X} \\ \dot{Y} \end{pmatrix}$ is expressed as $\dot{X}$ and $\begin{pmatrix} \dot{\theta}_1 \\ \dot{\theta}_2 \end{pmatrix}$ as $\dot{\theta}$, the rotation angle of each joint can be obtained from the hand position, as shown in Equation (5.2).

$$J^{-1}\dot{X} = \dot{\theta} \quad (5.2)$$

The matrix J shown in Equation (5.3) is Jacobian, and to find the inverse matrix J^{-1}, we need to find its determinant det(J) and calculate Equation (5.4).

$$J = \begin{pmatrix} L_1 \cos\theta_1 + L_2 \cos(\theta_1 + \theta_2) & L_2 \cos(\theta_1 + \theta_2) \\ L_1 \sin\theta_1 + L_2 \sin(\theta_1 + \theta_2) & L_2 \sin(\theta_1 + \theta_2) \end{pmatrix} \quad (5.3)$$

$$J^{-1} = \frac{1}{\det(J)} \begin{pmatrix} L_2 \sin(\theta_1 + \theta_2) & -L_2 \cos(\theta_1 + \theta_2) \\ -L_1 \sin\theta_1 - L_2 \sin(\theta_1 + \theta_2) & L_1 \cos\theta_1 + L_2 \cos(\theta_1 + \theta_2) \end{pmatrix} \quad (5.4)$$

When det(J) = 0, the relationship is as in Equation (5.5).

$$L_1 L_2 \sin\theta_2 = 0 \quad (5.5)$$

The values of θ_2 that satisfy this condition are 0° and 180° and are called the singular posture. Namely, when L_1 and L_2 form a straight line, IK cannot be used to control the arm. In the case of an average multi-axis robot, the joints are slightly tilted in the direction of bending to avoid a singular posture. However, in the case of the flexible arm used here, the initial posture is in a straight line, and the angle of each joint cannot be calculated with the usual IK. For this reason, a spline IK solver [105], in which the motion of the arm follows a non-uniform rational B-spline (NURBS) curve represented by the CG function to define the smooth shape, is used to represent the flexible arm bending angle. This enables the arm's free bending simulation in three dimensions by matching the joints on the NURBS curve. We decided to use it for the first time in the simulation of flexible arms.

The NURBS curve determines the shape using multiple control points, as shown in Figure 5.4. The curve is represented by a polynomial expression that follows the definition of a B-spline basis function. The point closest to the control point is affected by the curve. Therefore, if the control point is an element called a controller, for rotating the joints of the robot arm, the arm can be freely bent in three dimensions, unlike the method using IK, where the angle is strictly specified, and singular postures are avoided. The spline IK solver determines the start and endpoints of a NURBS curve and makes each control point follow the movement of the endpoint. Although the solver is not a feature of conventional robot simulation tools, it is incorporated in several CG tools, so we decided to use it for planning the robot's posture instead of the usual IK.

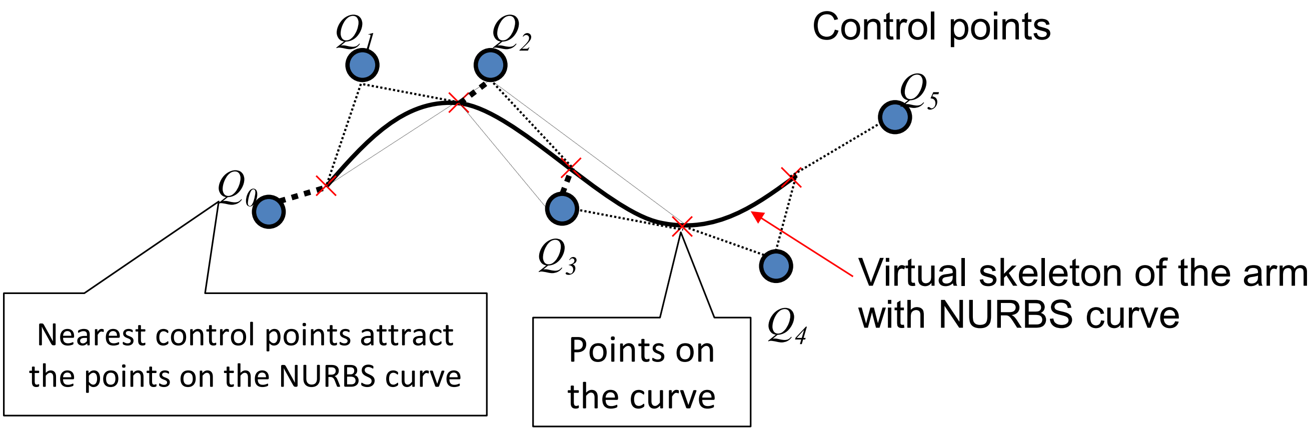

Figure 5.4 Sample curve drawn by NURBS for the spline IK method.

5.4 Real-time simulation of robots with flexible arms

5.4.1 Building environmental mesh objects from 3D point-cloud data

If the results of 3D measurements can be imported into the VR environment on the fly, the efficiency of preparing environmental models for remote operation support can be improved. Hence, a method for generating a mesh model for a VR environment in a few minutes in the field was developed based on 3D measured point-cloud data. Figure 5.5 shows the point cloud data obtained from 3D measurements conducted in a test space enclosed by partitions to verify the robot's operation in a narrow area. It is necessary to subsample the point cloud data to the order of 10^6 points because of the constraints of the development tool on its use in real-time in the VR environment. The figure compares the raw (total) point cloud data consisting of (a) $2x10^7$ points and (b) $1x10^6$ subsampled data points. Shapes common to both figures appear, but there is a gap between the points in (b) data such that the wall seems transparent. Therefore, generating a mesh model of the wall is necessary to prevent the other side from seeing when the robot is close to it and perform a collision check.

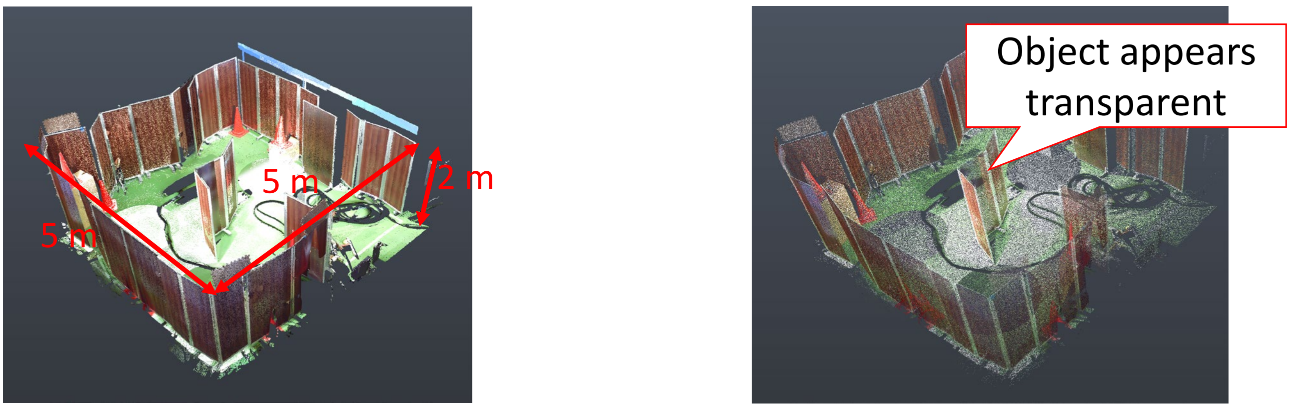

(a) Raw PCD (2.7 x 10^7 points) (b) Sub-sampled PCD (1 x 10^6 points)

Figure 5.5 Comparison between raw and sub-sampled point-cloud data for mesh modeling.

A method to enlarge the faces of the mesh model is to select three points and connect them with corresponding edges to form a face. Faces with similar normal vectors to adjacent faces are consolidated (Figure 5.6). Points of interest are selected from the point-cloud data to generate a mesh model (S-1). N points around the point of interest are chosen (S-2). A weighting factor is given according to distance from the point of interest (S-3). Then a face of the triangular mesh is set around the point of interest with maximum angle $\theta_{t,\ max,}$ and minimum angle $\theta_{t,\ min}$ (S-4). After the faces are generated, the normal vectors of the faces are calculated (S-5). If the angle θ_n between two normal vectors is more minor than $\theta_{n,\ max}$, the two normal vectors are considered similar, and the surfaces are merged (S-6). The above process is iterated to the maximum number of point-cloud data (S-7).

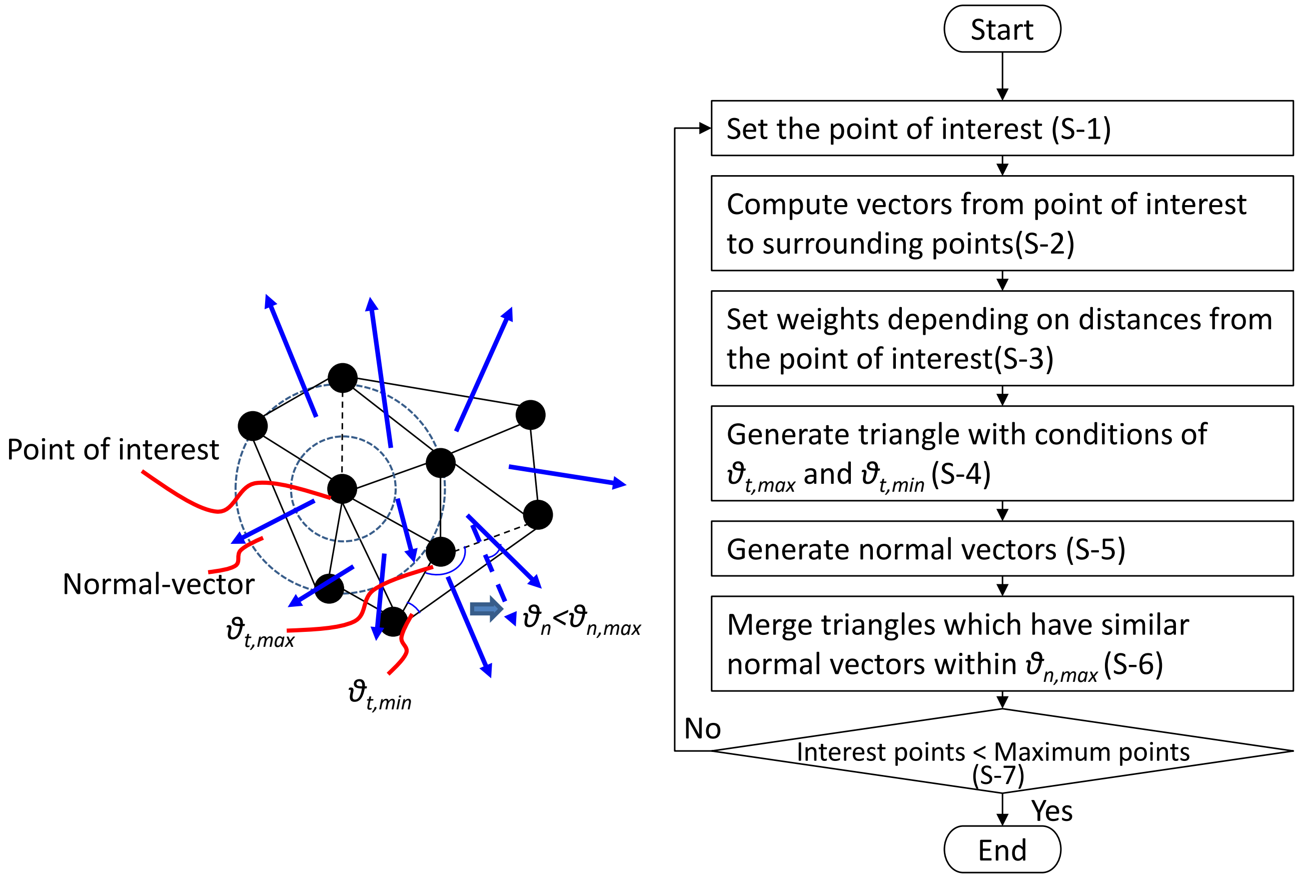

Figure 5.6 Flowchart of modeling mesh from point-cloud data.

5.4.2 Visualization of moving postures for flexible arms in a virtual reality environment

A CG model of a robot was created using a commercially available CG tool (Maya, Autodesk Inc. [106]). Figure 5.7 illustrates the metal plate springs covering the flexible arms and the internal structure. There are sets of hydraulically driven pistons. Each group consists of four pistons, cylinders, and tubes that inject and discharge water. The flexible arm can be bent in three dimensions by adjusting the amount of water injected into the cylinders. Each arm set can be bent up to 45 degrees relative to the x-, y-, and z-axes. Since the arm consists of an upper part and a forearm, it can bend up to 90 degrees relative to each axis. Therefore, by using a simple operation method with the spline IK solver, each piston is set to bend to an average of up to 45 degrees, and the ball joints connect pistons to bend two parts before and after each joint, it sets the constraint to be tilted upwards to 22.5 degrees in each piston alone.

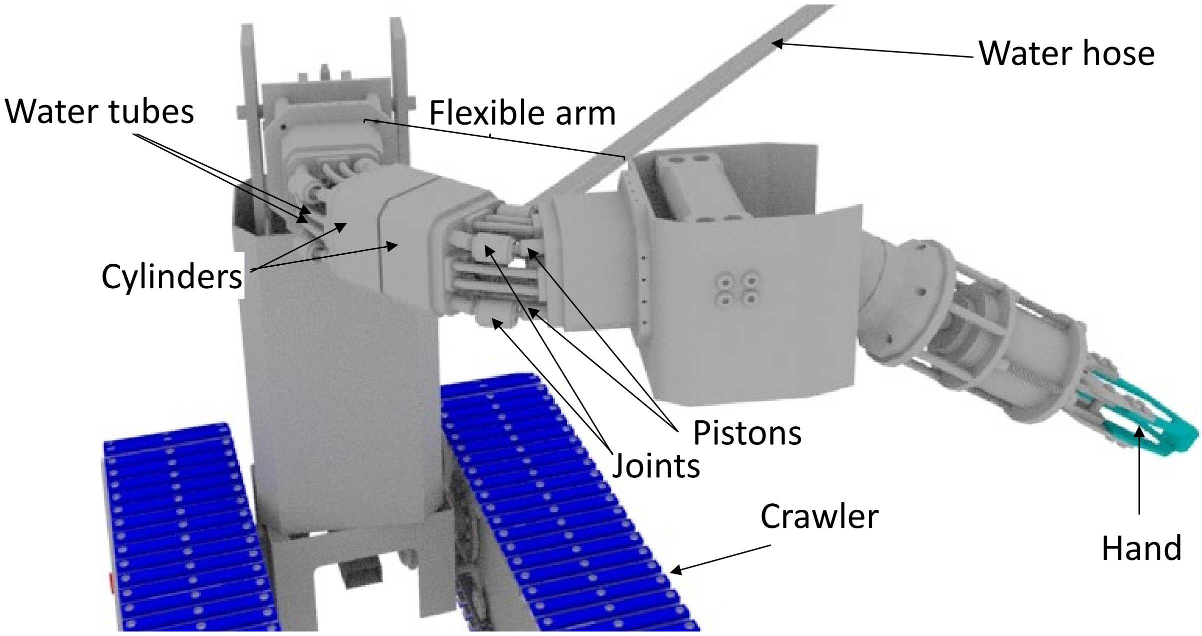

Figure 5.7 Simulation of movement for pistons and water tubes in the flexible arm.

5.4.3 Collision detection of arms objects with environmental meshes

Figure 5.8 shows the model used to check for collisions between the robot and objects in the area where it will be working. A real-time physics computation engine (open-source NVIDIA PhysX) is used for checking collisions [107]. Mesh with a geometric shape, called a mesh collider (the green wireframe part of the diagram), is used for detecting collision events. We decided that the mesh collider should be composed of simple geometric shapes to reduce the colliding portions and events because the processing becomes heavy when the mesh of the colliding body precisely matches the shape of part of the robot. Moreover, the robot's mesh collider was displaced 10 mm upward relative to the floor plane because the floor surface generated from the measured 3D point cloud data has an error of about several millimeters, and if the mesh collider remains in continuous contact with the floor, a state of collision persists. This robot VR application can calculate the duration of the robot's operation and recognize the actual robot's self-position from various three-dimensional views.

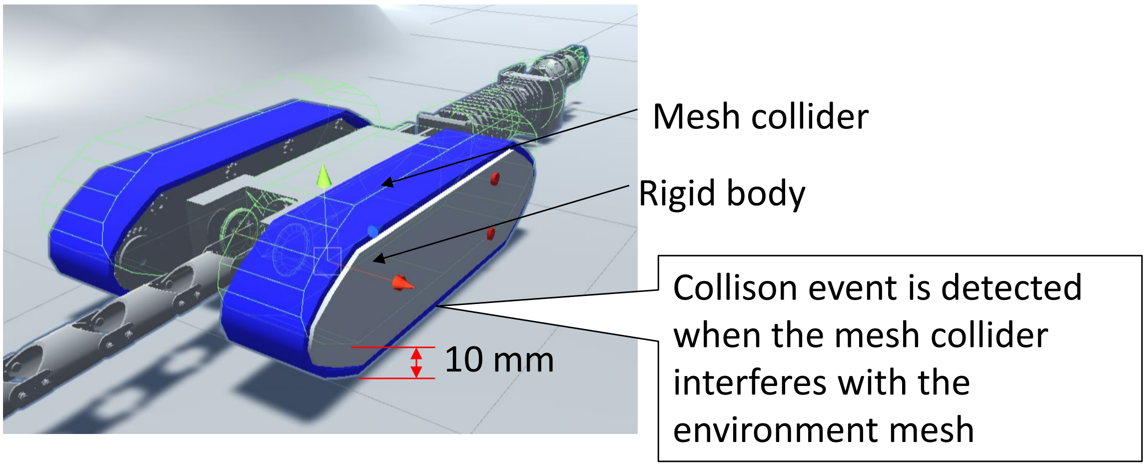

Figure 5.8 Geometric shapes for detecting collisions with a mesh collider based on the PhysX engine.

The relationship between the CG model of the robot and the operational parts is shown in Figure 5.9. The flexible arm and column can move relative to the chassis of the robot as follows: swing 1 move the column upwards through an angle, turn 1 rotates swing 1, swing 2 moves the flexible arm downwards through an angle, swing 3 moves the hand end effector downwards through an angle, suspension contracts the hand-end effector, and turn 2 rotates the hand end-effector. These operational parts of the arm can be bent up to 90 degrees in four directions (bend_up, bend_down, bend_left, and bend_right).

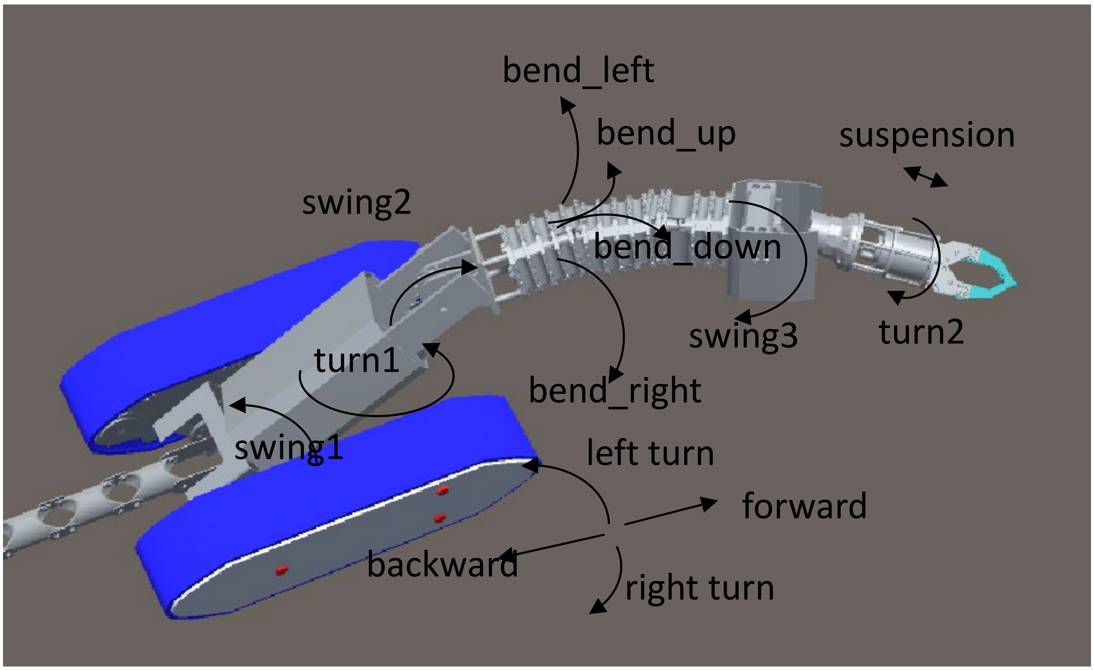

Figure 5.9 Parameters for operating the robot with a flexible arm.

5.5 Results and discussion

5.5.1 Generating a mesh model from a point-cloud data

As mentioned in section 5.4.1, the maximum number of meshes should be limited to 10^6 for a VR simulation to be carried out in real-time. The quality of the generated mesh models was compared to the processing time needed to generate the model.

An example of a mesh model generated from the point cloud data is shown in Figure 5.10. Figure 5.10 (a) shows the registrated point-cloud data obtained by 3D laser scanning of three locations in a field test. It consists of 2.7×10^7 points. Figures (b) and (c) show mesh models obtained from 10^6 and 10^7 points. In these models, the meshes of the wall do not appear transparent as the red cone in Figure 5.10 (a) when the robot is close to the obstacle and can be visualized as an obstacle. The number of mesh faces in each case is 1.9×10^6 and 1.8×10^7, and it is easy to see that the surfaces match those in the raw data.

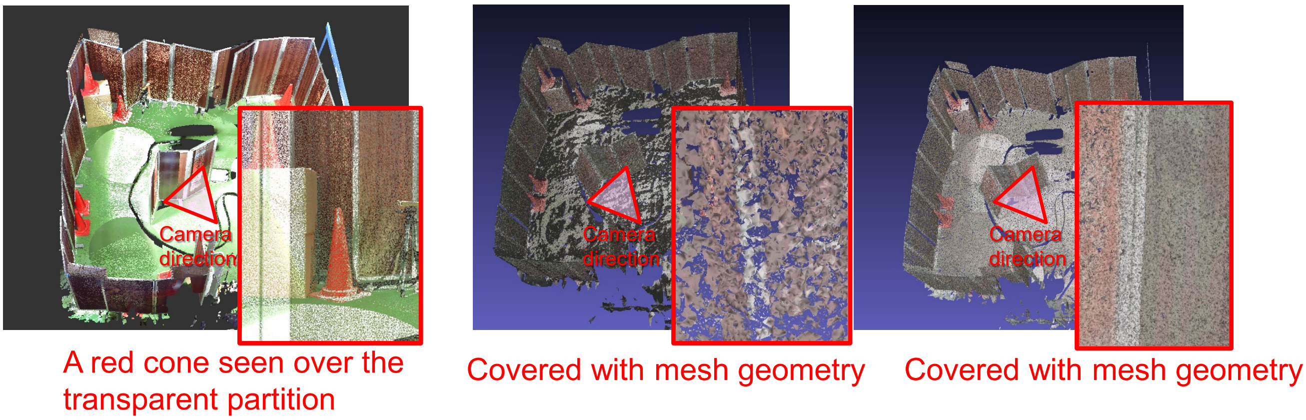

(a) Registered PCD (2.7×10^7 points)

(b) Mesh model generated from 10^6 subsampled PCD points (1.9×10^6 faces)

(c) Mesh model generated from 10^7 subsampled PCD points

Figure 5.10 Comparison of mesh models and corresponding point cloud data.

Figure 5.11 shows the time it takes to generate the mesh model from the point cloud data. It took 2 minutes to complete the processing of 10^6 points that were sub-sampled from the raw point-cloud data. When 10^5 points were obtained by the laser range finder (LRF) mounted on the robot, the model was completed in 20 seconds. When 10^7 points were used, it took 6 hours to make the model. Therefore, the processing time increased in proportion to the square of the number of points. If processing data can be done offline, 10^7 points could be used, and it would be possible to simulate in an environment model made of smooth geometric shapes. However, capturing the mesh model within a few minutes of making a 3D measurement in the field would be desirable. Therefore, we consider that 10^6 points of point-cloud data are a practical limit regarding the processing time of the mesh model.

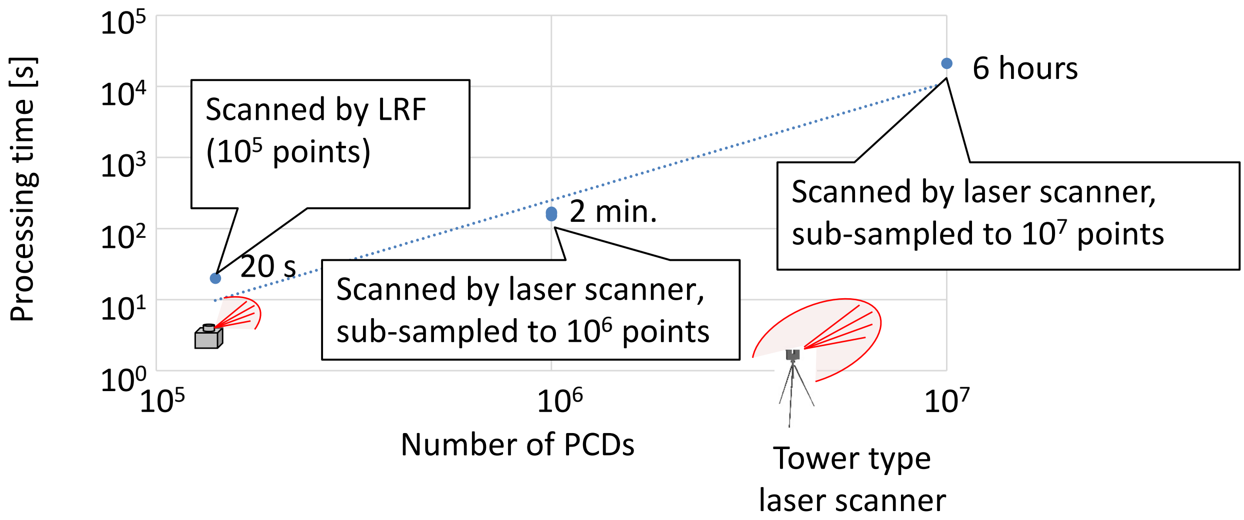

Figure 5.11 Relationship between mesh model size from point-cloud data and its generation time.

The screen update speed of the simulation was verified in the case of using a mesh model generated from large-scale point-cloud data. The verification used a PC equipped with an Intel Xeon ES-2603, 1.6 GHz 2CPU. The VR simulation of the mesh model generated from 10^7 points had a screen update speed of 1-2 frames per second; thus, a mesh model of this size is unsuitable for real-time operation. It is said that the screen update speed for real-time operation should be 30 frames per second or more. When the mesh model was generated from 10^6 points, the screen update speed in the VR simulation was 60 frames per second. Consequently, 10^6 point-cloud data was adequate for the VR simulation.

If the number of points is decreased, the geometric shape of the resulting mesh model will be of inferior quality, as shown in Figure 5.10 (b). We thought that the quality of the geometric shapes could be improved by adjusting the parameters when the mesh is generated. Figure 5.12 shows the relationship between the number of meshes generated with K_s points to be searched in the vicinity of the point of interest and the number of generated faces. The characteristics of a cone mesh model were examined for various values of K_s. The diameter of the bottom of the conical shape was 278 mm. It corresponds to the maximum size of small-bore piping components that would be cut and removed during decommissioning. Therefore, the cone was a reasonable size for this evaluation. K_s is a parameter that determines the complexity of the mesh shape that can be generated in the vicinity of a particular point.

The number of generated geometric faces increases as K_s increases, but the growth rate tends to saturate beyond a specific value of K_s. This tendency appears when there are fewer points in the neighborhood, and the resulting shape depends significantly on which points are chosen. When K_s is 20, the cone appears incomplete with numerous fractures. When K_s are 50 and 100, the cone is complete and has fewer fractures. Moreover, it is not efficient to increase the K_s more than necessary; it takes 18 minutes or more when K_s is 1000 but only 4 minutes when K_s is 100. Thus, K_s should be set from 50 to 100 to generate mesh models of equipment or piping components with many changes in shape.

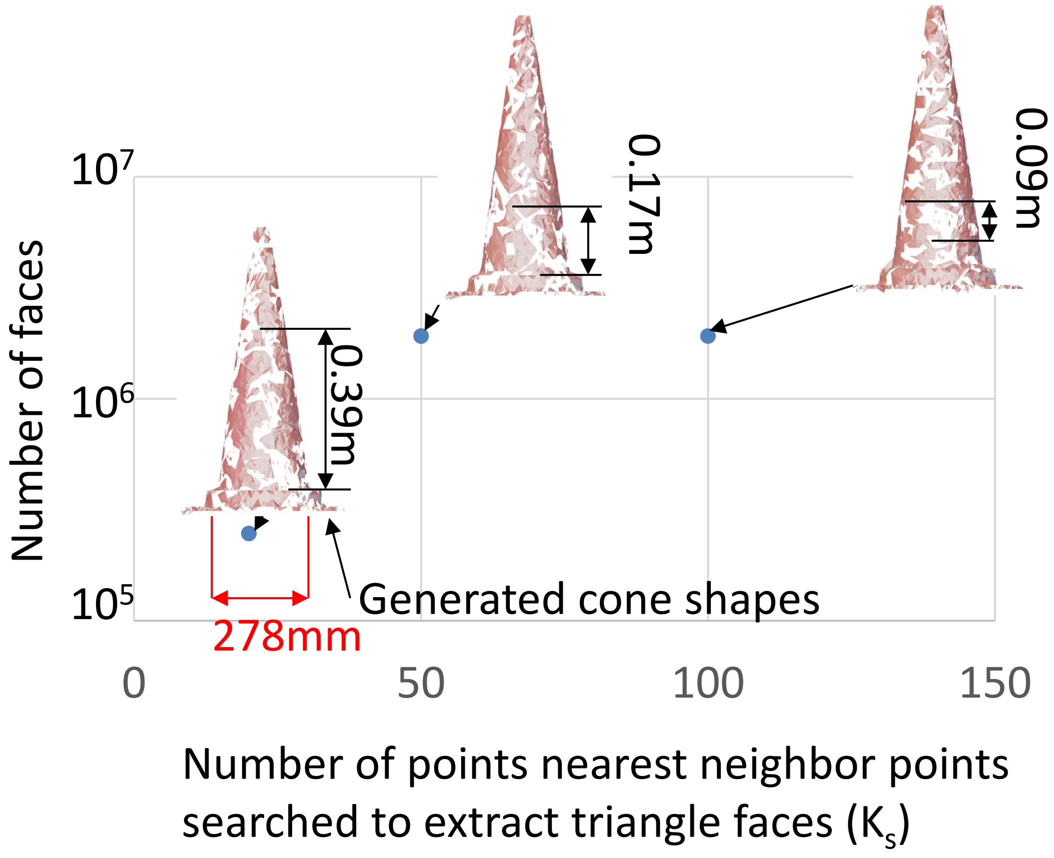

Figure 5.12 Quality of generated meshes.

5.5.2 Checking the collision detection function of the robot in the mesh model

Figure 5.13 shows the superimposed movement locus of the center coordinates of the crawler as blue points on the point-cloud data. The white square on the floor shows an area of 80 cm × 80 cm. This VR application can be used to confirm the coordinates 180 seconds after arrival at the endpoint of the center of the crawler and 20 seconds after the start of the movement. Moreover, it can confirm the robot's posture with the 3D isometric display. Therefore, the collision detection function enables users to ensure the postures of the robot even if obstacles impede the camera views.

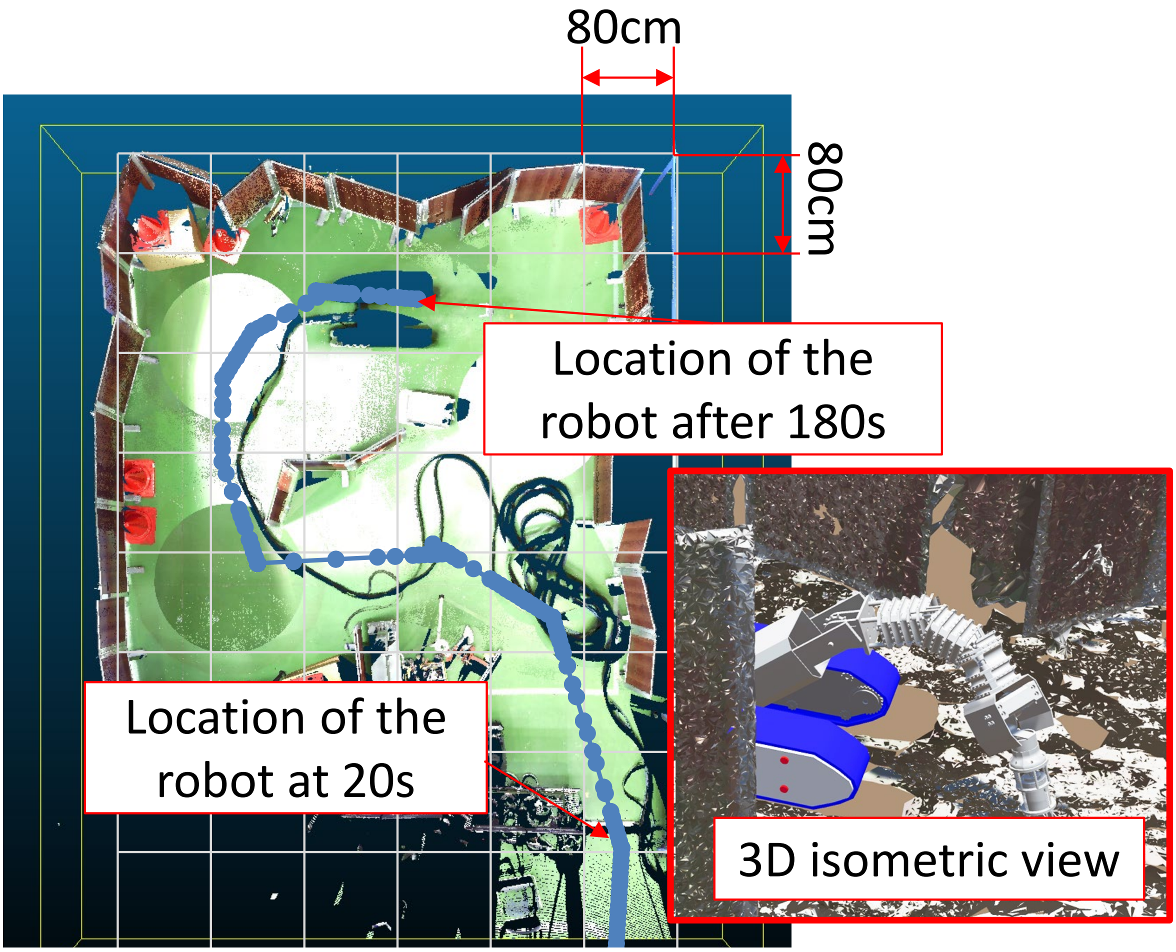

Figure 5.13 Trajectory of the robot in the field test.

Figure 5.14 shows how the robot hand detects rubble and its contact situation. The situation at the moment of contacting the rubble was detected from the posture. When a collision event was detected, processing temporarily increased; consequently, the screen was updated at about 30 frames per second, i.e., almost half that of a situation with no collision. Therefore, it was found that 60 frames per second or more is a desirable update speed when no collision occurs.

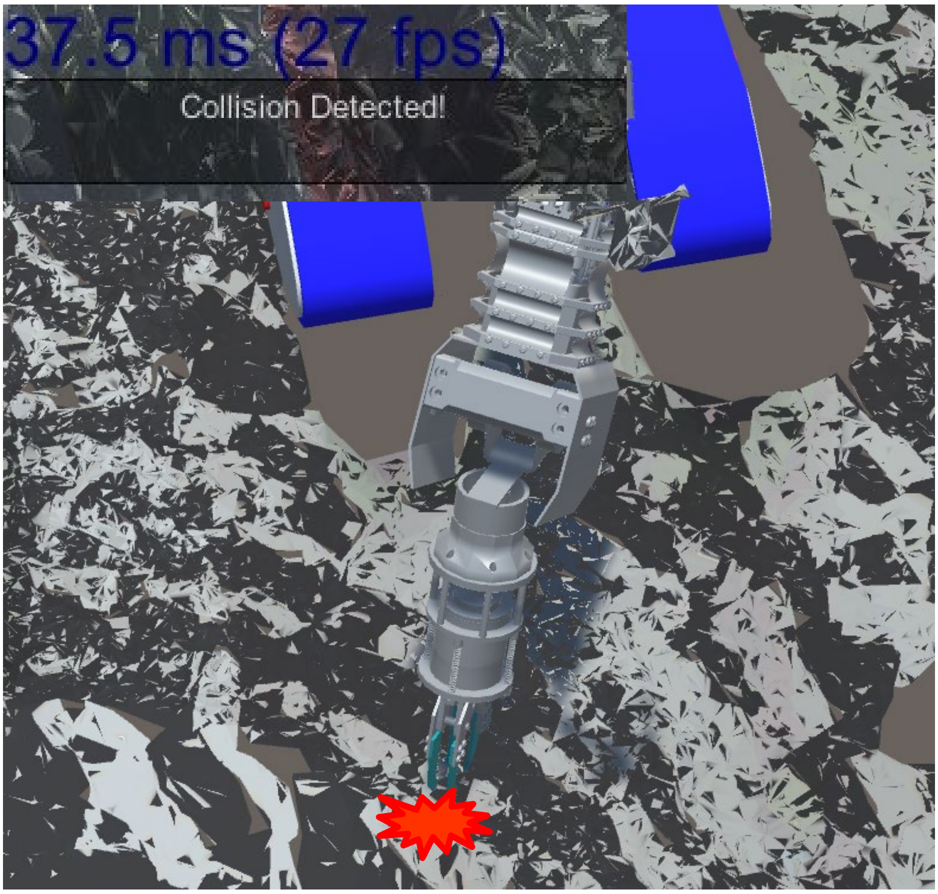

Figure 5.14 Example robot posture with flexible arm avoiding collisions against obstacles.

5.5.3 Evaluation of moving time of the robot

Figure 5.15 shows the recorded times of movements and changes in the angle of the flexible arm. By changing the angle of the arm (swing1 to swing3, bend_left, up, down, and right) at a rate of 10 degrees per second, the manual operation took 130 seconds to grasp and remove rubble. It took 13 operation steps to contact the rubble from the moment the rubble was recognized. The operator completed the movements (while looking at the screen) about three times faster than the robot's operation. The planned operation can be checked more quickly with the VR application than the actual robot hardware in a mockup field test. In addition, the difference between the start and the end of a series of operations can be assigned as the duration of the actual scheduled activity.

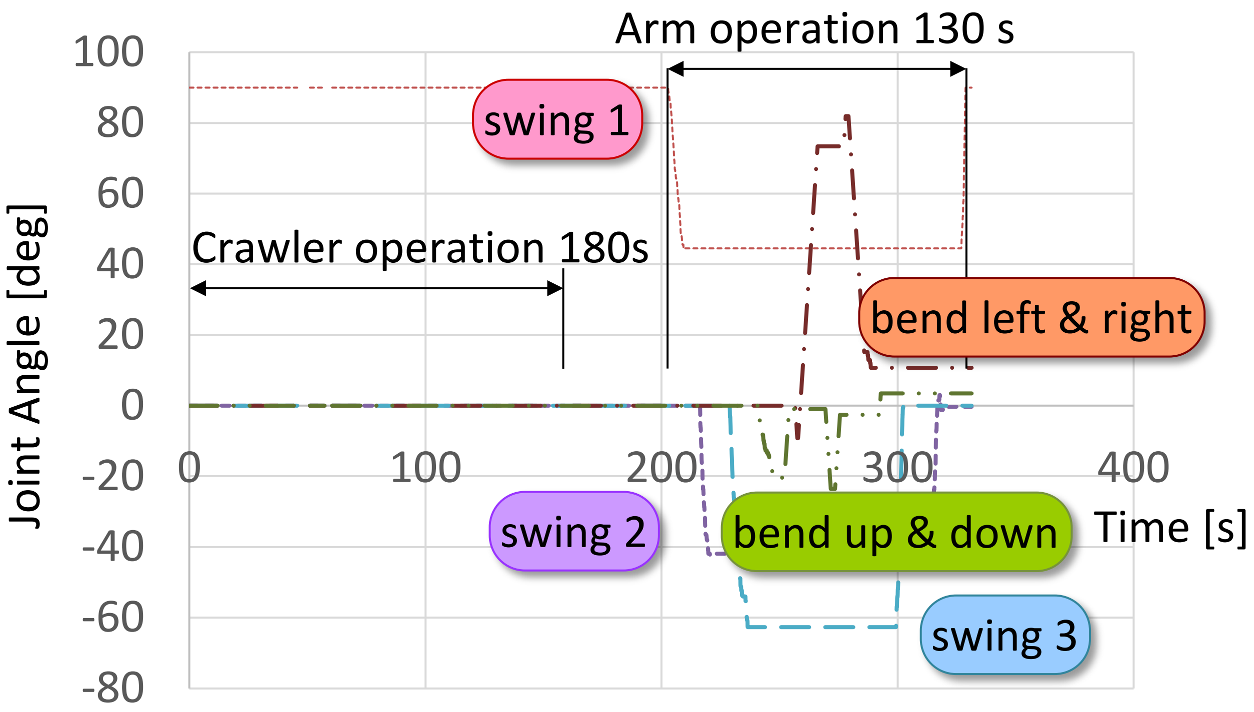

Figure 5.15 Recorded the time of the movement and the changes in the angle of the flexible arm of the robot.

The mesh is very coarse when the number of points is small, as shown in Figure 5.10 (b) because the normal vectors of the triangular mesh formed by the edge between points and the surface are not smoothed or optimized in the VR environment. The simulation in the VR environment used such a coarse mesh model because its purpose was to detect collision events. In contrast, more detailed simulations that incorporate the mechanical stability of the center of gravity of the robot on unstable surfaces, lifting of the object to be removed, and dynamics such as multi-legged walking will require more sophisticated processing such as smoothing of the mesh, repairing splits in the mesh surface, or replacing the point-cloud based mesh with a 3D CAD model. We will build mesh models that can be used for dynamics simulations in the future. In addition, we will use the calculated duration in this VR environment as input for the schedule optimization system. In this way, we will develop a schedule optimization technology that checks and updates the duration of an activity in the planned schedule corresponding to various operating scenarios.

5.6 Conclusion on real-time simulation methods for Robots with a flexible arm based on computer graphics technology

A support system of a robot operated remotely for high dose-rate environments plays a crucial role during decommissioning of NPPs, especially for the accident plant. Before deploying remote-controlled robots to a site, it is necessary to confirm that the operation plans are safe and efficient. In this research, we have developed the technology required to calculate the working duration by checking that the robot operates without colliding with obstacles, such as equipment and piping components on floors and walls, in a virtual environment made of a mesh model built from 3D point-cloud measurements.

A method that enlarges face surfaces was investigated to generate mesh models efficiently. It generates triangle surfaces by selecting three points for each face and consolidating the nearest surfaces with normal vectors in similar directions as one face. The appropriate number of point cloud data and parameters used for generating mesh models were evaluated by examining the quality of the generated mesh model and the processing time. As for the point cloud data, a 5 m x 5 m test field enclosed by partitions for testing the robot's behaviors in a narrow space was measured with a 3D scanner.

As a result of the evaluation, it was decided to generate mesh models from point cloud data consisting of 10^6 points, with which the operator's screen can be refreshed at 60 frames or more per second. The number of points to be searched in the vicinity of a point of interest should be 50 to 100 for generating faces with fewer cracks. In this case, the calculation time was less than two minutes.

As for detecting collisions, a CG model of a robot with a flexible arm was made, and collisions with obstacles were detected by simplifying the mesh shapes, including that of the robot.

With the developed functions, we confirmed that the movement trajectory of the robot and a three-dimensional isometric display from an arbitrary camera angle could be visualized by using the mesh model as the environment model of the robot. In addition, we confirmed that the moment of contact with rubble could be detected and displayed. The speed at which the user operates while looking at the screen is faster than the actual robot's angular change. Work planning can be shortened using this VR application instead of an actual hardware robot. The difference between the start and end times of a series of operations conducted in the VR environment can be scheduled as the duration of the actual working activity.

Previously, experts who know how to work in maintenance made engineering schedules for decommissioning projects. However, the schedules with Gantt-Charts made by experts show durations and milestones of the project mainly; the information for enough working space taken in each task is not well known. The developed technology to link the information between the duration of a specific task and the behavior of a remotely operated robot can be used for stakeholders to understand the decommissioning tasks in terms of time and robotic behaviors.

6 Summary of the research on decommissioning simulation based on plant lifecycle information management for NPPs

6.1 Summary of the research

Overviews of the dissertation as an introduction are described in chapter 1. Then, an integrated semantic model for plant lifecycle management that can be applied NPPs and its applicability to checking consistencies for engineering drawings among different sections in chapter 2. After that, a method that evaluates the quantity of waste for decommissioning an NPP is studied, and the procedure is verified with a whole 3D model of the NPP in chapter 3. Moreover, an exact number of dismantled fragments by cutting virtual 3D models of large equipment is described for examining and verifying the automatic generation of cut objects with a 3D model and its applicability for exposure dose evaluation in chapter 4. Finally, real-time simulation methods for robots with flexible arms based on computer graphics technology to support the planning of remote operations in a severe environment inside NPPs are described in chapter 5. In the following sentences, summaries of each chapter are stated.

6.1.1 Overview of the dissertation as an introduction

In this research, methods for data integrations and exchanges are studied for long lifecycles of NPPs over a hundred years, including the phase after the decommissioning of NPPs. Then, a support system for decommissioning engineering processes based on a 3D CAD model for a whole NPP and technologies for planning and estimating occupational exposure dose rate for workers related to cutting and dismantling large equipment are studied. As for the accident plant, work planning with remotely operated robots with water pressure controls can resist extraordinarily high dose rate areas.

In this research, there are four unique features. At first, core elements of information representation are extracted as a standard information model based on International Standards, such as STEP, ISO 15296, and so on. Then practical technologies for maintaining consistencies for engineering information related to plant lifecycles of an NPP have been evaluated. The link structures for objects with associations have been used for representing piping components and equipment for the NPP here, and it has been expressed with an original markup language. Following the network shape information, which consists of objects and associations, we can identify impacts by changing engineering information. With a design change, we can apply the data to maintain consistency between design data and actual project data. Hence, the resulting technologies have academic significance.

Secondly, based on the above information model, the radioactive waste inventory of an NPP is mapped to piping components and equipment as engineering attribute information with the 3D spatial distribution. The dose rates in the surrounding area are calculated automatically. With these functions, the economy, and the safety indexes of the decommissioning, such as waste quantities and occupational exposure dose, can be evaluated. Therefore, the developed technologies are applied to decommissioning engineering processes rationally and effectively.

Thirdly, based on 3D models for large equipment to be decommissioned, an automatic planning method for cutting virtually in the 3D space and formulating cutting procedures that consist of cutting sequence data based on multiple dismantling scenarios have been studied in this research. With the help of the study, the cutting sequence data can be used not only for generating segmented objects of equipment but also for calculating occupational exposure dose during dismantling work. Because of the evaluated results, workers at the dismantling site can avoid excessive exposure doses. We can minimize the number of containers for piping components and equipment waste. With these results, it is significant to do rational, detailed planning for the decommissioning project.

And finally, as for the accident plant, technologies for detailed planning with robots that have flexible arms controlled by water pressure in a virtual environment have been studied. The water pressure control is suitable for operating remotely in an extraordinarily high dose rate space. This research has developed simplified operation methods with a few virtual controllers for the complicated constraints of moving flexible arms. Then, a prototype system was designed to make moving sequences for planning robot operations. With the help of this research, the accuracy for dismantling work hours is calculated for dismantling tasks, and it supports recoveries from delays in the planned schedule. Consequently, the developed methods provide a significant work planning support system to judge feasible dismantling processes from ample search space.

6.1.2 Application of data model for a drawing data refining system according to plant product lifecycles

A drawing data refining system was developed based on the technical information infrastructure (TECHNOINFRA) set in the IMS/VIPNET project. Based on a common information model, CAD data translators from 2D drawings and 3D models were built, and their browsers were also made. A continuous drawing data refining system has been constructed to adopt every task in the plant-related work with its design data, such as process and instrumentation 2D drawings. This system verified and validated data consistency between actual project and design data. This drawing data refining system uses efficient mechanisms for piping lines with less memory. In evaluating this system, the efficiency and effectiveness of the achieved functions were shown.

6.1.3 The evaluation system of waste quantities for decommissioning planning of nuclear power plants

We have developed an intelligent 3D model that assigns radioactive inventory data that is substantial amounts of data to 3D objects and the ability to automatically generate the distribution of the spatial dose rate and the waste containment model. This allows the appropriate cutting lengths of equipment and piping components, the number of waste inmates required, and the calculation of the accumulated exposure dose based on various dismantling scenarios and can support the judgment related to the decommissioning plan. We also confirmed that we could support the decommissioning engineering systematically and efficiently by using simulation results related to waste volume and carrying out.

6.1.4 Evaluating the precise quantity of decommissioning waste by cutting virtual 3D models of large equipment

This research aimed to minimize the risk of overexposure to radiation and reduce the number of waste containers needed for cutting equipment and piping components into fragments. We developed an automatic planning method for virtually cutting 3D equipment objects given constraints on container size, radioactivity, weight, and dose rate to evaluate exposure and amount of waste. Cutting sequence data was used to formulate different cutting workflows, generate cut objects, and calculate the exposure dose from disassembling work.

Simulation results were shown for surface dose rate on waste containers, accumulated dose dependency on types of cutting procedures, and calculated results of waste quantities. If the cutting lengths are shorter, the exposure dose tends to become higher than longer lengths because the cutting time increases. This applies to highly contaminated components with radioactive materials as it takes time to complete disassembling. For the waste quantities and required number of waste containers, fragments decrease if the cutting length increases. Further, we verified that similar geometric shapes should be cut within their group to reduce the number of objects comprising the waste fragments. In contrast, the required number of waste containers was unchanged. This was due to the complexity of the geometric shapes.

By calculating the results of the required cutting length and dose-rate distribution for various cutting sequences of large equipment, the developed system is expected to support engineering planning. Using the method developed to estimate the amount of waste, we determined that the system can systematically and effectively support decommissioning engineering. Its ability to map radioactive inventory data to 3D objects enables the automatic dose rate calculation and waste container model generation.

6.1.5 Real-time simulation methods for robots with a flexible arm based on computer graphics technology

A support system of a robot operated remotely for high dose-rate environments plays a crucial role during decommissioning NPPs. Before deploying remote-controlled robots to a site, it is necessary to confirm that the operation plans are safe and efficient. In this research, we developed the technology required to calculate the working duration by checking that the robot operates without colliding with obstacles, such as equipment and piping components on floors and walls, in a virtual environment made of a mesh model built from 3D point-cloud measurements.

A method that enlarges face surfaces was investigated to generate mesh models efficiently. It generates triangular by selecting three points for each face and consolidating the nearest surfaces with normal vectors in similar directions as one face. The appropriate number of point cloud data and parameters used for generating mesh models were evaluated by examining the quality of the generated mesh model and the processing time. As for the point cloud data, a 5 m x 5 m test field enclosed by partitions for testing the robot's behaviors in a narrow space was measured with a 3D scanner.

As a result of the evaluation, it was decided to generate mesh models from point cloud data consisting of 106 points, with which the operator's screen can be refreshed at 60 frames or more per second. The number of points to be searched in the vicinity of a point of interest should be 50 to 100 for generating faces with fewer cracks. In this case, the calculation time was less than two minutes.

As for detecting collisions, a CG model of a robot with a flexible arm was made, and collisions with obstacles were detected by simplifying the mesh shapes, including that of the robot.

With the developed functions, we confirmed that the movement trajectory of the robot and a three-dimensional isometric display from an arbitrary camera angle could be visualized by using the mesh model as the environment model of the robot. In addition, we confirmed that the moment of contact with rubble could be detected and displayed. The speed at which the user operates while looking at the screen is faster than the actual robot's angular change. Work planning can be shortened using this VR application instead of an actual hardware robot. The difference between the start and end times of a series of operations conducted in the VR environment can be scheduled as the duration of the actual working activity.

6.2 Plans related to the decommissioning simulation

Many organizations study semantic model expressions. However, the standardization bodies, such as ISO and IEC, do not want to create duplicate ways of expression and overlapping between organizations. Therefore, ISO and IEC made a joint working group (JWG), as shown in Figure 6.1 [108]. On the ISO side, they have made International Standards, such as “industrial automation systems and integration — parts library — part 42: description methodology: a methodology for structuring parts families (ISO 13584-42) [109]”, “industrial automation systems and integration — integration of life-cycle data for process plants including oil and gas production facilities — part 4: initial reference data (ISO/TS 15926-4) [110]”, and “industrial automation systems and integration — Product data representation and exchange — part 239: Application protocol: product life cycle support (ISO 10303-239) [111].” On the other hand, on the IEC side, they have made International Standards relevant to all electrical, electronic, and related technologies, “standard data element types with an associated classification scheme for electric components - part 2: EXPRESS dictionary schema (IEC 61360-2) [112]”, and “standardized product ontology register and transfer by spreadsheets - part 1: logical structure for data parcels (IEC 62656-1) [113]”. Those standards are referred to and expanded to each industry. However, the methods to express dictionaries are different between ISO and IEC. Therefore, the ISO and IEC have formed a joint working group. Based on International Standards, reference data libraries (RDLs) have been made in the ISO at various levels, such as industrial RDLs, company RDLs, project RDLs, and private RDLs.

On the other hand, standard data dictionaries (CDDs) have integrated electrical and electronic components on the IEC side. Although each ISO and IEC organization has different schemes for expressing dictionaries, those organizations have started activities to be interoperable between technical dictionaries in each industry. The underlying concept is not inventing new methods and libraries that represent the same things. The perfect idea of expressing an item should be from one provenant database.

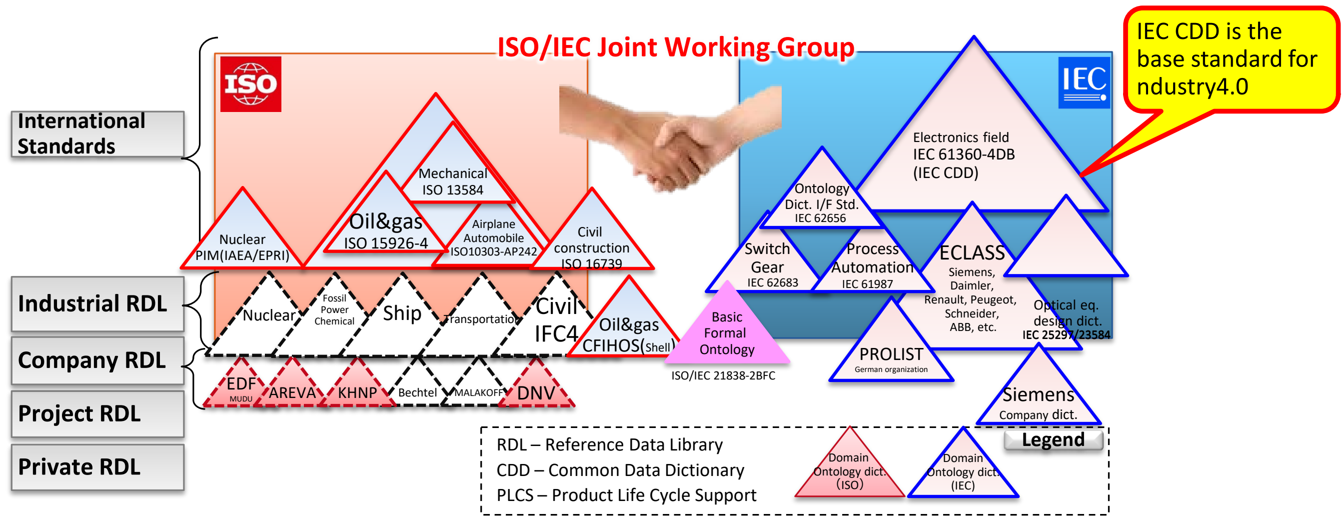

Figure 6.1 Joint standardization activities between ISO and IEC.

As for the decommissioning simulation, some integrated model to express information is needed, like Figure 6.2. This model can be defined based on Nuclear RDL. The NPPs consist of functional systems and spatial areas that a “system master table can manage” and an “area mater table.” The “system master table” has “contamination and activation” records as input data and “pipeline master” records. Each "contamination and activation" record consists of "nuclide inventory" records, such as radioactive nuclides of Tritium (H-3), Carbon-14 (C-14), Cobalt-60 (Co-60), and so on, to express degrees of radioactive contamination levels. "Pipe-line master" records consist of "pipe-parts" records, and "equipment master" records consist of "equipment-parts master" records.

Those "equipment-parts master" records and "pipe-parts master" records have "material" records and its "constituents" records to calculate dose-rate distribution based on their surrounding parts and spatial environmental model with "contamination and activation" records as radiation sources.

On the other hand, equipment and piping parts must be cut and packed into containers to store radioactive waste. So "equipment-parts master" records and "pipe-parts master" records also have "segmented-parts" records. For "segmented-parts" records, segmented IDs are allocated to identify the segmented objects uniquely. The IDs are used to track the waste fragment in conjunction with equipment-parts IDs or pipe-parts IDs to identify its origin. Segmented parts have volumes and radioactivity calculated by the original radioactivity of equipment or piping parts.

The "container material" table must manage waste containers, and the table includes "container summary" records and aggregations of "segmented parts" records.

Finally, the "area mater" table has the "container summary" table and the "dose-rate distribution" table to manage dismantling quantities and estimate the necessary cost of dismantling activities.

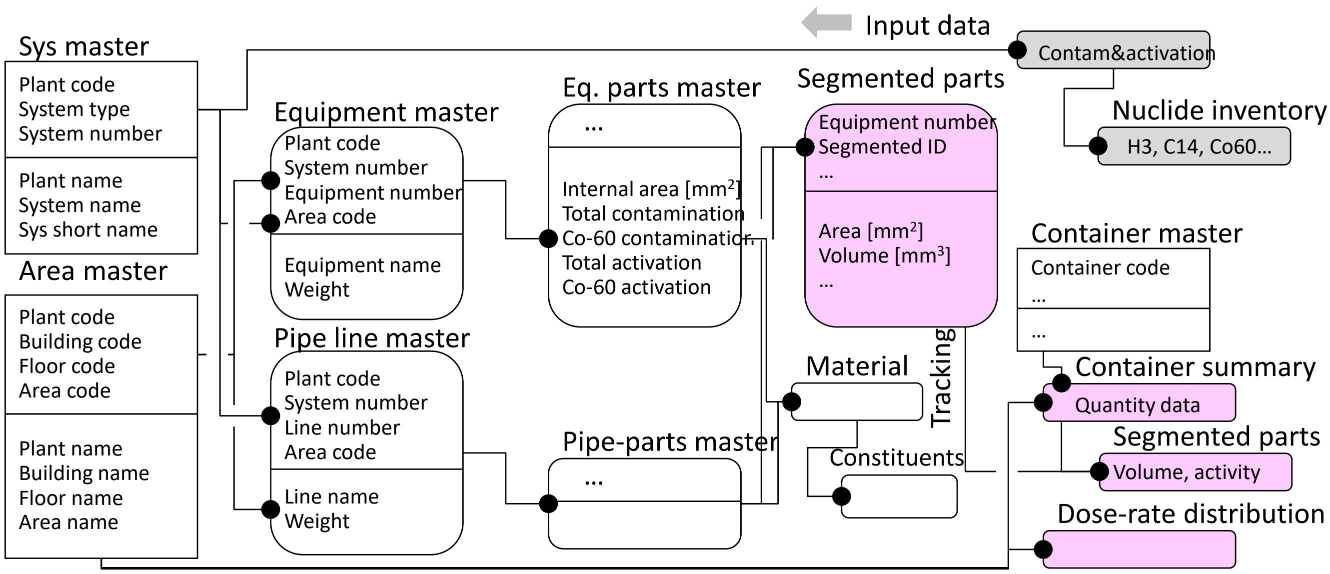

Figure 6.2 Database model to manage dismantling objects in conjunction with dose-rate distributions.

To plan and execute actual dismantling work remotely, we need to connect basic activities and virtualize robot behaviors in real-time. We have combined the control signals into a visualization module based on the developed VR technologies for visualizing robot behaviors. The developed system consists of the controlling PC for the robot and the visualization PC. Laser range finders since the robot's position (LRFs) is attached to the robot because enough optical cameras cannot be placed due to high radiation fields. The developed robot is controlled by water pressure to resist high dose-rate environments. The joint angle data is extracted from the water pressure data, and recognized location data is extracted. Then the information is published to the TCIP/IP communication module with the ROS processing function node [114]. The data encoded by the controlling PC is received by the TCP/IP communication module in the visualization PC, decoded by the ROS processing function node, and then passed to the developed robot visualization module. We have confirmed that the fundamental behavior of monitoring the actual robot by visualizing it in the virtual environment was successful. However, the noise on the signal causes the vibration of the location and the robot's joint angles. Therefore, we must reduce the effect of the noise with digital filters and implement other stabilization methods in the virtual environment.

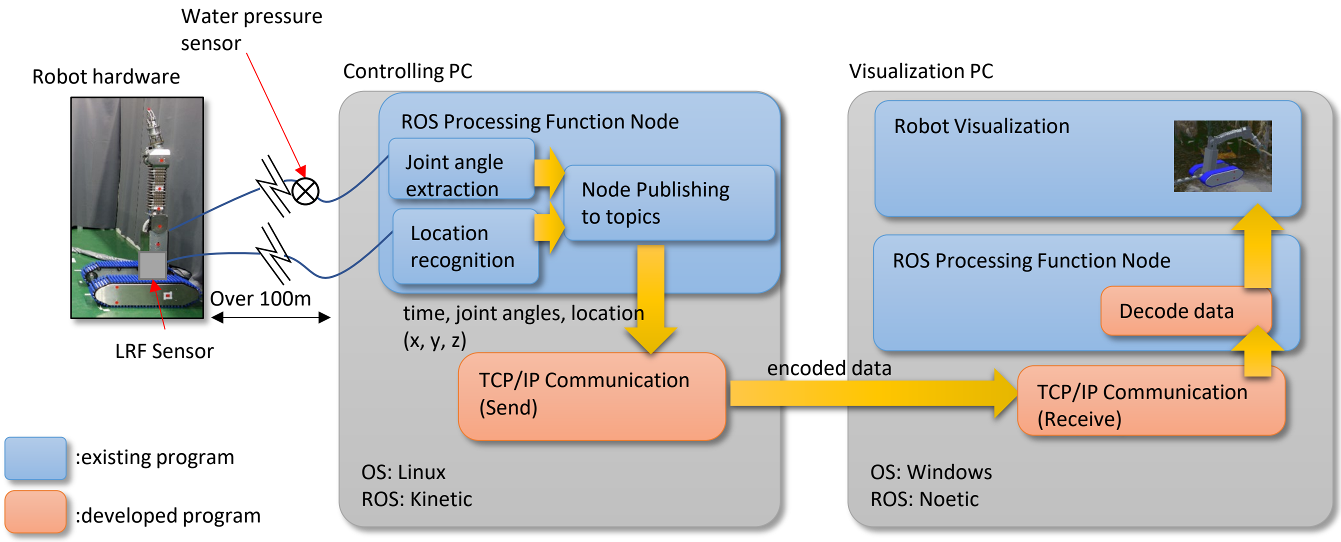

Figure 6.3 Real-time monitoring with visualizing in a virtual environment by communicating via ROS data from the actual hardware.

After confirming the monitoring functions for the actual robot behavior in the virtual environment, we will study the feasibility of controlling the robot from the virtual environment. We have developed the manual operation functions and gathering functions for operation logs. Several types of machine learning can be used for a VR simulator to calculate changing postures automatically [59]. Additionally, if kinematics and real-time dynamics are introduced to the VR simulator, the simulator can be used for training or planning the dismantling activities without mock-up facilities. Although experts make the initial dismantling schedules, the duration of each activity should be examined by testing with mock-up facilities and VR simulation. If the VR simulation can be used to investigate the validity of the durations of the dismantling schedule effectively, whether the planned schedule is feasible or not will be judged. Then, when the schedule is not possible, it should be adjusted. The dismantling schedule that cannot be feasible can be adjusted with optimization methods.

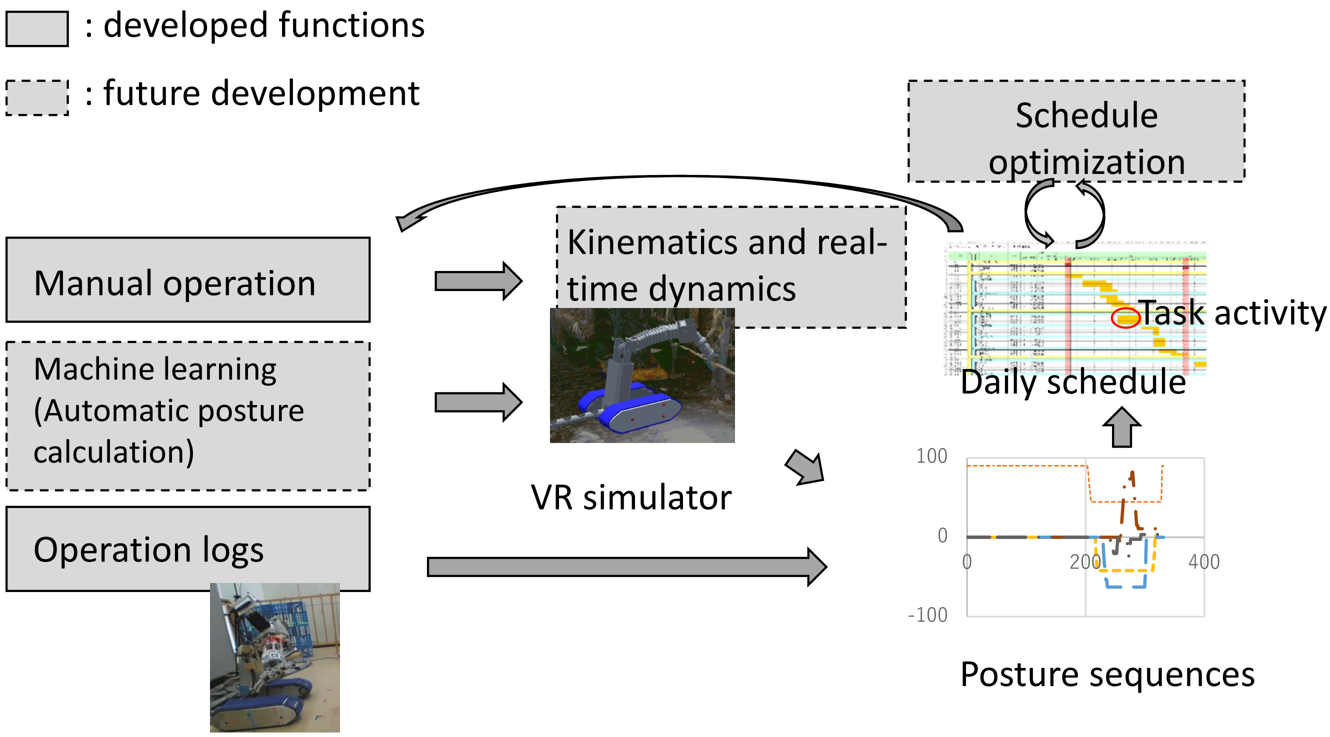

Figure 6.4 Bi-directional communication between the actual hardware and the software with optimized schedules.

As mentioned in 1.3.1, massive amounts of information can be gathered based on semantic technologies from online resources via the Internet. The decommissioning technologies for NPPs cannot be established by one organization; therefore, the whole structure of knowledge should be made efficiently and automatically by semantic technologies after enough knowledge is structured from the real world, understood, and converted from the real-world geometric shapes gathered by 3D scanning to meaningful objects, such as plant items defined by GPM stated in 2.2.3. Those technologies related to digital twins will be important for every industry. We should commit to developing automation methods to understand the real-world based on semantic technologies as one of the remaining issues to be resolved.

References

[1] W. J. O'Brien, "Fiatech: The Next Generation of the Capital Projects Technology Roadmap," *Journal of Construction Engineering and Management*, vol. 143, no. 9, p. 02517003, Sep. 2017, doi: 10.1061/(ASCE)CO.1943-7862.0001369.

[2] R. Volk, F. Hübner, T. Hünlich, and F. Schultmann, "The Future of Nuclear Decommissioning – A Worldwide Market Potential Study," *Energy Policy*, vol. 124, pp. 226–261, Jan. 2019, doi: 10.1016/J.ENPOL.2018.08.014.

[3] S. Yanagihara, "COSMARD: The Code System for Management of JPDR Decommissioning," *Journal of Nuclear Science and Technology*, vol. 30, no. 9, pp. 890–899, Sep. 1993, doi: 10.1080/18811248.1993.9734563.

[4] Y. Iguchi, Y. Kanehira, M. Tachibana, and T. Johnsen, "Development of Decommissioning Engineering Support System (DEXUS of the Fugen Nuclear Power Station," *Journal of Nuclear Science and Technology*, vol. 41, no. 3, pp. 367–375, Mar. 2004, doi: 10.1080/18811248.2004.9715497.

[5] METI, "Mid-and-Long-Term Roadmap towards the Decommissioning of TEPCO's Fukushima Daiichi Nuclear Power Station the Inter-Ministerial Council for Contaminated Water and Decommissioning Issues," *Ministry of Economy, Trade, and Industry (METI)*, 2019. https://www.meti.go.jp/english/earthquake/nuclear/decommissioning/pdf/20170926_01a.pdf (accessed Jan. 08, 2022).

[6] 石川 迪夫, "原子炉解体 廃炉への道," 講談社, 2011. https://www.amazon.co.jp/新装版-原子炉解体-廃炉への道-石川-迪夫/dp/4062170256 (accessed Jan. 08, 2022).

[7] Y. Miyasaka, "Planning and management for reactor decommissioning," *Dekomisshoningu Giho*, no. 24, pp. 48–59, 2001, Accessed: Jan. 08, 2022. [Online]. Available: http://inis.iaea.org/Search/search.aspx?orig_q=RN:33001436

[8] R. Lordan-Perret, R. D. Sloan, and R. Rosner, "Decommissioning the U.S. nuclear fleet: Financial assurance, corporate structures, and bankruptcy," *Energy Policy*, vol. 154, p. 112280, Jul. 2021, doi: 10.1016/j.enpol.2021.112280.

[9] T. Ishikura, "Trend on Decommissioning Technology of Nuclear Power Plants in 21 st Century (1)," *Journal of the Atomic Energy Society of Japan*, vol. 51, no. 8, pp. 625–629, 2009, doi: 10.3327/jaesjb.51.8_625.

[10] I. Lund, "Strategy Selection for the Decommissioning of Nuclear Facilities," *Strategy Selection for the Decommissioning of Nuclear Facilities*, pp. 67–70, 2004, Accessed: Jan. 08, 2022. [Online]. Available: http://www.copyright.com/.

[11] N. Watanabe, R. Miyoshi, T. Kozaki, S. Tanaka, and S. Yanagihara, "Cost Analysis for Decommissioning of Nuclear Power Plants with Uncertainties," *International Conference on Nuclear Engineering, Proceedings, ICONE*, vol. 7, Oct. 2018, doi: 10.1115/ICONE26-82572.

[12] N. Watanabe, R. Miyoshi, T. Kozaki, S. Tanaka, and S. Yanagihara, “Cost Analysis for Decommissioning of Nuclear Power Plants with Uncertainties,” *International Conference on Nuclear Engineering, Proceedings, ICONE*, vol. 7, Oct. 2018, doi: 10.1115/ICONE26-82572.

[13] S. Fillinger, E. Esche, G. Tolksdorf, W. Welscher, G. Wozny, and J. U. Repke, “Data Exchange for Process Engineering – Challenges and Opportunities,” *Chemie Ingenieur Technik*, vol. 91, no. 3, pp. 256–267, Mar. 2019, doi: 10.1002/CITE.201800122.

[14] M. Nakagami, “Project status of decommissioning Hamaoka NPS Unit 1 and Unit 2,” *Dekomisshoningu Giho*, no. 54, pp. 2–8, 2016, Accessed: Jan. 08, 2022. [Online]. Available: https://inis.iaea.org/search/searchsinglerecord.aspx?recordsFor=SingleRecord&RN=48071110

[15] Tokyo Electric Power Company Holdings (TEPCO), “Roadmap on the Way to Decommissioning -- Decommissioning Project｜Project Overview｜Tokyo Electric Power Company Holdings, Inc.” 2021. https://www.tepco.co.jp/en/hd/decommission/project/roadmap/index-e.html (accessed Jan. 08, 2022).

[16] Nuclear Damage Compensation and Decommissioning Facilitation Corporation (NDF), “Nuclear Damage Compensation and Decommissioning Facilitation Corporation,” 2021. Accessed: Jan. 08, 2022. [Online]. Available: http://archive.wmsym.org/2015/presentations/318.pdf

[17] Collaborative Laboratories for Advanced Decommissioning Science (CLADS), “Overall Map of Basic and Fundamental Research,” 2021. https://clads.jaea.go.jp/en/rd/map/map.html (accessed Jan. 08, 2022).

[18] R. H. Adams, J. de Grosbois, and M. Gladyshev, “Application of Plant Information Models to Manage Design Knowledge through the Nuclear Power Plant Life Cycle,” *IAEA-TECDOC-1919*, 2018.

[19] International Standard Organization (ISO), “ISO 10303-227:2005 - Industrial automation systems and integration — Product data representation and exchange — Part 227: Application protocol: Plant spatial configuration,” 2005. https://www.iso.org/standard/34006.html (accessed Jan. 08, 2022).

[20] International Standard Organisation (ISO), “ISO 10303-221:2007 - Industrial automation systems and integration — Product data representation and exchange — Part 221: Application protocol: Functional data and their schematic representation for process plants,” 2007. https://www.iso.org/standard/36771.html (accessed Jan. 08, 2022).

[21] D. Mun, J. Hwang, S. Han, H. Seki, and J. Yang, “Sharing product data of nuclear power plants across their lifecycles by utilizing a neutral model,” *Annals of Nuclear Energy*, vol. 35, no. 2, pp. 175–186, Feb. 2008, doi: 10.1016/j.anucene.2007.06.018.

[22] T. Yoshinaga *et al.*, “2514 Development of Technology Knowledge Infrastructure: Outline of IMS-VIPNET Project,” *The proceedings of the JSME annual meeting*, vol. 2005.4, no. 0, pp. 27–28, 2005, doi: 10.1299/jsmemecjo.2005.4.0_27.

[23] International Standard Organization (ISO), “ISO 15926-1:2004 - Industrial automation systems and integration — Integration of life-cycle data for process plants including oil and gas

production facilities — Part 1: Overview and fundamental principles," 2004. https://www.iso.org/standard/29556.html (accessed Jan. 08, 2022).

[24] D. Leal, "ISO 15926 'Life Cycle Data for Process Plant': an Overview," *Oil & Gas Science and Technology*, vol. 60, no. 4, pp. 629–637, Jul. 2005, doi: 10.2516/ogst:2005045.

[25] L. van Ruijven and J. Novack, "'Car wash for data': Best practices for information and configuration management applied at Pallas nuclear facility - Revista Nuclear España," *Nuclear España*, 2021. https://www.revistanuclear.es/wp-content/uploads/2021/09/Art.-Dynatec-v1.pdf (accessed Jan. 08, 2022).

[26] International Standard Organization (ISO), "ISO 10303-1:2021 - Industrial automation systems and integration — Product data representation and exchange — Part 1: Overview and fundamental principles," 2021. https://www.iso.org/standard/72237.html (accessed Jan. 08, 2022).

[27] A. B. Feeney, "The STEP Modular Architecture," *Journal of Computing and Information Science in Engineering*, vol. 2, no. 2, pp. 132–135, Jun. 2002, doi: 10.1115/1.1511520.

[28] M. Hardwick, K. C. Morris, D. L. Spooner, T. Rando, and P. Denno, "Lessons learned developing protocols for the industrial virtual enterprise," *Computer-Aided Design*, vol. 32, no. 2, pp. 159–166, Feb. 2000, doi: 10.1016/S0010-4485(99)00098-6.

[29] Y. Koizumi, H. Seki, and T. Yoon, "Data Integration Framework based on a Generic Product Model," in *Proceedings of the Tools and methods of competitive engineering (TMCE) 2004*, 2004, pp. 891–902.

[30] F. Tanaka, "Trends in international standard development to support smart machining," *Journal of Systems, Control and Information Engineers*, vol. 63, no. 5, pp. 182–187, 2019.

[31] International Standard Organization (ISO), "ISO/TC 184/SC 4 Industrial Data." https://committee.iso.org/home/tc184sc4 (accessed Jan. 08, 2022).

[32] X. Yang and C. McGreavy, "Requirements for sharing process data in the life cycle of process plants," *Computers & Chemical Engineering*, vol. 20, no. SUPPL.1, pp. S363–S368, Jan. 1996, doi: 10.1016/0098-1354(96)00071-3.

[33] W. J. O'Brien, "Fiatech: The Next Generation of the Capital Projects Technology Roadmap," *Journal of Construction Engineering and Management*, vol. 143, no. 9, p. 02517003, Jun. 2017, doi: 10.1061/(ASCE)CO.1943-7862.0001369.

[34] S. B. Kim, "Assessment of CII Best Practices usage in the construction industry," *KSCE Journal of Civil Engineering 2014 18:5*, vol. 18, no. 5, pp. 1228–1238, May 2014, doi: 10.1007/S12205-014-0221-Z.

[35] S. M. E. Sepasgozar, R. Karimi, S. Shirowzhan, M. Mojtahedi, S. Ebrahimzadeh, and D. McCarthy, "Delay Causes and Emerging Digital Tools: A Novel Model of Delay Analysis, Including Integrated Project Delivery and PMBOK," *Buildings 2019, Vol. 9, Page 191*, vol. 9, no. 9, p. 191, Aug. 2019, doi: 10.3390/BUILDINGS9090191.

[36] R. Michele, "Data Centric Verification to Streamline Project Planning and Execution," Aug. 2021, doi: 10.4043/31113-MS.

[37] E. van der Bijl, “The Importance of Standardization and Recommended Practices for Ei Equipment in the Oilgas Industry,” *Petroleum and Chemical Industry Conference Europe Conference Proceedings, PCIC EUROPE*, vol. 2018-June, Oct. 2018, doi: 10.23919/PCICEUROPE.2018.8491412.

[38] R. M. Doe, M. Selway, and M. Stumptner, “A Review of Interoperability in the AECO Sector compared with the Oil & Gas Sector”.

[39] B. Dafflon, N. Moalla, and Y. Ouzrout, “The challenges, approaches, and used techniques of CPS for manufacturing in Industry 4.0: a literature review,” *International Journal of Advanced Manufacturing Technology*, vol. 113, no. 7–8, pp. 2395–2412, Apr. 2021, doi: 10.1007/S00170-020-06572-4/TABLES/7.

[40] International Standard Organization (ISO), “ISO - ISO/TC 184/SC 4 - Industrial data,” 2022. https://www.iso.org/committee/54158.html (accessed Apr. 10, 2022).

[41] International Atomic Energy Agency (IAEA), “Exploring Semantic Technologies and Their Application to Nuclear Knowledge Management,” 2021. Accessed: Jun. 20, 2022. [Online]. Available: https://www.iaea.org/publications/13469/exploring-semantic-technologies-and-their-application-to-nuclear-knowledge-management

[42] H. Seki, M. Imamura, and H. Nagase, “Evaluating Precise Quantity of Decommissioning Waste by Cutting Virtual 3D Models of Large Equipment,” *http://www.sciencepublishinggroup.com*, vol. 5, no. 3, p. 36, 2020, doi: 10.11648/J.NS.20200503.12.

[43] G. Rindahl and N. K. F. Mark, “Innovative and Adaptive Technologies in Decommissioning of Nuclear Facilities Final report of a coordinated research project 2004-2008,” *IAEA-TECDOC*, no. 1602, 2008.

[44] Y. Ohga, M. Fukuda, K. Shibata, T. Kawakami, and T. Matsuzaki, “A system for the calculation and visualisation of radiation field for maintenance support in nuclear power plants,” *Radiation Protection Dosimetry*, vol. 116, no. 1–4, pp. 592–596, Dec. 2005, doi: 10.1093/rpd/nci014.

[45] T. Paviot, C. Mouton, and S. Lamouri, “Long term control of 3D engineering data for nuclear power plants,” in *Proceedings of the 18th International Conference on 3D Web Technology - Web3D ’13*, 2013, p. 205. doi: 10.1145/2466533.2466563.

[46] J. Lee *et al.*, “Establishment of the framework to visualize the space dose rates on the dismantling simulation system based on a digital manufacturing platform,” *Annals of Nuclear Energy*, vol. 95, pp. 161–167, Sep. 2016, doi: 10.1016/j.anucene.2016.05.013.

[47] I. Kim *et al.*, “A framework for a flexible cutting-process simulation of a nuclear facility decommission,” *Annals of Nuclear Energy*, vol. 97, pp. 204–207, Nov. 2016, doi: 10.1016/j.anucene.2016.07.004.

[48] C. Zhang, M. Hu, F. di Maio, B. Sprecher, X. Yang, and A. Tukker, “An overview of the waste hierarchy framework for analyzing the circularity in construction and demolition waste management in Europe,” *Science of The Total Environment*, vol. 803, p. 149892, Jan. 2022, doi: 10.1016/J.SCITOTENV.2021.149892.

[49] M. Schmittem, "Nuclear Decommissioning in Japan-Opportunities for European Companies-EU-Japan Centre for Industrial Cooperation," *EU–Japan Centre for Industrial Cooperation*, 2016.

[50] P. A. Grossi, R. de Oliveira Segabinaze, C. C. Oliveira De Tello, and V. Daniška, "Cost Estimation for Decommissioning of Research Reactors," *2013 International Nuclear Atlantic Conference - INAC 2013*, 2013.

[51] I. Szőke, M. N. Louka, T.-R. Bryntesen, S.-T. Edvardsen, and J. Bratteli, "Comprehensive support for nuclear decommissioning based on 3D simulation and advanced user interface technologies," *Journal of Nuclear Science and Technology*, vol. 52, no. 3, pp. 371–387, Mar. 2015, doi: 10.1080/00223131.2014.951704.

[52] S. Okada, K. Hirano, R. Kobayashi, and Y. Kometani, "Development and Application of Robotics for Decommissioning of Fukushima Daiichi Nuclear Power Plant," *Hitachi Review*, vol. 69, no. 4, pp. 562–563, 2020.

[53] T. George Thuruthel, Y. Ansari, E. Falotico, and C. Laschi, "Control Strategies for Soft Robotic Manipulators: A Survey," *Soft Robotics*, vol. 5, no. 2, pp. 149–163, Apr. 2018, doi: 10.1089/soro.2017.0007.

[54] J. M. Aitken *et al.*, "Autonomous Nuclear Waste Management," *IEEE Intelligent Systems*, vol. 33, no. 6, pp. 47–55, Nov. 2018, doi: 10.1109/MIS.2018.111144814.

[55] E. Jharko, R. Meshcheryakov, and V. Promyslov, "Aspects of Nuclear Power Plant Digital Decommissioning," *SIBCON 2021 - International Siberian Conference on Control and Communications*, May 2021, doi: 10.1109/SIBCON50419.2021.9438885.

[56] H. Seki, K. Tatehora, and Y. Oomasa, "Drawing data refining system according to plant product life cycle," in *Information Control Problems in Manufacturing 2006*, Elsevier, 2006, pp. 745–750. doi: 10.1016/B978-008044654-7/50256-9.

[57] H. Seki, A. Enomoto, H. Nagase, M. Imamura, and J. Tahata, "Evaluation system of waste quantities for decommissioning planning of nuclear power plants," *Dekomisshoningu Giho*, no. 57, pp. 36–43, 2018.

[58] H. Seki, M. Imamura, and H. Nagase, "Evaluating Precise Quantity of Decommissioning Waste by Cutting Virtual 3D Models of Large Equipment," *Nuclear Science*, vol. 5, no. 3, p. 36, 2020, doi: 10.11648/j.ns.20200503.12.

[59] H. Seki, K. Ueno, and K. Hirano, "Real-time Simulation Methods for Robots with a Flexible Arm Based on Computer Graphics Technology," *International Journal of Mechanical Engineering and Applications*, vol. 9, no. 6, pp. 90–97, 2021, doi: 10.11648/j.ijmea.20210906.12.

[60] D. Mun, J. Hwang, S. Han, H. Seki, and J. Yang, "Sharing product data of nuclear power plants across their lifecycles by utilizing a neutral model," *Annals of Nuclear Energy*, vol. 35, no. 2, pp. 175–186, Feb. 2008, doi: 10.1016/J.ANUCENE.2007.06.018.

[61] A. B. Feeney, "The STEP Modular Architecture," *Journal of Computing and Information Science in Engineering*, vol. 2, no. 2, pp. 132–135, Jun. 2002, doi: 10.1115/1.1511520.

[62] M. Hardwick, K. C. Morris, D. L. Spooner, T. Rando, and P. Denno, "Lessons learned developing protocols for the industrial virtual enterprise," *Computer-Aided Design*, vol. 32, no. 2, pp. 159–166, Feb. 2000, doi: 10.1016/S0010-4485(99)00098-6.

[63] X. F. Zha and H. Du, "A PDES/STEP-based model and system for concurrent integrated design and assembly planning," *Computer-Aided Design*, vol. 34, no. 14, pp. 1087–1110, Dec. 2002, doi: 10.1016/S0010-4485(01)00186-5.

[64] J. Liang *et al.*, "Synthesis of consolidated data schema for engineering analysis from multiple STEP application protocols," *Computer-Aided Design*, vol. 31, no. 7, pp. 429–447, Jun. 1999, doi: 10.1016/S0010-4485(99)00041-X.

[65] T. YOSHINAGA *et al.*, "Development of Technology Knowledge Infrastructure: Outline of IMS-VIPNET Project," *The proceedings of the JSME annual meeting*, vol. 2005.4, no. 0, pp. 27–28, 2005, doi: 10.1299/JSMEMECJO.2005.4.0_27.

[66] H. Seki, "Virtual Production Enterprise Network (VIPNET)," *IMS 0431 Summary Report*, 2005.

[67] P. R. Weems and M. Hwang, "Overview of issues common to structuring, negotiating and documenting LNG projects," *The Journal of World Energy Law & Business*, vol. 6, no. 4, pp. 267–299, Dec. 2013, doi: 10.1093/JWELB/JWT016.

[68] R. Cutler, "Kazakhstan's offshore Kashagan deposit set for first oil in 2012," *Central Asia–Caucasus Institute*, 2011, Accessed: Apr. 10, 2022. [Online]. Available: http://www.cacianalyst.org/publications/analytical-articles/item/12292-analytical-articles-caci-analyst-2011-5-25-art-12292.html

[69] K. Miller, "Piper Alpha and the Cullen Report," *Industrial Law Journal*, vol. 20, 1991, Accessed: Apr. 17, 2022. [Online]. Available: https://heinonline.org/HOL/Page?handle=hein.journals/indlj20&id=190&div=&collection=

[70] M. E. Patc-Cornell', "Learning from the Piper Alpha Accident: A Postmortem Analysis of Technical and Organizational Factors," vol. 13, no. 2, 1993.

[71] S. Kwon, B. Kim, K. An, D. Ryu, D. Mun, and S. Han, "Standardized exchange of plant equipment and materials data based on ISO 15926 methodology in nuclear power plants," *Annals of Nuclear Energy*, vol. 118, pp. 185–198, Aug. 2018, doi: 10.1016/J.ANUCENE.2018.04.001.

[72] K. Iwahara, Y. Higashikawa, M. Matsuura, and H. Seki, "Development of NPM/XML-based data integration framework and nuclear plant engineering support system," in *Proceedings of the 11th international conference on nuclear engineering*, 2003, p. ICONE-36565.

[73] M. West, *Developing high quality data models*. Elsevier, 2011.

[74] Y. Koizumi, H. Seki, and T. Yoon, "Data integration framework based on a generic product model," in *Proceedings of the TMCE*, 2004, pp. 891–902.

[75] G. and Rindahl and N. K. F. Mark, "Norway: VRdose and emerging 3D software solutions to support decommissioning activities. Experiences and expectations from development and deployment of innovative technology," *IAEA-TECDOC-1602*, 2008, Accessed: Mar. 31, 2022. [Online]. Available: https://www.osti.gov/etdeweb/biblio/21156590

[76] Y. Ohga, M. Fukuda, K. Shibata, T. Kawakami, and T. Matsuzaki, "A system for the calculation and visualisation of radiation field for maintenance support in nuclear power plants," *Radiation Protection Dosimetry*, vol. 116, no. 1–4, pp. 592–596, Dec. 2005, doi: 10.1093/RPD/NCI014.

[77] J. Lee *et al.*, "Establishment of the framework to visualize the space dose rates on the dismantling simulation system based on a digital manufacturing platform," *Annals of Nuclear Energy*, vol. 95, pp. 161–167, Sep. 2016, doi: 10.1016/J.ANUCENE.2016.05.013.

[78] T. Paviot, C. Mouton, and S. Lamouri, "Long term control of 3D engineering data for nuclear power plants," *Proceedings - Web3D 2013: 18th International Conference on 3D Web Technology*, p. 205, 2013, doi: 10.1145/2466533.2466563.

[79] I. Kim *et al.*, "A framework for a flexible cutting-process simulation of a nuclear facility decommission," *Annals of Nuclear Energy*, vol. 97, pp. 204–207, Nov. 2016, doi: 10.1016/J.ANUCENE.2016.07.004.

[80] Y. Nonaka, E. N. Yamamoto, K. Oya, A. Enomoto, and E. H. Seki, "Development of IT-driven Power Plant Engineering Work Support Systems," *Hitachi Review*, vol. 65, no. 4, 2016.

[81] H. Seki, M. Imamura, T. Hirashige, H. Nagase, S. Tamata, and A. Enomoto, "Estimation and Visualization of Decommissioning Wastes based on Plant 3D Model," 2015.

[82] T. Sato *et al.*, "Particle and Heavy Ion Transport code System, PHITS, version 2.52," *Journal of Nuclear Science and Technology*, vol. 50, no. 9, pp. 913–923, Sep. 2013, doi: 10.1080/00223131.2013.814553.

[83] E. D.-N. mathematik and undefined 1959, "A note on two problems in connexion with graphs," *ir.cwi.nl*, vol. 1, pp. 269–271, 1959, Accessed: Mar. 31, 2022. [Online]. Available: https://ir.cwi.nl/pub/9256/9256D.pdf

[84] A. Enomoto *et al.*, "Multiple Path Finding System for Replacement Tasks," *Procedia CIRP*, vol. 33, pp. 3–8, Jan. 2015, doi: 10.1016/J.PROCIR.2015.06.003.

[85] A. Okabe *et al.*, "Automatic Route-finding with Non-monotonic-trend Factor for Large-scale Plant Maintenance Task," *Procedia CIRP*, vol. 41, pp. 550–555, Jan. 2016, doi: 10.1016/J.PROCIR.2015.12.001.

[86] M. Schmittem, "Nuclear Decommissioning in Japan-Opportunities for European Companies-EU-Japan Centre for Industrial Cooperation," 2016.

[87] P. A. Grossi, R. de Oliveira Segabinaze, C. C. Oliveira De Tello, and V. Daniška, "Cost Estimation for Decommissioning of Research Reactors," 2013.

[88] I. Szőke, M. N. Louka, T. R. Bryntesen, S. T. Edvardsen, and J. Bratteli, "Comprehensive support for nuclear decommissioning based on 3D simulation and advanced user interface technologies," *http://dx.doi.org/10.1080/00223131.2014.951704*, vol. 52, no. 3, pp. 371–387, Mar. 2014, doi: 10.1080/00223131.2014.951704.

[89] I. Szőke *et al.*, "Real-time 3D radiation risk assessment supporting simulation of work in nuclear environments," *Journal of Radiological Protection*, vol. 34, no. 2, p. 389, Apr. 2014, doi: 10.1088/0952-4746/34/2/389.

[90] H. Seki, M. Imamura, T. Kitahara, and A. Enomoto, “Estimation of Decommissioning Quantity Based on 3D Intelligent Model-17075,” 2017.

[91] H. Seki, A. Enomoto, A. Imamura, H. Nagase, J. Tahata, and E. A. Y. T. I. M. N. H. and T. J. Seki H, “Holistic Nuclear Power Plant Decommissioning Management System,” 2018.

[92] K. Ishigure, “Decommissioning strategies and programme developments of Japan (Conference) | ETDEWEB,” 2003. Accessed: Mar. 31, 2022. [Online]. Available: https://www.osti.gov/etdeweb/biblio/20521799

[93] H. Seki, J. Tahata, M. Imamura, H. Nagase, and L. Hitachi, “Evaluating Quantity of Decommissioning Waste by Cutting Virtual 3D Objects in Large Equipment,” *Proceedings of the 45th Annual Waste Management Conference International Conference (WM2019)*, p. 19111, 2019.

[94] H. Seki, M. Imamura, and H. Nagase, “Evaluating Precise Quantity of Decommissioning Waste by Cutting Virtual 3D Models of Large Equipment,” *http://www.sciencepublishinggroup.com*, vol. 5, no. 3, p. 36, 2020, doi: 10.11648/J.NS.20200503.12.

[95] S. Okada, K. Hirano, R. Kobayashi, and Y. Kometani, “Development and Application of Robotics for Decommissioning of Fukushima Daiichi Nuclear Power Plant: Hitachi Review,” *Hitachi Review*, vol. 69, pp. 562–563, 2020, Accessed: Mar. 31, 2022. [Online]. Available: https://www.hitachi.com/rev/archive/2020/r2020_04/04d02/index.html

[96] T. George Thuruthel, Y. Ansari, E. Falotico, and C. Laschi, “Control Strategies for Soft Robotic Manipulators: A Survey,” *Soft Robotics*, vol. 5, no. 2, pp. 149–163, Apr. 2018, doi: 10.1089/SORO.2017.0007/ASSET/IMAGES/LARGE/FIGURE12.JPEG.

[97] V. H. Andaluz *et al.*, “Unity3D-MatLab Simulator in Real Time for Robotics Applications,” *Lecture Notes in Computer Science (including subseries Lecture Notes in Artificial Intelligence and Lecture Notes in Bioinformatics)*, vol. 9768, pp. 246–263, 2016, doi: 10.1007/978-3-319-40621-3_19.

[98] P. Besset and C. J. Taylor, “Inverse kinematics for a redundant robotic manipulator used for nuclear decommissioning,” *2014 UKACC International Conference on Control, CONTROL 2014 - Proceedings*, pp. 56–61, Oct. 2014, doi: 10.1109/CONTROL.2014.6915115.

[99] A. Borboni, R. Bussola, R. Faglia, P. L. Magnani, and A. Menegolo, “Movement optimization of a redundant serial robot for high-quality pipe cutting,” *Journal of Mechanical Design, Transactions of the ASME*, vol. 130, no. 8, pp. 0823011–0823016, Aug. 2008, doi: 10.1115/1.2918907/418177.

[100] F. Pin, L. Love, and D. Jung, “Automated Kinematics Equations Generation and Constrained Motion Planning Resolution for Modular and Reconfigurable Robots,” *Proceedings of the 227th ACS National Meeting*, 2004. https://www.osti.gov/biblio/826014 (accessed Mar. 31, 2022).

[101] K. Shoji, “Possibility of applying large-scale point cloud/mixed reality technology in decommissioning of nuclear facilities,” *Dekomisshoningu Giho*, vol. 55, pp. 8–21, 2017, Accessed: Mar. 31, 2022. [Online]. Available: https://inis.iaea.org/search/search.aspx?orig_q=RN:48071118

[102] T. Li, J. Wang, H. Liu, and L. gang Liu, “Efficient mesh denoising via robust normal filtering and alternate vertex updating,” *Frontiers of Information Technology & Electronic Engineering 2017 18:11*, vol. 18, no. 11, pp. 1828–1842, Jan. 2018, doi: 10.1631/FITEE.1601229.

[103] Unity, “Graphics performance fundamentals,” *Unity Documentation*, 2020. https://docs.unity3d.com/Manual/OptimizingGraphicsPerformance.html (accessed Apr. 01, 2022).

[104] M. Srinivasan Ramanagopal, A. P. van Nguyen, and J. le Ny, “A Motion Planning Strategy for the Active Vision-Based Mapping of Ground-Level Structures,” *IEEE Transactions on Automation Science and Engineering*, vol. 15, no. 1, pp. 356–368, Jan. 2018, doi: 10.1109/TASE.2017.2762088.

[105] X. Shi, H. Fang, and L. Guo, “Multi-objective optimal trajectory planning of manipulators based on quintic NURBS,” *2016 IEEE International Conference on Mechatronics and Automation, IEEE ICMA 2016*, pp. 759–765, Sep. 2016, doi: 10.1109/ICMA.2016.7558658.

[106] Autodesk, “Maya Software,” 2022. https://www.autodesk.com/products/maya/overview?term=1-YEAR&tab=subscription (accessed Apr. 01, 2022).

[107] NVIDIA, “NVIDIA PhysX System Software,” 2019. https://www.nvidia.com/en-us/drivers/physx/physx-9-19-0218-driver/ (accessed Apr. 01, 2022).

[108] D. Leal, A. Cook, C. Partridge, J. Sullivan, and M. West, “A Survey of Industry Data Models and Reference Data Libraries-to identify requirements for, and to provide input to, a Foundation Data Model,” 2020, Accessed: Apr. 02, 2022. [Online]. Available: https://www.repository.cam.ac.uk/bitstream/handle/1810/324263/Industry%20data%20models%20and%20Reference%20Data%20Libraries.pdf?sequence=1

[109] International Standard Organization (ISO), “ISO - ISO 13584-42:2010 - Industrial automation systems and integration — Parts library — Part 42: Description methodology: Methodology for structuring parts families,” 2010. https://www.iso.org/standard/43423.html (accessed Apr. 16, 2022).

[110] International Standard Organization (ISO), “ISO - ISO/TS 15926-4:2019 - Industrial automation systems and integration — Integration of life-cycle data for process plants including oil and gas production facilities — Part 4: Initial reference data,” 2019. https://www.iso.org/standard/73830.html (accessed Apr. 16, 2022).

[111] International Standard Organization (ISO), “ISO - ISO 10303-239:2012 - Industrial automation systems and integration — Product data representation and exchange — Part 239: Application protocol: Product life cycle support,” 2012. https://www.iso.org/standard/54791.html (accessed Apr. 16, 2022).

[112] International Electrotechnical Commission (IEC), “IEC 61360-2 - Standard data element types with associated classification scheme for electric components – Part 2: EXPRESS dictionary schema,” 2012. https://standards.globalspec.com/std/1547933/iec-61360-2 (accessed Apr. 16, 2022).

[113] International Electrotechnical Commission (IEC), "IEC 62656-1 - Standardized product ontology register and transfer by spreadsheets – Part 1: Logical structure for data parcels," 2014. https://standards.globalspec.com/std/9862932/IEC%2062656-1 (accessed Apr. 16, 2022).

[114] Open Robotics, "ROS/Tutorials/Writing Publisher Subscriber(c++) - ROS Wiki," 2022. https://wiki.ros.org/ROS/Tutorials/WritingPublisherSubscriber%28c%2B%2B%29 (accessed Apr. 16, 2022).

Acknowledgment

I want to express my deep and sincere gratitude to Professor Satoshi Tadokoro. Despite the inconvenient situation of having face-to-face meetings due to COVID-19 effects, we had fruitful conversations, and he gave me insightful advice for my dissertation work via a Web meeting tool.

I also would like to thank Professor Yutaka Watanabe, Professor Takayuki Okatani, and Professor Kazunori Ohno for their excellent detailed advice in completing this dissertation.

As for supporting and giving opportunities for research and development in this area, I appreciate the people in the Research and Development Group of Hitachi, Ltd., and Hitachi GE Nuclear Energy Ltd.

I also thank my parents and family for supporting me in the Tohoku University doctoral course.

List of publications

1. Original papers

1) H. Seki, A. Enomoto, H. Nagase, M. Imamura, and J. Tahata. "Evaluation System of Waste Quantities for Decommissioning Planning of Nuclear Power Plants [in Japanese]" *Journal of the RANDEC* (57), pp. 11-19 (2018). [関　洋ほか、"原子力発電プラントの廃止措置における廃棄物等評価システム," デコミショニング技法No. 57, pp. 11–19 (2018)] related to Chapter 3.
2) H. Seki, Mitsutaka Imamura, and Hiroshi Nagase. "Evaluating Precise Quantity of Decommissioning Waste by Cutting Virtual 3D Models of Large Equipment." Nuclear Science 5(3), pp. 36-43 (2020), related to Chapter 4.
3) H. Seki, K. Ueno, and K. Hirano, "Real-Time Simulation Methods for Robots with Flexible Arms Based on Computer Graphics Technology," International Journal of Mechanical Engineering and Applications 9(6), pp. 90-97(2021), related to Chapter 5.

2. Presentation at international conferences

1) H. Seki, K. Tatehora, and Y. Oomasa, "Drawing data refining system according to plant product life cycle," *IFAC Proceedings* Volumes 39.3, pp. 789-794, St. Etienne, France (2006), (peer-reviewed), related to Chapter 2.
2) H. Seki. "Development of Decommissioning Engineering Platform Based on Plant 3D Model," Bentley Systems, Be Inspired 2014 Innovation in Power Generation, London, UK (2014).
3) H. Seki, M. Imamura, T. Hirashige, H. Nagase, S. Tamata, and A. Enomoto. "Estimation and Visualization of Decommissioning Wastes based on Plant 3D Model." ICONE23-1015, Narashino, Japan (2015).
4) H. Seki, A. Enomoto, M. Imamura, and T. Kitahara. "Decommissioning Engineering Support Systems Based on 3D CAD Models," ICMST 2016, Shenzhen, China (2016).
5) H. Seki, M. Imamura, T. Kitahara, and A. Enomoto. "Estimation of decommissioning quantity based on 3D intelligent model." In Proceedings of the 45th Annual Waste Management Conference International Conference (WM2017), vol. 17075. Phoenix, AZ, USA (2017).
6) H. Seki, A. Enomoto, M. Imamura, and T. Kitahara. "Decommissioning engineering support system based on an intelligent 3D model database." In Proceedings of International Congress on Advances in Nuclear Power Plants (ICAPP 2017), Kyoto, Japan (2017).
7) H. Seki, A. Enomto, T. Yoshida, M. Imamura, H. Nagase, and J. Tahata. "Holistic nuclear power plant decommissioning management system." In Proceedings of the 12th International Workshop on the Integrity of Nuclear Components (ASINCO 12), Hualien, Taiwan (2018).
8) H. Seki, M. Imamura, and H. Nagase. "Evaluating Quantity of Decommissioning Waste by Cutting Virtual 3D Objects in Large Equipment," In Proceedings of the 47th Annual Waste Management Conference International Conference (WM2019), vol. 19111. Phoenix, AZ, USA (2019).
9) H. Seki. "Decommissioning Engineering Support System Based on Building Information Modeling," International Workshop on Structural Safety Technology for Nuclear Back-end Management at Institute of Nuclear Energy Research, Taoyuan, Taiwan (2019).
10) H. Seki, K. Hirano, and K. Ueno. "Development of Real-Time Simulation Technology for Robots with Flexible Arms Based on Three-Dimensional Computer Graphics (CG) Methods." ICONE28-60410, Online (2021).

3. Presentation at Japanese conferences

1) 関洋, 笠原孝保, 太田吉美. “原子力プラントの設計に関わるノウハウ活用システムの開発” 平成 12 年電気学会全国大会論文集, pp. 1249-1252 (1996).
2) 関洋，三宅俊之. “4D CADを用いた建設シミュレーション基盤技術の開発” 平成21年電気学会　電子・情報・システム部門大会　GS18-1 (2009).
3) 関洋, 片岡一郎, 今村光孝. “プラント 3D モデルに基づく 廃炉エンジニアリング・システム基盤の開発” 原子力学会2014年春の年会, I61. (2014).
4) 関洋，杉本洋平，榎本敦子，今村光孝，平重貴之，玉田慎，長瀬博. “廃止措置エンジニアリング技術. の開発；（1）プラント 3D モデルに基づく大規模廃棄物量算出の自動化” 原子力学会2015年秋の大会, G01. (2015).
5) 関洋，榎本敦子，今村光孝，北原隆. “3D CADモデルに基づく廃止措置エンジニアリング支援，” 日本保全学会 第１３回学術講演会，H-2-2-5 (2016).
6) 関洋. “3Dモデルを活用した原子力プラント廃止措置計画支援の取り組み,” Autodesk University Japan (2016).

4. Patents

1) 特開2003-044529号「データベース統合支援方法およびシステム」（登録3854825号）
2) 特開2005-301630号「ＣＡＤデータ変換装置および方法ならびにプログラム」（登録4410595号）
3) 特開2008-287300号「設計支援装置」（登録4935494号）
4) 特開2010-211736号「設計支援装置、設計支援方法およびプログラム」（登録5028439号）
5) 特開2012-014309号「建設シミュレーション方法、及び、装置」（登録5557622号）
6) 特開2012-180191号「プラント建設支援方法およびプラント建設支援装置」（登録5452524号）
7) WO/2013/051080 ”Site Management method and site management device”「現場管理方法および現場管理装置」（登録5798632号）
8) 特開2015-087300号「プラント解体計画支援装置及びプラント解体計画支援方法」（登録6300345号）
9) 特開2015-230223号「放射性廃棄物収納計画支援システム」（登録6297929号）
10) 特開2016-090545号「放射線源マッピングシステムおよび処理方法」（登録448317号）
11) 特開2016-211952号「解体手順計画システム」（登録6588732号）
12) 特開2017-194274号「廃棄工程管理装置、および、廃棄工程管理方法」（登録6626398号）
13) 特開2018-205974号「空間表示装置、および、空間表示方法」（登録6867883号）